1-1-1975

Compatibility of the system; poly(2,6-Dimethyl phenyleneoxide)/poly(styrene coparachlorostyrene).

James J. Tkacik
University of Massachusetts Amherst

COMPATIBILITY OF THE SYSTEM:
POLY (2,6-DIMETHYL PHENYLENEOXIDE)/
POLY (STYRENE CO-PARACHLOROSTYRENE)

A Dissertation Presented

By

James J. Tkacik

Submitted to the Graduate School of the
University of Massachusetts in partial
fulfillment of the requirements for the degree of

DOCTOR OF PHILOSOPHY

December 1975

Polymer Science and Engineering

COMPATIBILITY OF THE SYSTEM: POLY (2,6-DIMETHYL PHENYLENEOXIDE)/ POLY (STYRENE CO-PARACHLOROSTYRENE)

A Dissertation

By

James J. Tkacik

Approved as to style and content by:

W.J. MacKnight, Chairman of Committee

F.E. Karasz, Member

I.C. Sanchez, Member

R.S. Porter,
Department Head

Polymer Science and
Engineering

December 1975

A C K N O W L E D G E M E N T S

I would like to thank W.J. MacKnight and F.E. Karasz for their professional guidance and concern throughout the course of this research.

I would like to extend my gratitude to the Plastics Institute of America for the financial assistance of my fellowship while performing this research.

A C K N O W L E D G E M E N T S
(A N D A P O L O G I E S)

I would especially like to thank Bill MacKnight for all of his efforts to aid in my personal and professional development. For the interest, assistance and friendship (not to mention free meals and the trip to England !), I extend my gratitude.

Unfortunately, however, much of his sage advice was not appreciated or, still worse, blatantly ignored. (Margaritas ante porcos.) For this, I apologize.

A B S T R A C T

Compatibility characteristics of the polymer blend system of poly(2,6-dimethylphenelyeneoxide)(PPO) and poly(styrene co-parachlorostyrene)(PCS) were investigated. These blends were analyzed by differential scanning calorimetry (DSC), dynamic mechanical and dielectric relaxations and electron microscopy to elucidate factors influencing compatibility, especially as a function of the chemical composition of the PCS copolymer.

PCS copolymers of various p-Cl styrene contents were synthesized and blended with PPO by solution techniques (e.g., freeze drying, coprecipitation). The criterion for compatibility is the existence of a single, compositionally dependent Tg (DSC) for each binary blend of PPO and PCS. PCS copolymers with a p-Cl styrene content of >60 (mole) % were incompatible with PPO; those with $\leq$ 60% were compatible.

Electron microscopy provided complementary evidence for these compatibility assignments. Blends ascertained to be incompatible by DSC exhibited large scale (5-10 μ) phase separation, with domain structures a function of blend composition. Compatible blends

exhibited no such discernible phase separation.

Dielectric relaxation studies provided a consistent assessment of compatibility by monitoring the relaxation of the dipolar PCS component of the blend. Compatible PPO/PCS blends exhibited one compositionally dielectric loss peak at temperatures intermediary to those of the components. Incompatible blends exhibited a PCS loss peak unchanged from the pure PCS component.

Frohlich analysis of the dielectric results provided information about the environments of dipoles within the blends as a function of compatibility. For the incompatible blends the dipole orientation correlation factor (g) was independent of blend composition, which in consistent with phase separation. In the compatible blends g increases as the PCS component becomes more dilute. This effect has been attributed to inter- and/or intramolecular factors which influence dipolar environments, indicating intimate mixing.

Analysis of compatibility by dynamic mechanical experiments was somewhat more complex. Incompatible systems exhibited two distinct mechanical damping peaks as a function of temperature. Compatible blends exhibited one major loss peak and a minor secondary peak attributed to a PCS-rich phase.

C O N T E N T S

LIST OF FIGURES

LIST OF TABLES

C H A P T E R I

SURVEY OF RELATED RESEARCH

A. Introduction

Polymer blends have stimulated a considerable amount of interest from both purely scientific and commercial aspects. From the point of view of a polymer physical chemist, polymer-polymer interactions are of great interest, relating such basic factors as molecular interactions, blend morphology and bulk properties. Commercially, polymer blends represent an increasingly large portion of marketable polymeric products. A review of recent patents would reveal that the formulation of polymer blends (both compatible and incompatible) have beneficially modified properties such as impact resistance,[1] tensile strength,[2] and processibility.[3] Unfortunately, despite the large scope of the commercial investigation and production, advances are often empirical (or even "black art") in nature and have not been accompanied by comparable progress in the basic understanding of the principles involved in polymer blending, compatibility or molecular interactions.

B. Polymer Compatibility

Generally, the term polymer blend refers to physical mixtures of two or more polymeric components which are not covalently linked.* Soluble (or miscible) polymer systems are described as being compatible. This polymer compatibility is characterized by physical properties analogous to those exhibited by miscible mixtures of low molecular weight organic molecules (e.g., the formation of a single continuous, homogeneous phase). Polymer pairs which are incompatible (i.e., immiscible) exhibit large scale phase separation; this phase separation is generally greater than the order of magnitude necessary to scatter light (i.e., greater than several thousand Angstroms). Within this incompatible system each component is macroscopically segregated. Therefore, in an incompatible blend of poly-A and poly-B, the polymer chains of either homopolymer experience an environment which is essentially identical to that of a chain in an isolated (i.e., unblended) block of its own pure homopolymer. The effect of this type of phase separation is that the presence of one component of the blend not greatly influence the polymer chains of the other com-

---

* These components are also generally considered to be randomly fused into a macroscopic mass, thus eliminating trivial examples of polyblends such as mixtures of powders of two polymers or polymer laminates.[4]

ponent. Physically, the result is that the incompatible polymer blend retains distinct properties of each of the components. For example, incompatible polymer blends exhibit two distinct glass transition temperatures (Tg), one corresponding to the Tg of each of the components. Similarly, each isolated phase will exhibit a dynamic relaxation (for, e.g., mechanical and dielectric experiments) corresponding to those of the immiscible components.

In compatible systems the polymer chains of both components are intermixed on a microscopic scale (i.e., on a sub-macromolecular scale). These systems also do not scatter light, thus limiting any phase separation to domains of less than ca. 1000 A. This intimate mixing influences the environment of each polymer chain. Generally, physical properties of the compatible polyblends reflect the presence of this modified homogeneous phase. A primary example is the existence of a single, calorimetrically determined Tg for compatible blends.[5] Verily, it is this characteristic of a single Tg that is the most common criterion for compatibility of polymers in the solid state.

The existence of compatible polymer pairs is the exception rather than the rule in the realm of blending. In a survey by Krause,[5] of ca. 300 reported blending

attempts (of various polymer pairs), under 40 were judged to be compatible at all blend compositions. It is obvious from this survey that polymer compatibility cannot be predicted or rationalized by simple criteria useful in the study of mixtures of small molecules. For example, the venerable rule of "like dissolves like" is not necessarily true for polymer pairs. For instance, two homopolymers as chemically similar as polystyrene and poly(α-methyl styrene) are incompatible. Other relatively dissimilar polymers such as polyacrylic acid and polyethylene oxide can form "pseudo-compatible" blends by means of specific interactions and complex formation over a limited composition range.[5]

C. Thermodynamics of Polymer Blending

The phenomenon of polymer mixing and compatibility can be investigated on various levels from the macroscopic (involving, e.g., thermodynamics or rheological studies) to the microscopic where segmental molecular interactions are considered. Attempts have been made to relate thermodynamic mixing theory to polymer compatibility based on structural features. Unfortunately, this effort has not met with a great deal of success with regard to general applicability.

The theoretical approach for the evaluation of the mixing process involving two polymeric species is analogous to that for small molecules. Generally, two chemical species are miscible if the free energy of mixing is ≤ 0. The free energy of mixing is defined by

$$\Delta G_m = \Delta H_m - T \Delta S_m \qquad (1)$$

ΔG_m = free energy of mixing

ΔH_m = enthalpy of mixing

ΔS_m = entropy of mixing

By an extension of the Flory-Huggins theory (developed for concentrated polymer-solvent systems), ΔG_m can be expressed in terms which represent molecular properties. In a mixture of poly-A and poly-B which have degrees of polymerization, x_A and x_B, volume fractions, ϕ_A and ϕ_B, and a polymer-polymer interaction paramater, χ_{AB}, the free energy of mixing can be expressed:[6]

$$\Delta G = \frac{RTV}{V_r} \{\chi_{AB}\phi_A\phi_B + \frac{\phi_A}{x_A}\ln\phi_A + \frac{\phi_B}{x_B}\ln\phi_B\} \qquad (2)$$

where V is the volume of the mixture and V_r is some reference volume (e.g., usually the polymer repeat unit volume). If both components have long chain lengths (i.e., x_A, x_B are large), the entropic contribution

$$\frac{\phi_A}{x_A}\ln\phi_A + \frac{\phi_B}{x_B}\ln\phi_B$$

will favor mixing but will be very small. The factor

determining compatibility will be the enthalpic term, $\chi_{AB}\phi_A\phi_B$. For a polymer pair to be compatible, this enthalpic term must be very small (or negative). For macromolecules of comparable molecular weights, the polymer-polymer interaction parameter can be written

$$\chi_{AB} = \frac{V_r}{RT}\{\delta_A - \delta_B\}^2 \qquad (3)$$

where δ_A and δ_B are the solubility parameters of poly-A and poly-B, respectively.* To achieve miscibility, the difference in solubility parameters must be minimal. Krause has estimated that in a binary polymer system where $x_A = x_B$ = 10,000 (i.e., molecular weight of ca. 100,000), the critical limit for the solubility parameter difference is 0.11. Therefore, polymer pairs whose solubility parameters differ by more than 0.11 are predicted to be incompatible.

D. PPO/Polystyrene Blend Systems

The polymer blend which is being investigated in this study is comprised of modified polystyrenes and poly(2,6-dimethylphenyleneoxide) (also known as poly (2,6-xylenol)), generally referred to as PPO.[7] The

---

* This theory is not valid for polymer pairs which exhibit specific interactions (e.g., hydrogen bonding) which result in exothermic mixing processes (i.e. $\Delta H_m < 0$).

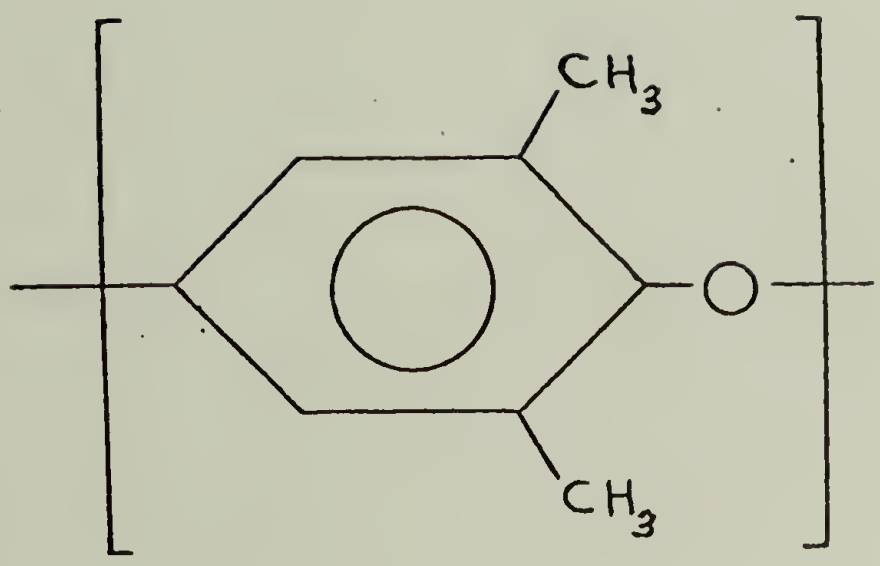

Figure 1. Repeat unit of poly(2,6-dimethylpheneylene oxide) (PPO)

repeat unit of PPO is shown in Figure 1.

Basic studies of the blend system PPO/(atactic polystyrene)[8] were performed by MacKnight et al., in which the calorimetric, dielectric and dynamic mechanical properties were ever so thoroughly investigated.[9,10] These studies revealed that this polymer pair formed a compatible system. The criterion for this compatibility classification was that the blends exhibited a single glass transition at a temperature which was intermediary to those of the components at all blend compositions, with the value of the Tg dependent on the ratio of components. Additionally, blend samples formed clear films; this homogeneity substantiated their classification as compatible.

In the cases of the calorimetric and dielectric studies the classification of compatibility was unambiguous.[10] However, for the dynamic mechanical experiments, in addition to the main relaxation (corresponding to the compatible blended phase), relaxations were also detected at temperatures corresponding to transitions of the pure components. This characteristic was attributed to component rich phases within the compatible system.

Preliminary studies for this present investigation indicated that PPO and poly(para-chlorostyrene) were

incompatible as determined by calorimetric and dielectric relaxation techniques. The investigation originally was intended to synthesize random copolymers of styrene and para-chlorostyrene of various compositions and investigate the compatibility characteristics of these copolymers with PPO.

In the early stages of the project, similar work by A.R. Shultz [11] was revealed in which the compatibility of the above system was studied as a function of the chemical composition of the copolymer. His research indicated an abrupt shift from compatibility to incompatibility as the p-chlorostyrene content of the copolymer exceeds a critical limit of ca. 64 (mole)%.

The research described in this thesis investigates the blend system PPO/ poly(styrene co-parachlorostyrene). By observing thermal transitions, dynamic mechanical and dielectric relaxations and blend morphologies, attempts have been made to elucidate factors influencing the system's compatibility characteristics. Emphasis has been placed on the dielectric relaxation experiments as that technique is the most specific in investigating molecular interactions within the blend system.

E. Dielectric Analysis of Molecular Properties

Previously, compatibility of polymer blends have

been studied by dynamic relaxation techniques (e.g., dielectric,[9] dynamic mechanical [10] relaxations). However, these techniques have generally been limited to the detection of relaxations as a means to assess the compatibility of polymer blends. Additionally, however, dielectric relaxation experiments offer the advantage that they can be utilized to relate macroscopic (e.g., dielectric constant) and microscopic properties (e.g., environment of dipoles. Evaluation and comparison of the environment of dipoles of polymer chains can elucidate differences between compatible and incompatible blends on a microscopic scale. This information can be obtained by analysis of the dipole orientation correlation factor of the Frohlich equation (development in Appendix II):

$$g = \frac{9kT}{4\pi N \mu_o^2} \cdot \frac{(2\varepsilon_R + \varepsilon_U)(\varepsilon_R - \varepsilon_U)}{\varepsilon_R(\varepsilon_R + 2)^2} \qquad (4)$$

g= dipole orientation correlation factor
k= Boltzmann's constant
T= absolute temperature
N= number of dipoles per cm^3
μ_o = dipole moment of an isolated dipole unit
ε_R, ε_U = relaxed, unrelaxed dielectric constants

Considering short range interactions, the dipolar environment of a dipole, i, is related to g by:

$$g = 1 + z\,\overline{\cos\,\gamma} \qquad (5)$$

where $\overline{\cos\gamma}$ is the average cosine value of the angle, γ, between dipole 1 and its z nearest neighbors.

For an ideal freely rotating polymer chain with dipoles a tetrahedral angles to the chain (e.g., polyparachlorostyrene dipole), the g value is calculated to be 0.92.[12] Experimental studies indicate that g is in the range of o.65 to 0.80.[13] This reduction of the correlation factor has been attributed to internal barriers to rotation of the macromolecules. From these results and Equation 5 we see that cosγ must be negative; as z decreases, g will increase to the theoretical maximum. Therefore, as the effective dipole concentration of the system decreases, the number of nearest neighbors (z) decreases, resulting in an increase in the orientation correlation factor. This effect has been observed in a series of random copolymers of parachlorostyrene and styrene by solution dielectric studies;[14] as the number of chlorostyrene dipole units per chain decreases, the correlation factor increases. Analogously, for any of these copolymers in solution, g increases as the solution concentration becomes more dilute.

The dipole orientation correlation factor is also sensitive to the configuration of the macromolecule in solution. Studies on polyparachlorostyrene related the

correlation factor to chain expansion in solution. By coupling viscosity and dielectric measurements, it was shown that the g factor increases as the quality of the solvent increases (i.e., as the chain expands, g increases).[15] For dilute solutions intrinsic viscosity and molecular size is related by:[16]

$$[\eta] = \frac{\Phi \langle h^2 \rangle^{3/2}}{M} \qquad (6)$$

$[\eta]$ = intinsic viscosity

Φ = Kirkwood-Riseman empirical hydrodynamic constant
h = radius of gyration of the polymer chain
M = molecular weight

For linear polymers $\langle h^2 \rangle$ is related to the mean squared end to end distance, $\langle r^2 \rangle$, by:[17]

$$r^2 = 6 \langle h^2 \rangle \qquad (7)$$

Therefore, for a given polymer (M being constant), r is proportional to h which varies as the cube root of the intrinsic viscosity:

$$r \propto g \propto [\eta]^{1/3} \qquad (8)$$

For polyparachlorostyrene, through a series of solvents in which the intrinsic viscosity increased from 0.57 to 1.25, the dipole orientation correlation factor increased from 0.55 to 0.77.[15] This variation in vis-

cosity corresponds to an increase of 30% in the chain end to end distance which results in a similar increase in the dipole orientation correlation factor.

C H A P T E R II

EXPERIMENTAL AND COMPUTATIONAL PROCEDURES

A. Polymer Synthesis

Copolymers of styrene and parachlorostyrene (designated PCS copolymers) of suitable compositions were prepared by free radical polymerization. The radical copolymerization curve for this system (solid line in Figure 2) reveals that these two monomers deviate only slightly from an "ideal" copolymerization pair [18] (i.e., monomers which would be randomly placed in the polymer chain, represented by a dashed line in the same figure). The random, atactic nature of the monomer placement has been experimentally verified by polarization studies of similar polymers.[20] As a result of the nature of the reaction kinetics of this system, it is possible to synthesize a series of random, atactic copolymers of various controlled compositions.

Monomeric styrene and p-chlorostyrene were purchased from Polysciences, Inc. and purified by removal of the inhibitor (tert-butylcatechol) by repeated washings with 0.1 M aqueous solution of NaOH and drying over molecular sieves.

Mixtures of the monomers of suitable proportions were combined with ca. 30 volume percent toluene; this

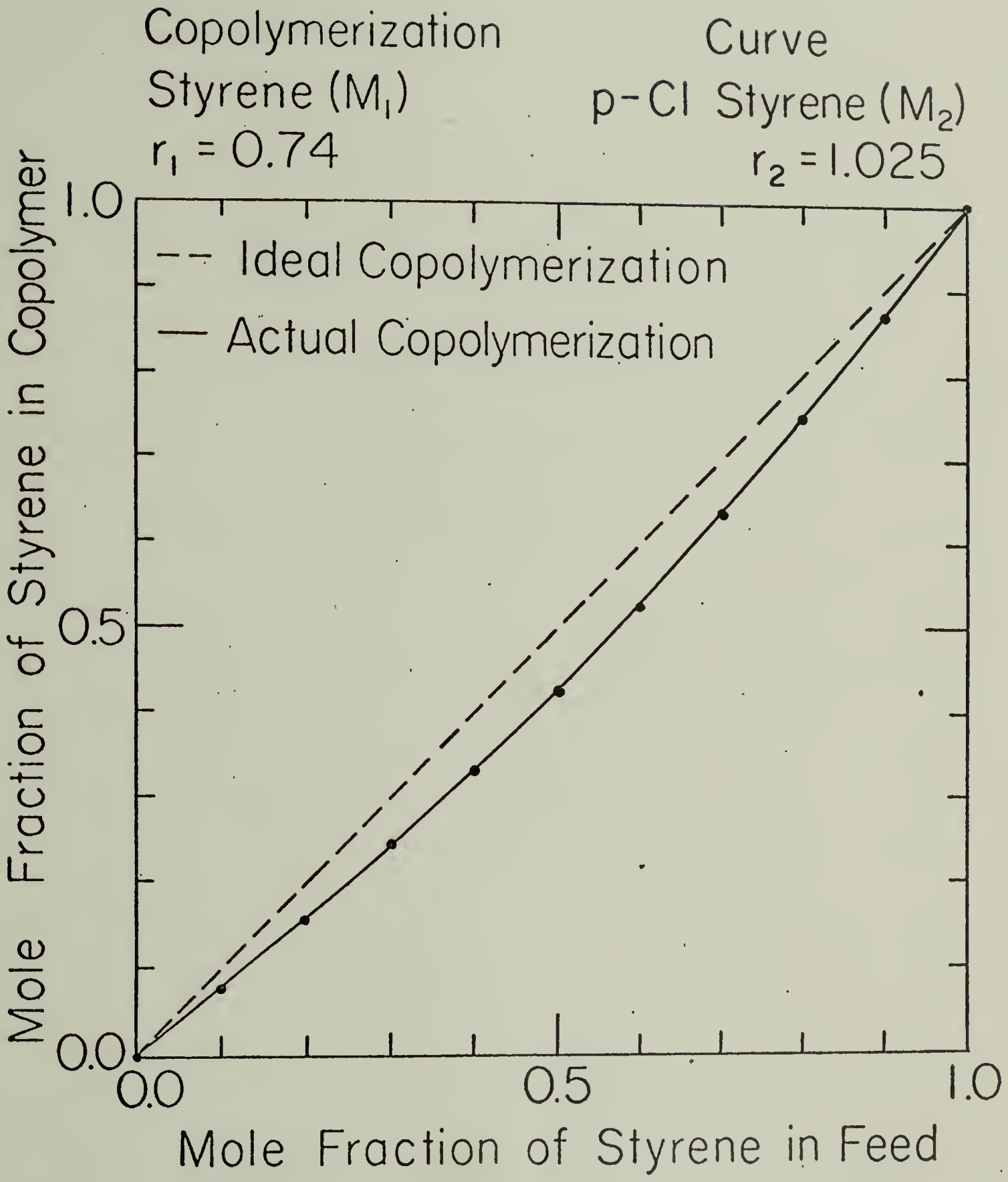

Figure 2. Copolymerization curve for styrene and parachloro-styrene.[18,19]

solution was bubbled with nitrogen gas for one hour to remove dissolved oxygen which inhibits radical reactions.

The reaction vessel consisted of a 250 ml round bottom flask equipped with a mechanical stirrer, thermometer, mantle heater, reflux condenser and addition dropping funnel. During the course of the reaction, the interior of the apparatus was subjected to a constant flowing blanket of nitrogen.

For the radically initiated reactions a toluene solution of benzoyl peroxide (weight of benzoyl peroxide was o.1% of total monomer weight) was added dropwise to the reaction mass which was maintained at 75°C. Thermal polymerizations were carried out by maintaining the reaction temperature at 110°C (i.e., the boiling point of toluene). In all polymerizations toluene was added to the system to limit the viscosity to a level at which mixing and heat transfer were acceptable.

The copolymerizations were reacted for approximately 24 hours; in all cases yields were 60 to 70%. The viscous reaction products were diluted with toluene to 500 ml total volume, filtered through sintered glass filters and added dropwise to a 3.5 litre volume of vigorously stirred methanol, in which the polymeric product precipitates from the nonsolvent alcohol. The precipi-

tated product was isolated by filtration and dried in vacuo for ca. 48 hours at 100°C. This procedure of dissolution, filtration, precipitation and drying was repeated to further purify the product.

Elemental analysis for chlorine was performed on the reaction products to determine the relative p-chlorostyrene content of the copolymers. Analysis of the reproducibility of the analytic technique revealed that the composition estimates are accurate to ± 1 mole per cent of parachlorostyrene content.

The molecular weight characteristics of the PCS polymers were determined by gel permeation chromatography. The synthesized PCS copolymers were essentially constant in molecular weight properties (e.g., molecular weights and molecular weight distributions) as exhibited in Table I. Other polymeric materials used in this study included high molecular weight, additive free PPO (courtesy of General Electric Co.) and atactic polystyrene (provided by Montsanto Co.).

Compression molding of the samples was performed on the dried precipitate by a typical molding cycle which has been found to produce the most consistent, bubble-free films. An excess of dried polymeric product is placed in the annulus of a spacer of the desired thickness and enclosed between aluminum foil sheets

Table I. Characterization data for PCS copolymers.

Polymer	Initiation mechanism	p-Cl styrene content (mole percent)	M_n (x 10^{-4})	M_w/M_n
PCS-1	Radical	100	12	2.8
PCS-3	"	68	11	2.1
PCS-5	"	47	9.2	2.5
PCS-6	Thermal	60	10	2.2
PPO	-	-	(M_v =) 2.3	

between the heated platens of the molding press without pressure. When the platen temperature well exceeds the Tg of the polymer (e.g., at ca. 200°C for the pure PCS polymers), platen pressure is increased to 10,000 pounds. The temperature and pressure are maintained at these levels for approximately 45 minutes, after which the sample is slowly cooled to room temperature under pressure. To inhibit oxidative degradation, a flowing nitrogen blanket envelpped the platen area whenever its temperature exceeded 100°C.

Difficulties were encountered in making transparent copolymer samples. A certain turbidity was present in both compression molded and solution cast films. This cloudiness could not be eliminated by typical physical purification techniques (e.g., filtration of polymer solutions through carbon black adsorbants, repeated precipitations in methanol, prolonged extraction of the polymeric product with hot methanol). An independent investigation of this problem indicates that the turbidity of the solid polymer was probably caused by the presence of trace amounts of silicone grease which contaminated the polymer in the synthesis step.[21]

B. Preparation of Polymer Blends

Blends of the individual PCS copolymers and PPO

were prepared by coprecipitation from toluene solutions. Dilute cosolutions (2% (g/ml) of total polymer weight per solution volume) of specific compositions were prepared. All solutions were clear, regardless of the fact that some of the resultant blends were incompatible. These solutions were filtered and added dropwise to a large (15X) excess of vigorously stirred methanol. The precipitates were isolated by filtration, air dried for 24 hours and vacuum dried at 100°C for an additional 48 hours.

Some samples were also blended by freeze-drying of dilute cosolutions. Benzene solutions (2% weight/ volume) were filtered, cooled to ca. 10°C (slightly above the freezing point of benzene) in an airtight brass container; the solution was then quickly quenched to -78°C in a dry ice/isopropanol bath. A vacuum was applied to the system, and the vacuum chamber was maintained at a temperature of 0°C in an ice/water bath. When ca. 95% of the benzene was sublimed from the polymer system, the temperature of the vacuum chamber was slowly raised to room temperature and maintained under vacuum for at least 12 hours.

Compression molded samples were formed from the dry coprecipitate or freeze-dried material utilizing a molding cycle as described for the PCS polymers except

that the molding temperature was maintained at ca. 280°C for the blends (or for pure PPO).

C. Calorimetric Studies

Glass transition temperatures (Tg's) of the molded samples were obtained by calorimetric analysis on a Perkin-Elmer DSC-2 differential scanning calorimeter. An indium reference sample (melting point of 156°C) was used for the calibration reference. A uniform heating rate of 20°C per minute was employed for all measurements. For all samples the Tg is taken to be the temperature of the intersection of the baseline and the rising edge of the transition endotherm (i.e., the onset of the transition) as shown in Figure 3 which is the thermograph of PPO.

D. Dielectric Analysis

Measurements of dielectric properties were performed on a General Radio 1620-A Capacitance Measuring Assembly. The instrument was used in the dissipation factor mode in which the electronic bridge creates a circuit with equivalent dielectric properties of the test sample. This equivalent circuit is described by a variable resistance and capacitance in series as shown schematically in Figure 4. The dielectric prop-

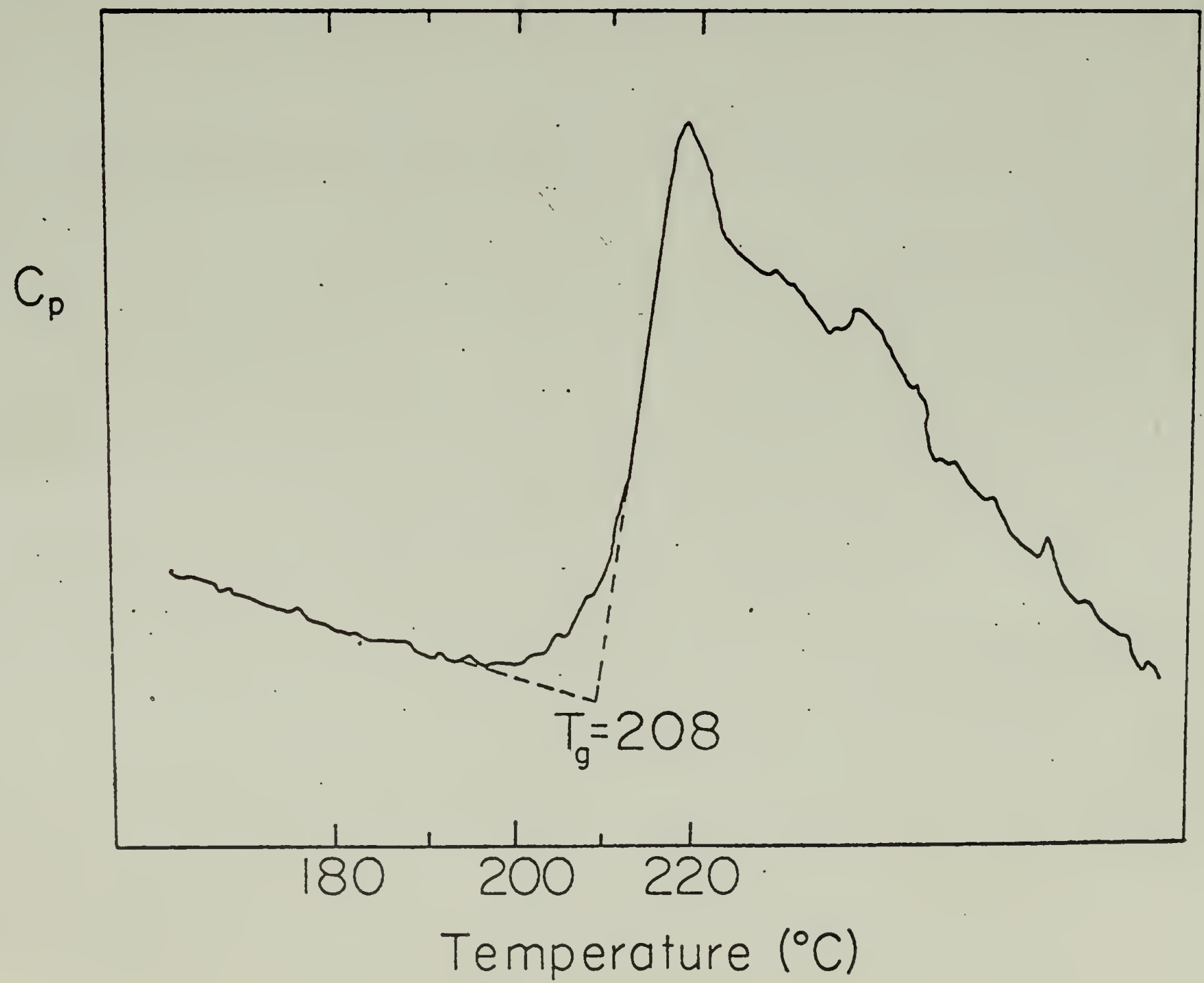

Figure 3. Typical DSC trace (PPO) indicating method of Tg designation.

erties of the sample can be calculated from sample dimensions and the instrument read-out values of the dissipation factor and the capacitance using the relationships of Equations (9) through (12).[22]

$$\tan \delta_e = R_x C_x \omega \tag{9}$$

$$\varepsilon' = \frac{C_x}{C_o (1 + \tan^2 \delta_e)} \tag{10}$$

$$\varepsilon'' = \frac{C_x \tan \delta_e}{C_o (1 + \tan^2 \delta_e)} \tag{11}$$

$$C_o = \frac{A \varepsilon_o}{d} \tag{12}$$

$R_x C_x$ = dissipation factor reading

C_x = capacitance reading

d = sample thickness
A = capacitor electrode area
ε_o = capacitance of air

ω = frequency (in KHz)

The terms ε' and ε'' represent the real and imaginary (loss) components, respectively, of ε^*, the complex dielectric constant as in the relationship:

$$\varepsilon^* = \varepsilon' - i\varepsilon'' \tag{13}$$

Measurements of the dielectric properties of the polymer blends were conducted over a frequency range of

Figure 4. Schematic diagram of series approximation for dielectric properties evaluation.

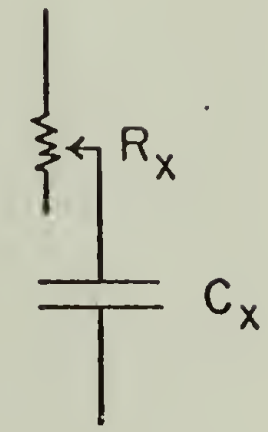

Figure 5. Sample grips for Vibron shear mode.

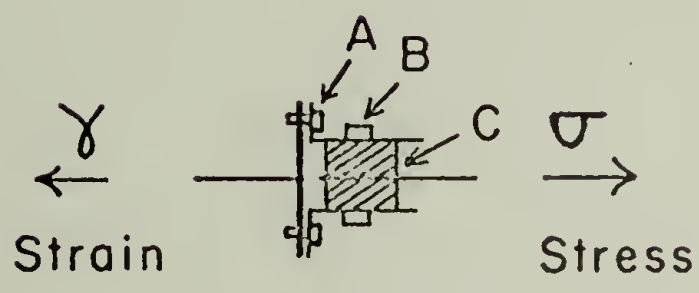

Adjustable side plates grip the sample blocks (C) by means of tightening screws (A) and compression clip (B).

200Hz to 10 KHz and a temperature range of 25°C to 250°C. The sample cell consisted of a parallel plate assembly equipped with a micrometer to monitor plate separation (i.e., sample thickness) and a grounded third terminal guard ring to eliminate fringing electrical fields. Temperature control was achieved by allowing the cell to reach thermal equilibrium with a variable temperature, thermostated oil bath. To prevent oxidative degradation of the sample, a nitrogen flow was maintained through the cell. The electrical circuitry permitted the measurement of the direct current conductivity of the sample at each temperature; the correction for this conductive effect became significant at temperatures above the Tg of the sample.

E. Dynamic Mechanical Studies

Measurements of dynamic mechanical properties were performed on a Toyo Rheovibron DDV II-B Direct Reading Dynamic Viscoelastometer. Measurements were made in the shear mode in order to traverse high temperature, multiple transition regions in which extended tensile stress might lead to loss of the sample's shape and mechanical integrity. Two equal size blocks of the sample (ca. 0.25 x 0.25 x 0.05 inches) were placed in special shear grips represented in Figure 5.

From the instrument read-out of dynamic force and tan δ and knowledge of the sample size, the mechanical properties were calculated by Equations (14) through (17):[23]

$$G^* = \frac{L}{XY\ (D-K)} \times 10^9 \text{ dyne/cm}^2 \qquad (14)$$

$$G' = G^* / (1 + \tan^2 \delta) \qquad (15)$$

$$G'' = (G^* \tan \delta) / (1 + \tan^2 \delta) \qquad (16)$$

$$G^* = G' + i\, G'' \qquad (17)$$

X,Y = length, width of sample (cm)
L = thickness of sample (cm)
D = dynamic force reading
K = instrument displacement error constant

Analogous to the dielectric properties, G' and G" are the real (storage) and imaginary (loss) components of G*, the complex shear modulus.

Samples were measured in a temperature range of 25° to 250°C and a frequency range of 3.5 to 110 Hz. The test temperature was increased at a rate of about 1°C per minute. The sample was subjected to a flowing nitrogen blanket throughout the run.

F. Electron Microscopy

Transmission electron micrographs were taken of

fracture surface replications of the polymer blends. Samples were fractured at a temperature above the Tg of the PCS component but below that of PPO (i.e., at ca. 170°C) to maximize the difference in fracture properties of the two components if they are segregated into two phases. Replicas of the fracture surfaces were prepared on carbon supports using gold-palladium shadowing.

Scanning electron micrographs were also taken of the blend fracture surfaces. Samples were fractured as for the transmission samples above; they were then decorated with gold coating.

C H A P T E R I I I

RESULTS AND DISCUSSION

A. Calorimetric Studies

Analysis of the blends of PPO and PCS copolymers by DSC yieldied information regarding their thermal properties, especially glass transition temperatures. All polymers used in this study proved to be amorphous materials with one glass transition above room temperature.

Characteristic DSC thermographs of the PPO-PCS polymer blends are displayed in Figures 6 through 11. Figures 6,7 and 8 show DSC traces for blends of PPO and PCS-3 of various compositions. It is apparent that each of these blends exhibit two distinct Tg's as designated in the figures. By definition, therefore, blends of PPO and PCS-3 are incompatible. Figures 9, 10 and 11 are thermographs of PPO/PCS-5 blends. These traces obviously differ from the PPO/PCS-3 system in that only one Tg exists for each polymer blend. The existence of this sole intermediary Tg indicates a compatible blend system.

Figure 12 summarizes the calorimetric measurements for the blends of the various PCS copolymers and PPO, showing the dependence of Tg on blend compo-

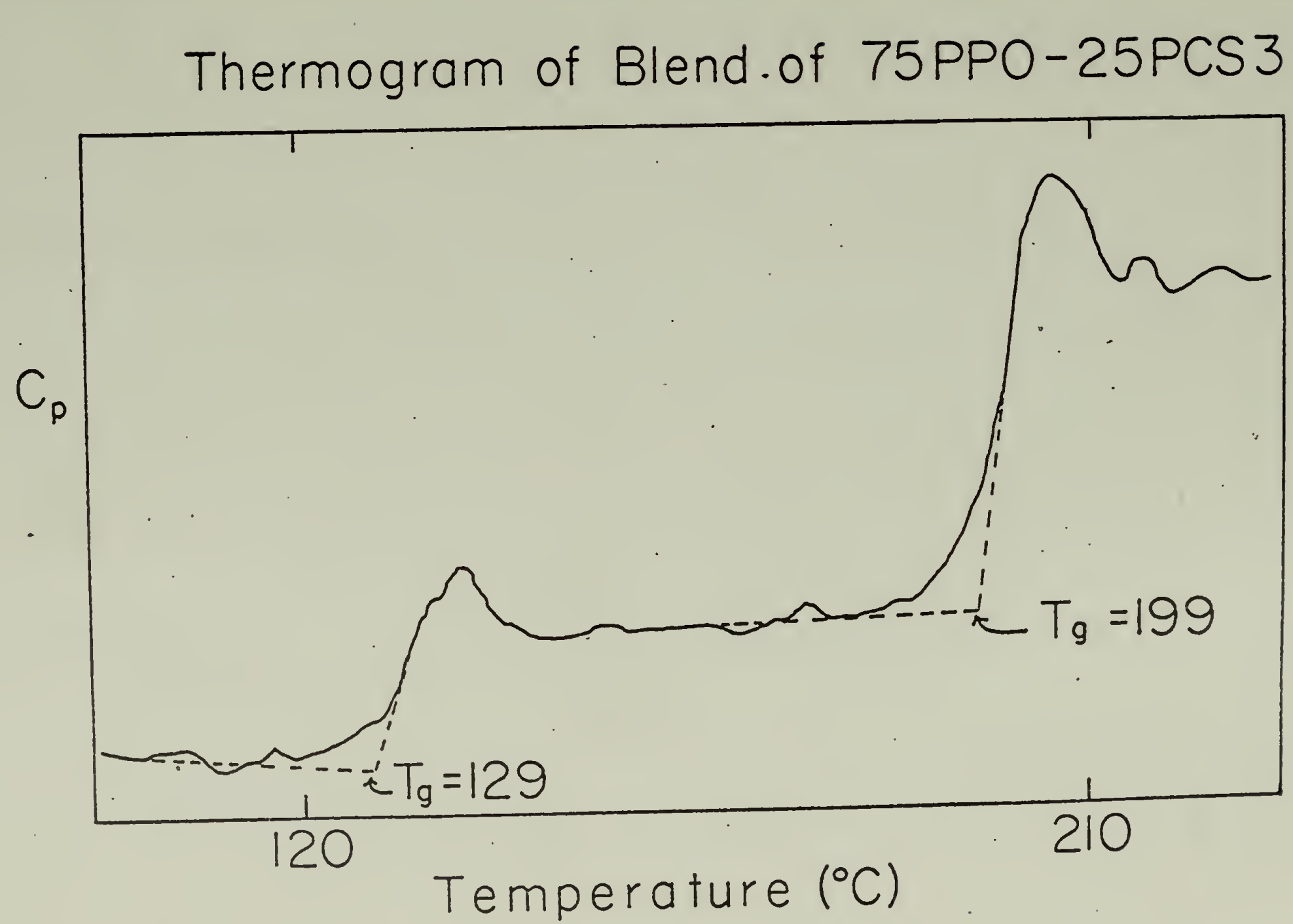
Thermogram of Blend of 75PPO-25PCS3
C_p
T_g =129
T_g =199
120
210
Temperature (°C)

Figure 8.

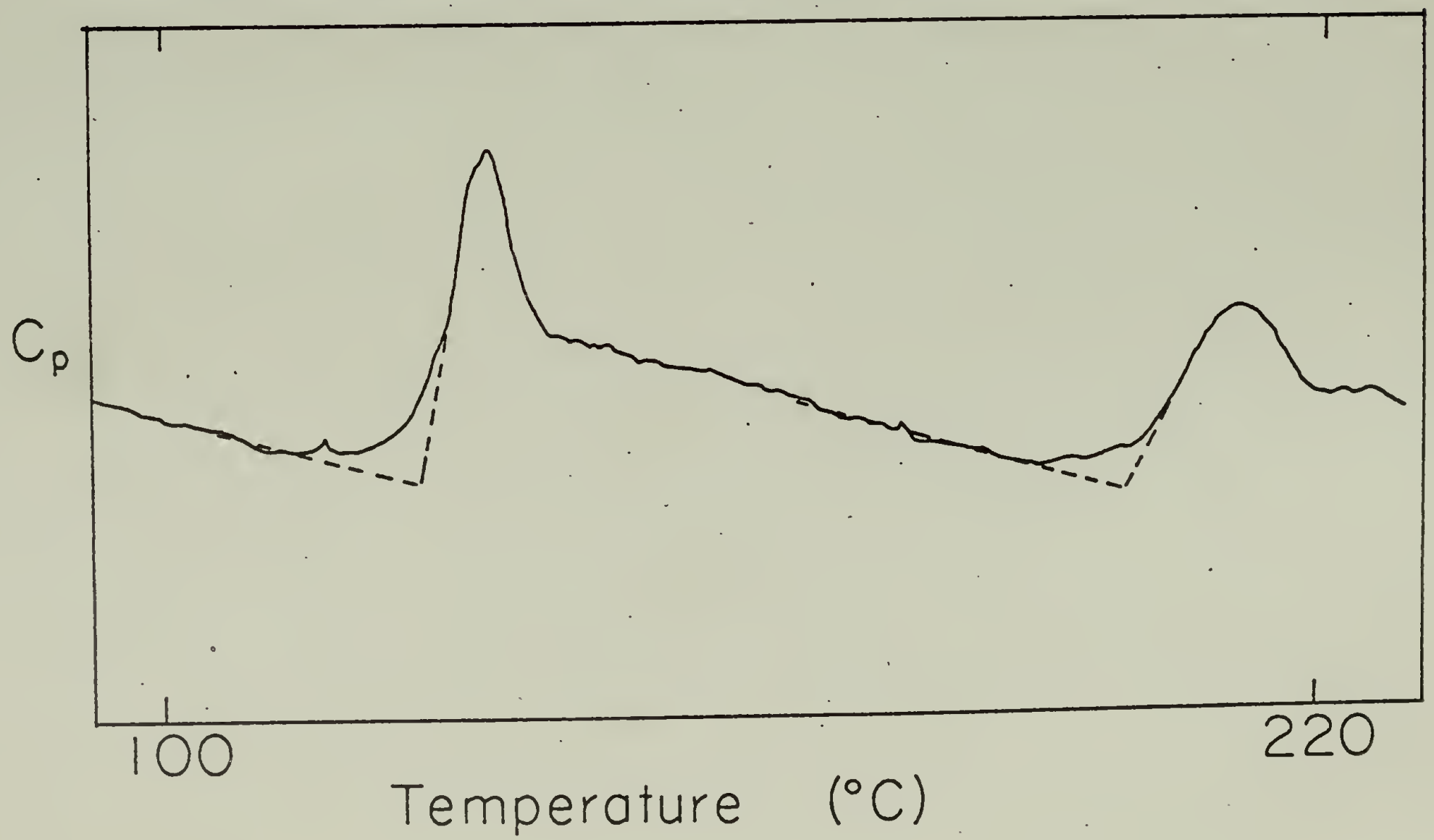
Thermogram of Blend of 50 PPO-50 PCS 3
Cp
100
220
Temperature (°C)

Figure 7.

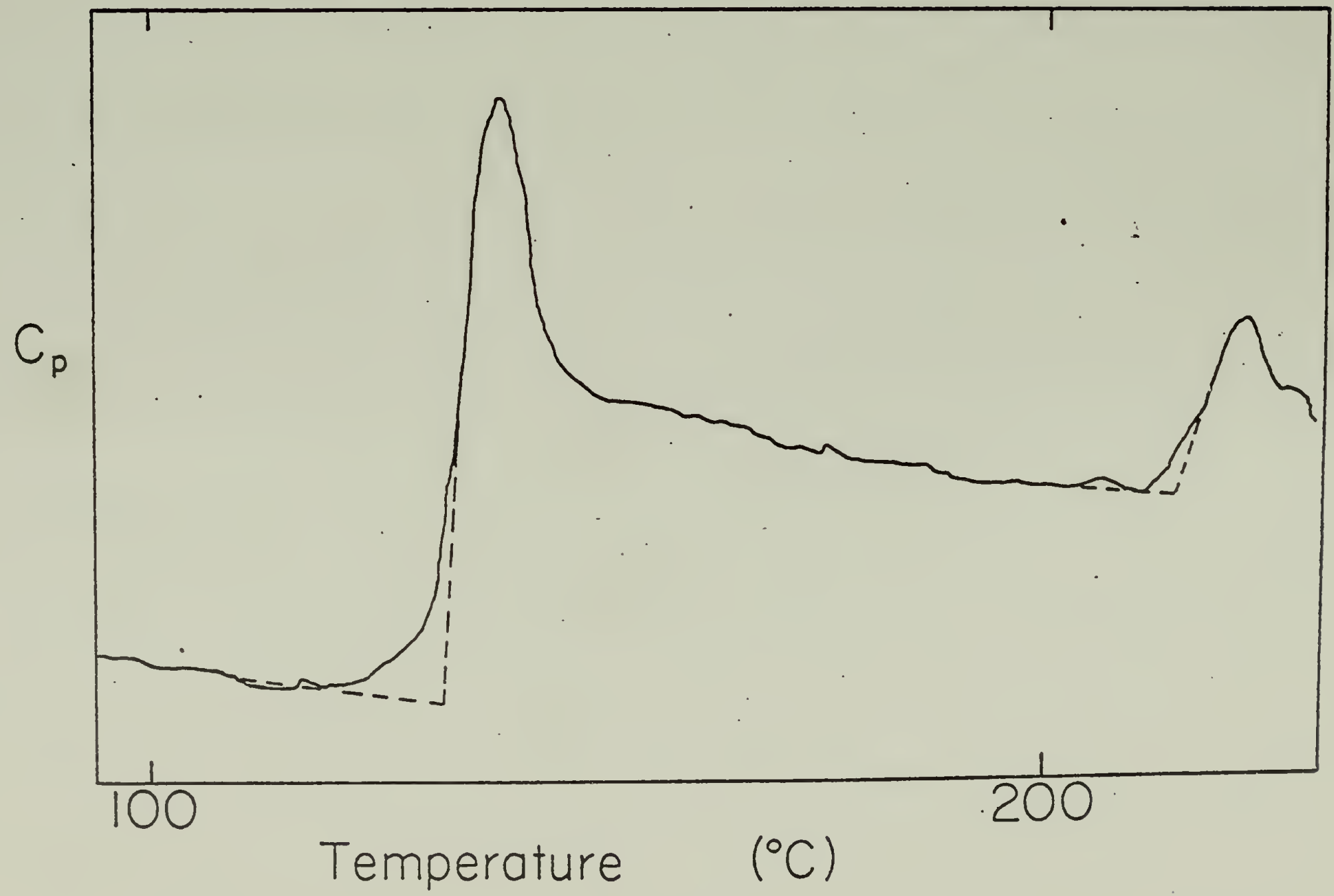
Thermogram of Blend of .25PPO-75PCS3
C_p
100
200
Temperature (°C)

Figure 6.

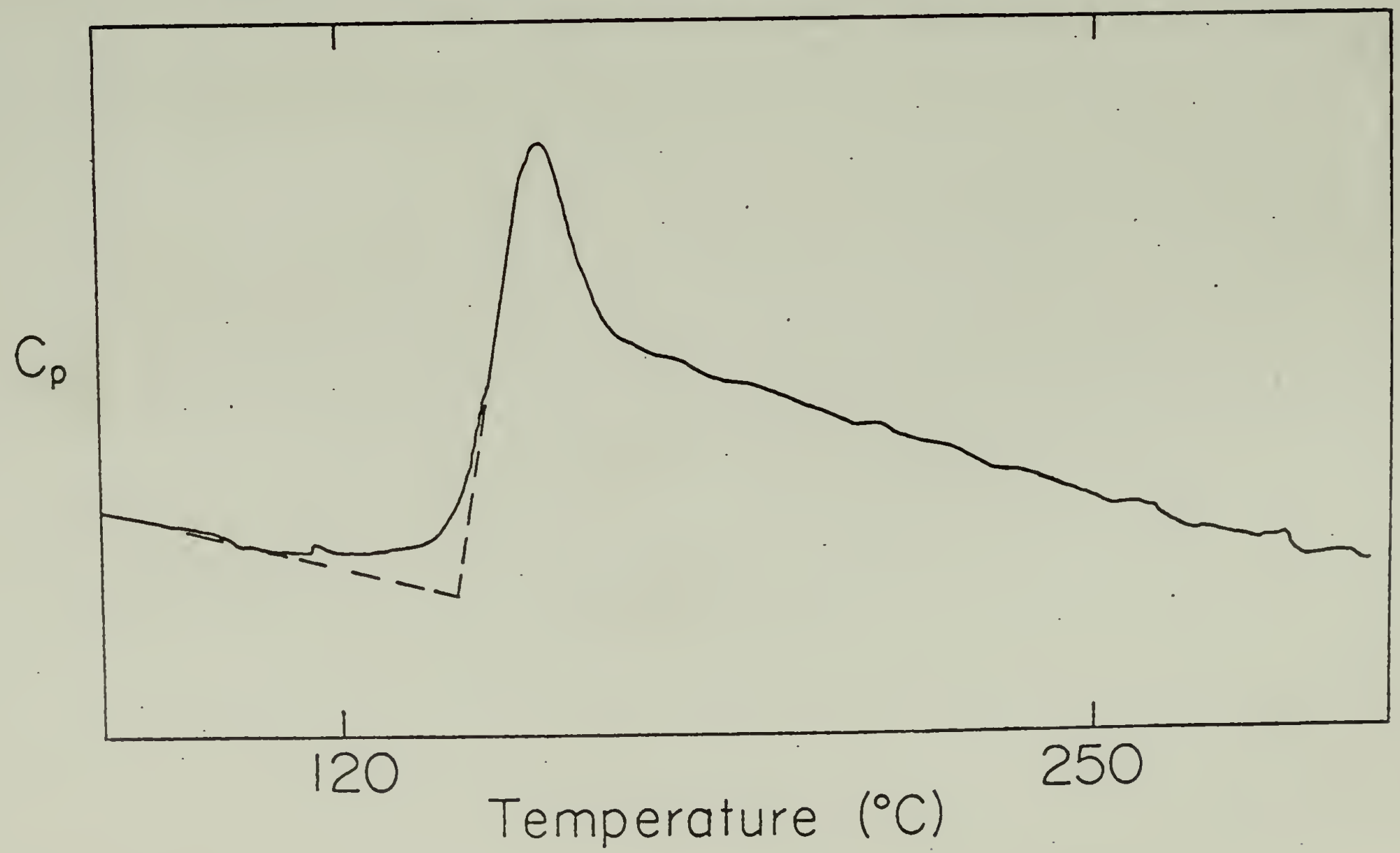
Thermogram of Blend of 25PPO-75PCS5
C_p
120
250
Temperature (°C)

Figure 9.

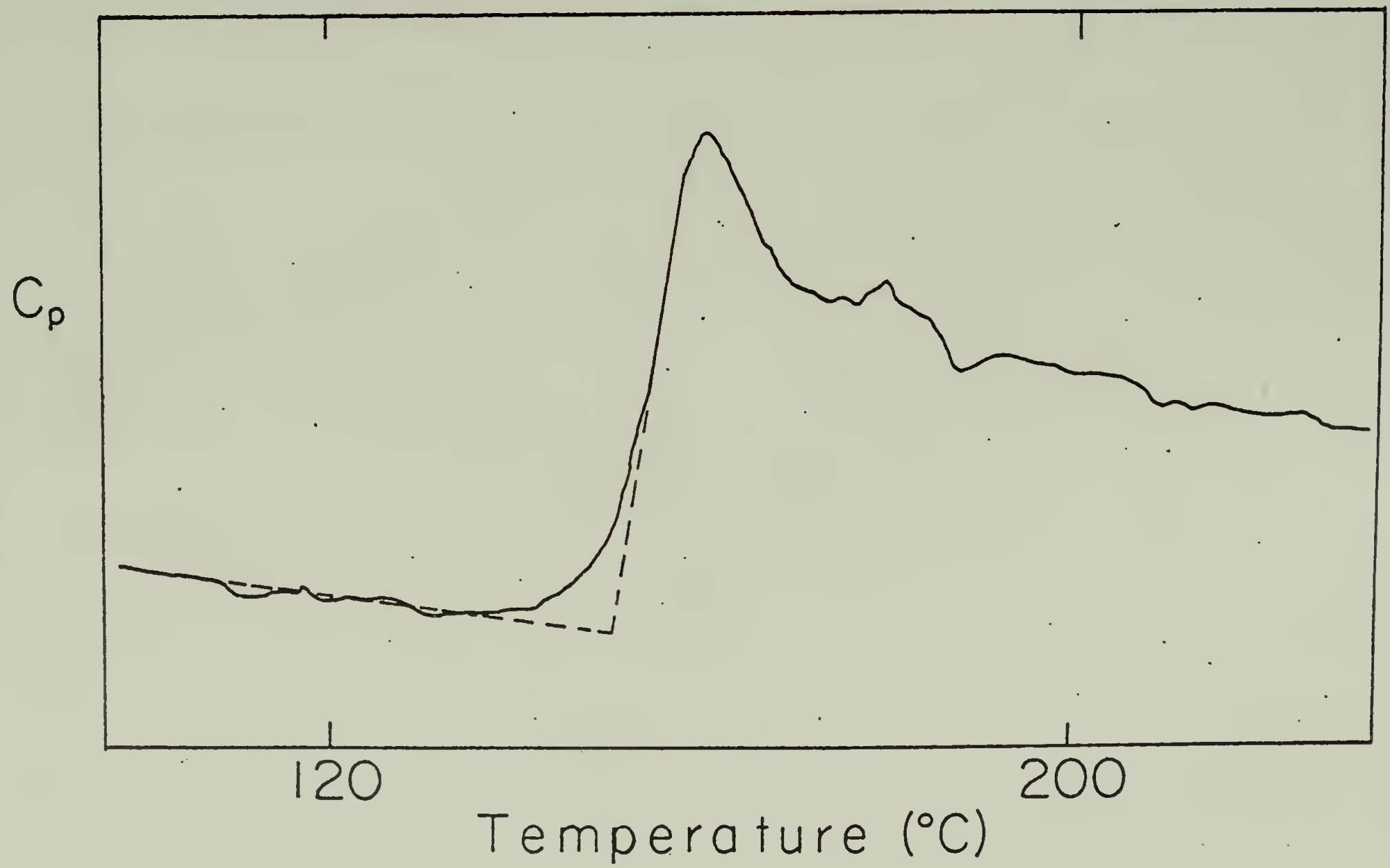
Thermogram of Blend of 50PPO-50PCS5
C_p
120
200
Temperature (°C)

Figure 10.

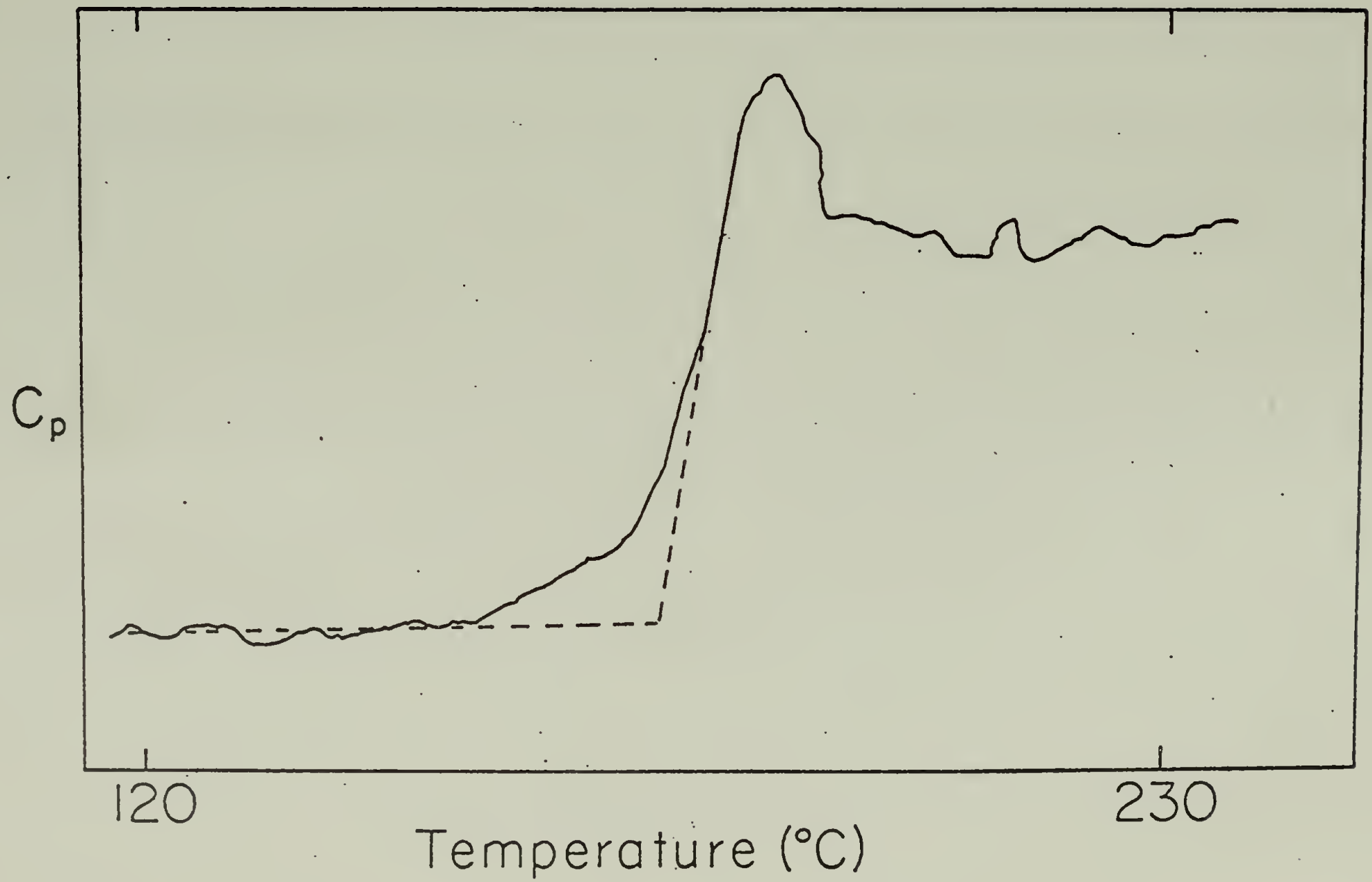
Thermogram of Blend of 75PPO-25PCS5
C_p
120
230
Temperature (°C)

Figure 11.

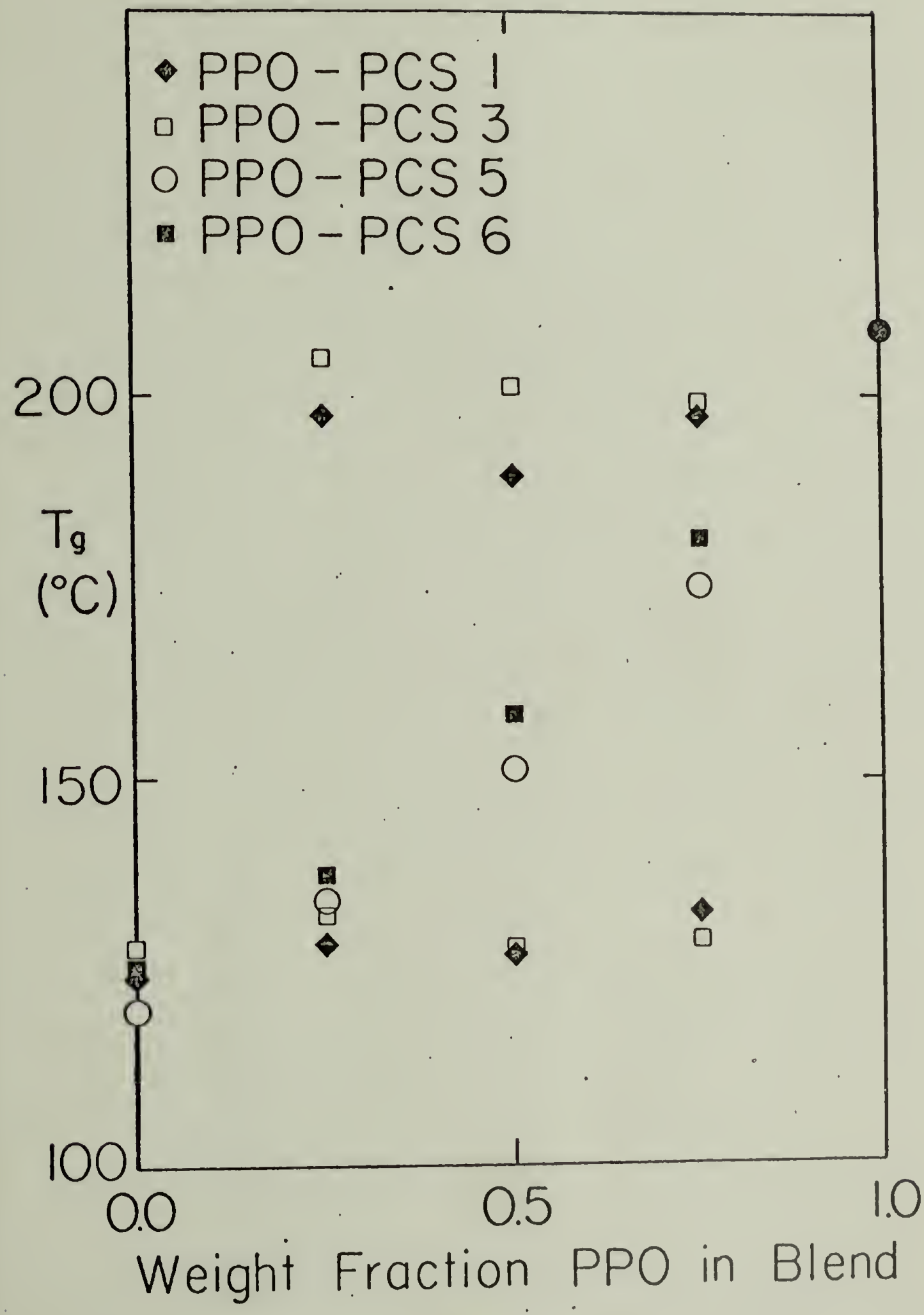

Figure 12. Compositional dependence of Tg for PPO/PCS blends.

sition. It is immediately apparent that blends of PPO and PCS-1 or PCS-3 are incompatible as each blend exhibits two distinct Tg's at each blend composition. These Tg's are essentially composition independent and occur at temperatures corresponding to those of the pure components of the blend. There is some evidence for a slight elevation of the lower Tg above that of the pure PCS component and a slight depression of the upper Tg below that of pure PPO, but no trends can be discerned.

The behavior of the blends of PPO with PCS-5 or PCS-6 differ from that of the above incompatible blends. Mixtures of PPO/PCS-5 or PPO/PCS-6 form compatible blends with a single Tg intermediary to those of the pure components. The composition dependence of the Tg is quite similar to that exhibited by the PPO/ polystyrene blend system.[9]

These results indicate that there is not a continuous variation of compatibility as the chemical composition of the polystyrene component changes (i.e., as the parachlorostyrene content increases in the PCS copolymer series). Rather, there is an abrupt shift from compatible to incompatible behavior as the parachlorostyrene content of the blended copolymer exceeds a critical limit. This critical limit has been established by

Shultz as 64 mole percent parachlorostyrene.[11]

With regards to compatibility characteristics, it is significant to note that, for any PCS copolymer, the compatibility properties are consistent over the entire composition range (e.g., all compatible mixtures are compatible at all blend ratios).

B. Electron Microscopy

Electron microscopy provided complementary evidence for the compatibility studies of the PPO/PCS blends. In all cases where incompatibility is indicated by calorimetry, large scale (i.e., 5-10 μ) phase separation is observed. Figures 13a, b and c display fracture surface replications (transmission mode) of blends of PPO and PCS-1. When PPO is the minor blend component (i.e., 25% PPO in Figure 13a), the predominant feature of the micrograph is the ridge-like structure which appears to be an extended ductile fracture surface of a layer of PPO embedded in the PCS-1 continuous phase. (N.B.,The ductile nature of the fracture of the PPO phase reflects the fact that the fracture was performed above the Tg of the PCS but below that of the PPO). As the portion of PPO in the blend increases to 50% (Figure 13b), the PPO domains tend toward larger aggregations embedded in the PCS-1

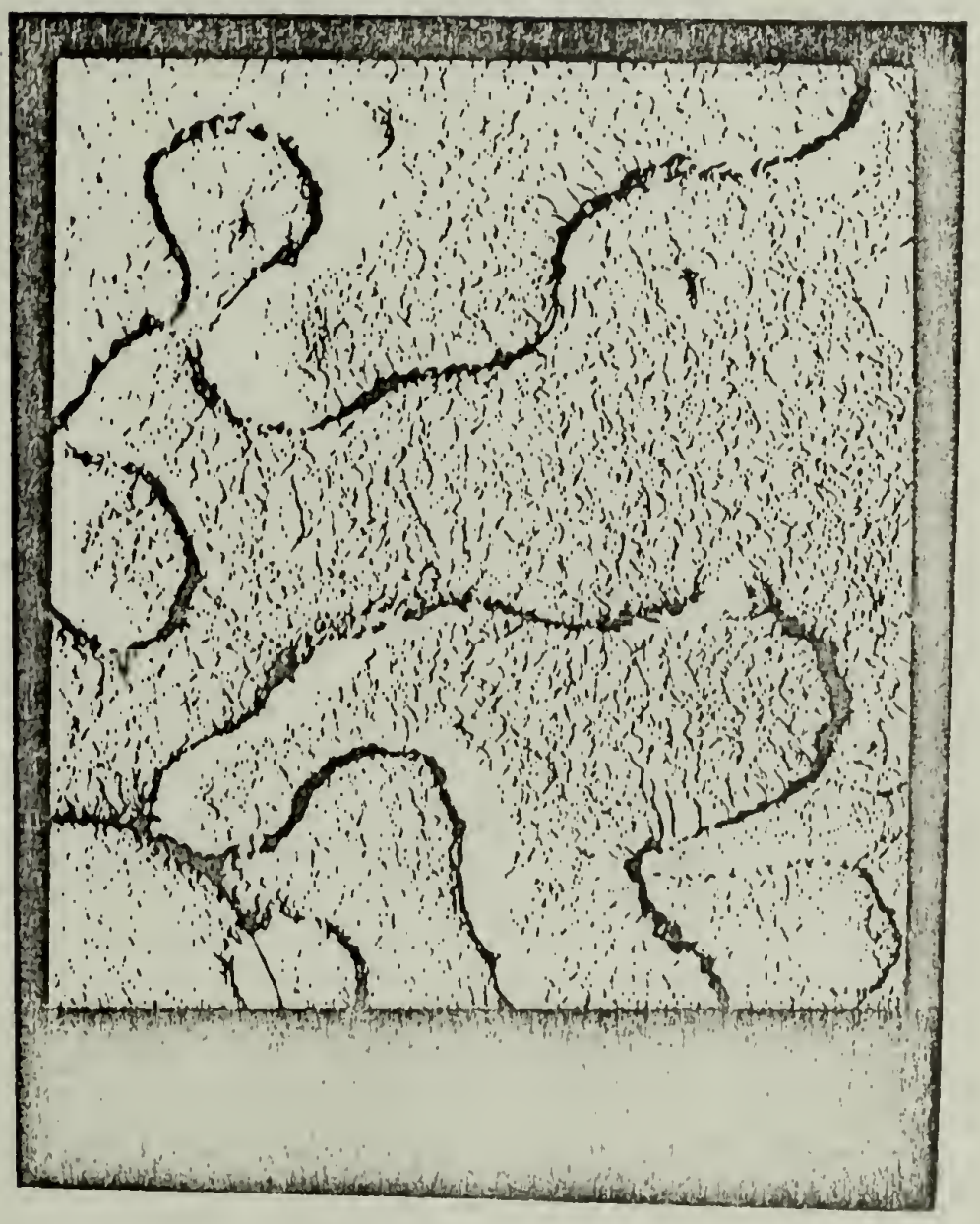

5μ

Figure 13a. Transmission electron micrograph, 25/75:PPO/PCS-1.

Figure 13b. Transmission electron micrograph 50/50:PPO/PCS-1

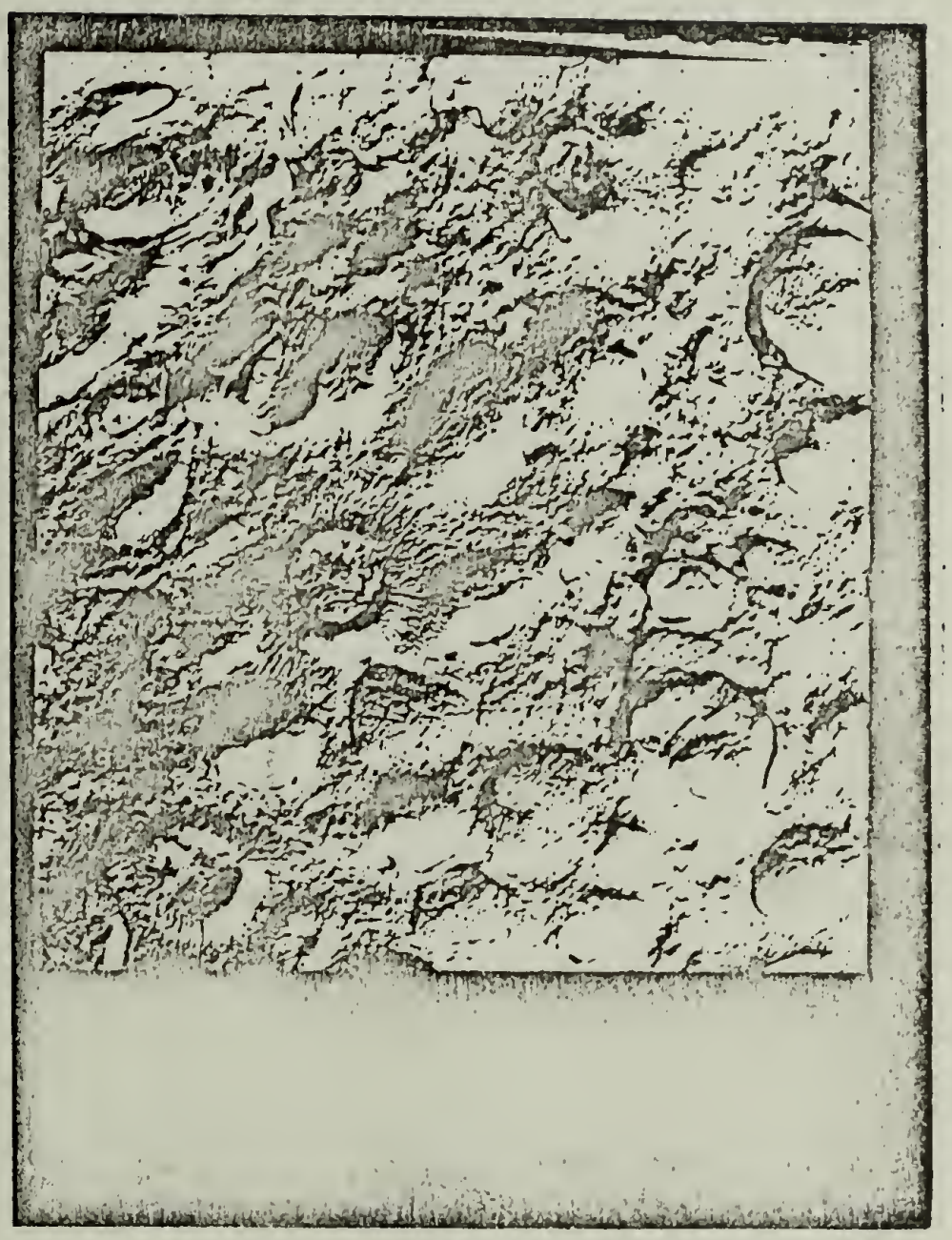

Figure 13c. Transmission electron micrograph, 75/25:PPO/PCS-1.

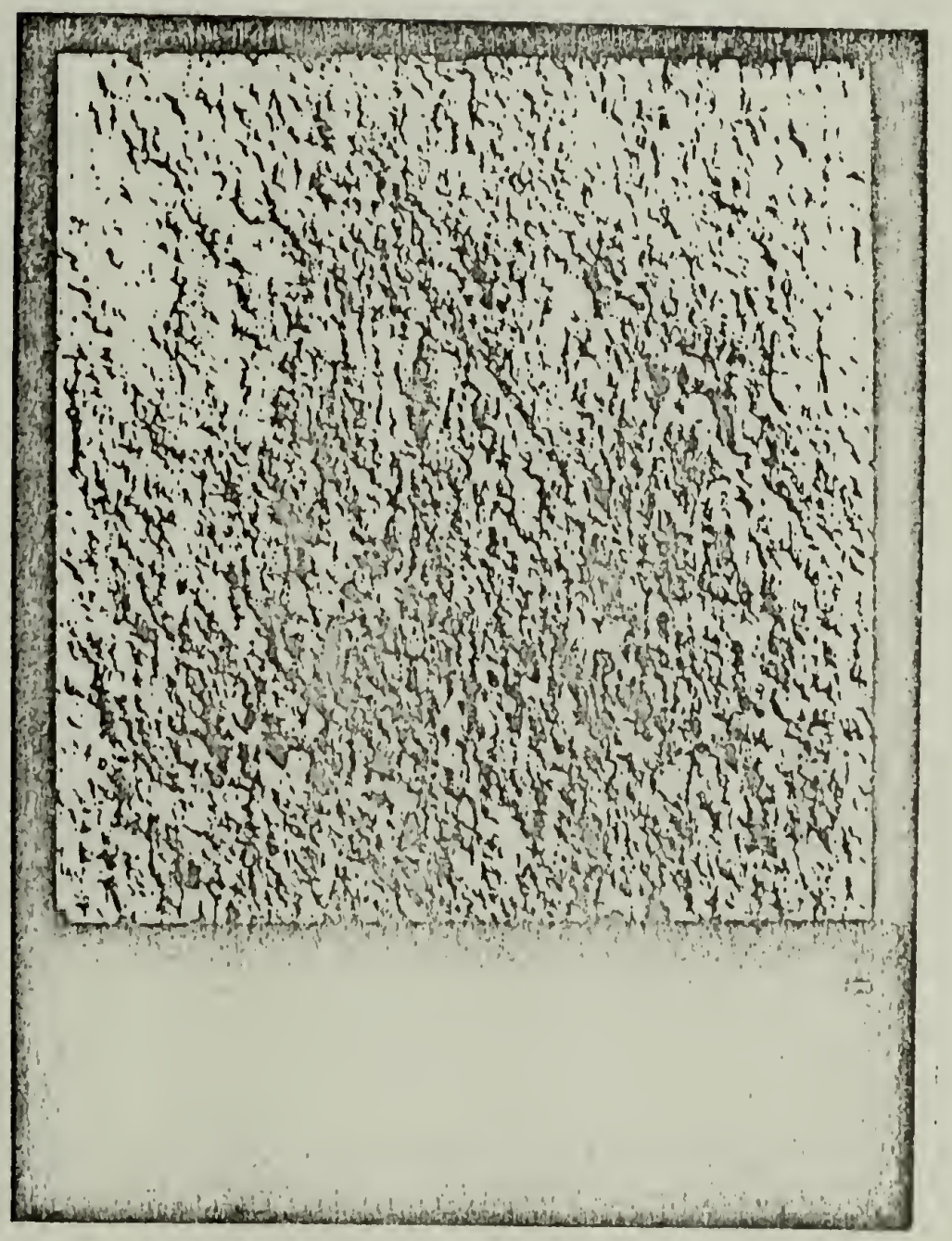

Figure 14. Transmission electron micrograph, 50/50: PPO/polystyrene.

continuum. As the composition changes to 75/25:PPO/PCS-1 (Figure 13c), a phase inversion occurs, and PPO constitutes the continuous medium with dispersed spherical regions of PCS-1.

A similar situation is observed for the other incompatible system of PPO/PCS-3 shown in the scanning micrographs of Figures 15,16 and 17. The blend of 25% PPO (Figure 15) exhibits ridgelike (and larger) aggregates on the order of 2-5 μ . Figure 16 displays the fracture surface of a 50/50 blend where the ductile fracture extensions of PPO are much more predominant. Finally, in a blend of 75/25:PPO/PCS-3, the PPO forms the continuous phase, with the hollow areas representing the nonductile areas of fracture (i.e., the PCS-3 inclusions) of ca. 2 μ in size.

It must be noted that from studies relating the size and shapes of microphase separations in incompatible systems,[24] these domain structures are a function of molding conditions (e.g., flow patterns, melt viscosities, shear rates, etc.) and not strictly a function of the polymers being blended. So it is in this case of the incompatible PPO/PCS blends. The particular microphase separation occurring in these blends affect the material properties. However, these structures are a result of the specific molding conditions employed in

5μ

Figure 15. Scanning electron micrograph, 25/75:PPO/PCS-3.

Figure 16. Scanning electron micrograph, 50/50:PPO/PCS-3.

Figure 17. Scanning electron micrograph, 75/25:PPO/PCS-3.

5μ

Figure 18. Scanning electron micrograph, 50/50:PPO/PCS-5.

these studies and not an inherent material property of the blend system.

Electron microscopy detected no such phase separation in the case of the blends classified as compatible by DSC. Figure 14 shows a transmission micrograph of a fracture surface replica for a blend of 50/50: PPO/polystyrene; Figure 18 is a scanning micrograph of a 50/50:PPO/PCS-5 blend. In neither blend phase separation is discernible.

As this microscopy demonstrates, the incompatible blends display heterogeneous morphologies with large scale phase separations. This segregation of polymer components gives rise to the physical properties characteristic of incompatible blends.

C. Dielectric Relaxation Measurements

Samples of the PPO/PCS blend systems were analyzed by dielectric techniques to evaluate material characteristics which reflect molecular relaxation properties (see Appendix I). For example, molecular relaxation processes which involve a dipole reorientation result in a dielectric loss and an increase in the dielectric constant. Figure 19 demonstrates these effects as a function of temperature for a typical polymer blend (50/50:PPO/PCS-3) in its dielectric relaxation

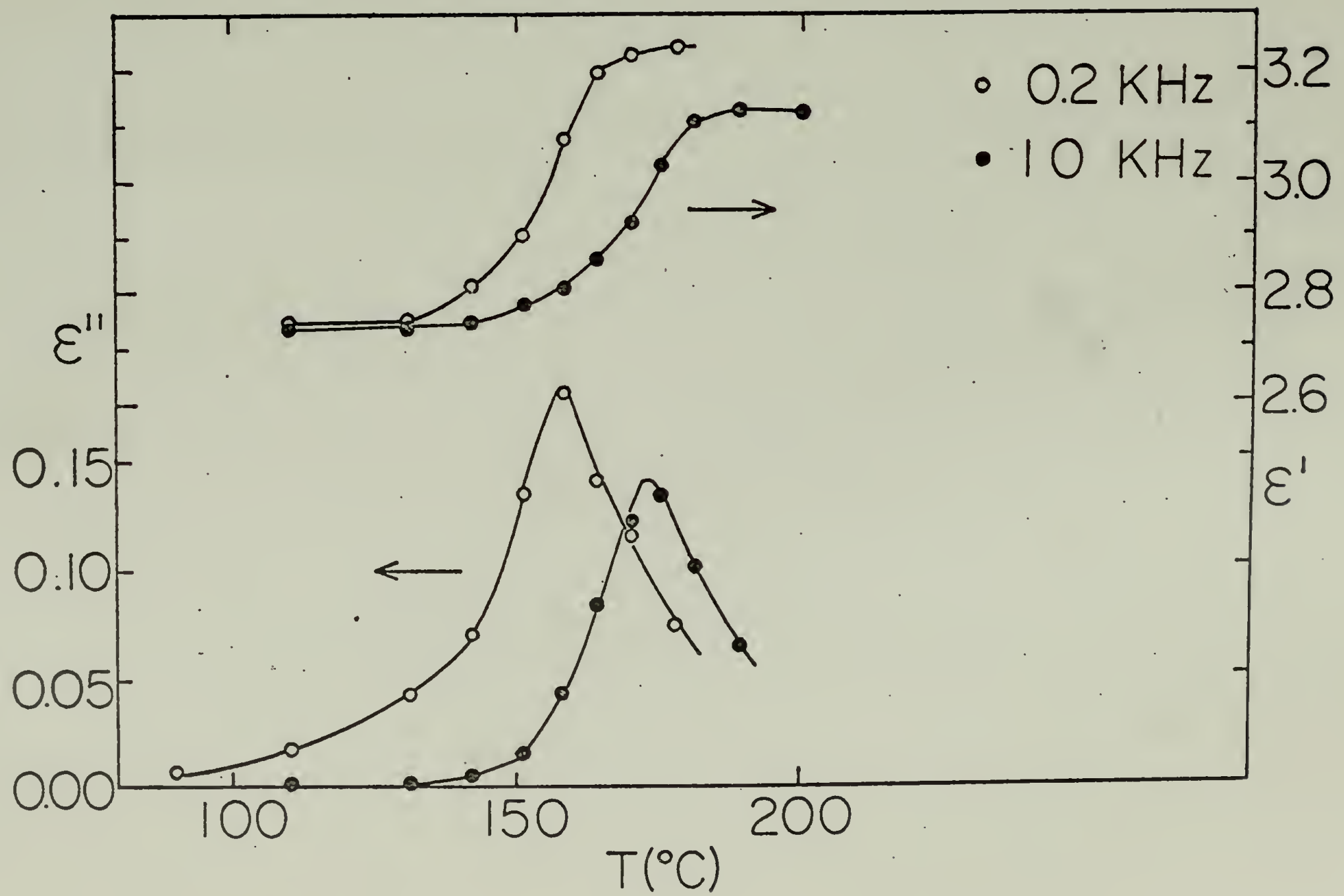

Figure 19. Typical plot of '' and '' as a function of temperature.

region; dielectric constant, ε', and dielectric loss, ε'', are plotted versus temperature at the frequency limits of the study (0.2 and 10 KHz).

The temperature at which the loss factor is a maximum (designated as $T_{\varepsilon''max}$) is the temperature at which the molecular relaxation process is the greatest. This temperature can be considered to be the dielectric analogue of the calorimetric Tg . Figure 20 summarizes the composition dependence of $T_{\varepsilon'' max}$ (at 1 KHz) for the PPO/PCS blends. The incompatible blends (PPO/PCS-1 and PPO/PCS-3) have a PCS loss peak at a temperature corresponding to the loss peak of the pure PCS copolymer. (Due to the fact that the intensity of the dielectric loss of PCS is about three orders of magnitude greater than that of PPO, the only loss peak observed was that of PCS.) Analogous to the DSC results, the compatible blends (PPO/PCS-5 and PPO/PCS-6) exhibit a loss peak maximum at a temperature intermediary to those of the blend components. Another characteristic difference between the loss peaks of the incompatible and compatible systems is that the relaxation process of the latter occurs over a wider temperature range. Figure 21 demonstrates this effect in the plot of ε'' versus temperature for an incompatible (50/50:PPO/PCS-3) and a compatible (50/50:PPO/PCS-5) system.

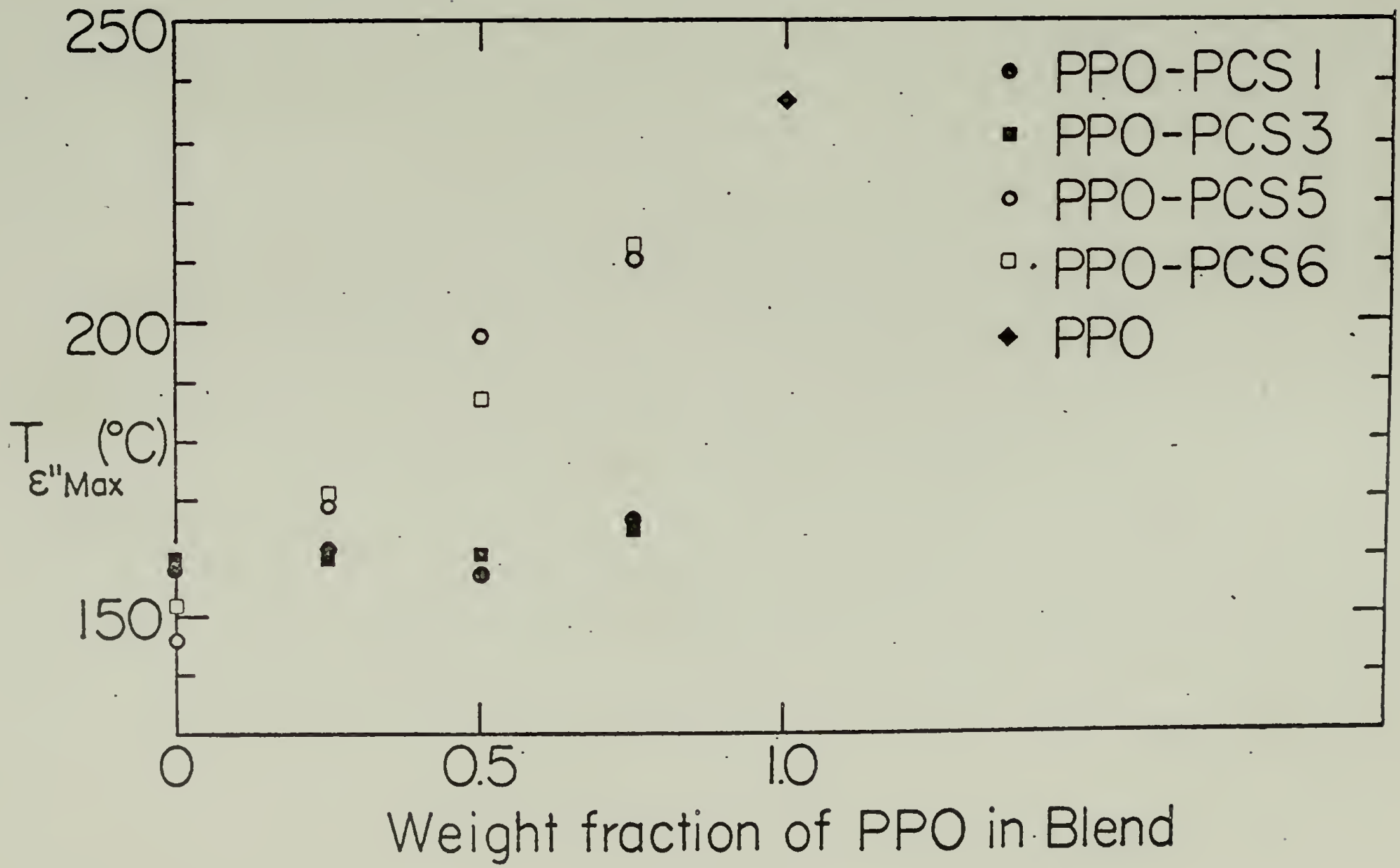

Figure 20. Compositional dependence of $T_{\varepsilon''max}$ for the PPO/PCS blends.

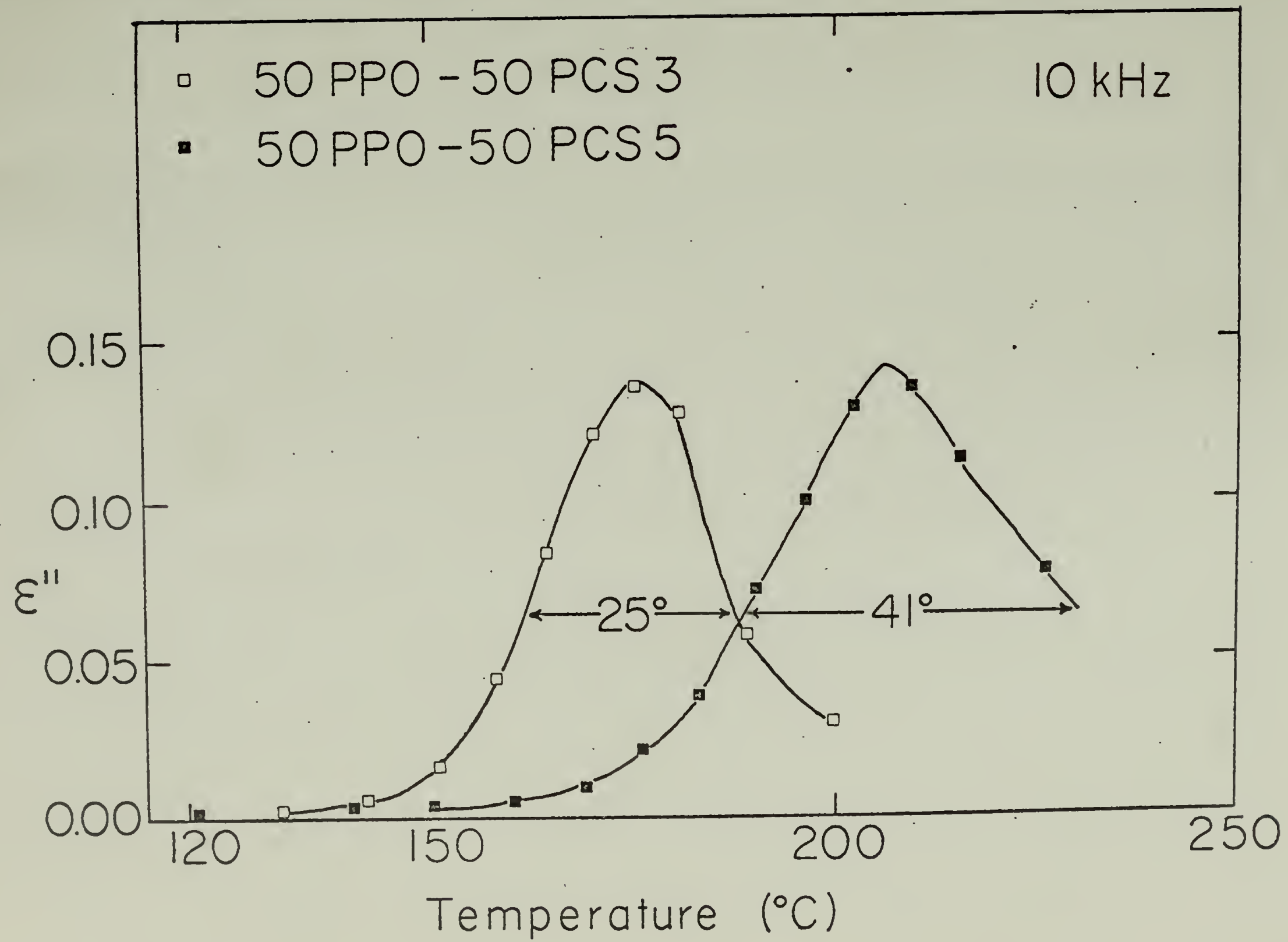

Figure 21. Comparison of dielectric loss peak width for PPO/PCS blends.

The peak width of the relaxation region (as measured by peak width at one half peak height) for the incompatible system is considerably less than that for the compatible blend (25° and 41°C, respectively).

The dielectric loss peak intensities are proportional to the PCS content for both compatible and incompatible systems, confirming that the dielectric loss is a reflection of motion occurring in the PCS component. Similar evidence is obtained by data exhibited in Figures 22 through 25 which are Arrhenius plots for the PPO/PCS blends. In both incompatible (Figures 22 and 23) and compatible systems (Figures 24,25), the slopes of the plots for the blends are essentially unchanged from those of the pure PCS components. Therefore, the dielectric relaxation activation energy is the same for the pure PCS component and its blends. Although the values of $T_{\varepsilon''max}$ for the compatible blends are proportional to the PPO content, the presence of the PPO does not seem to affect the activation energy of the dipole orientation of the PCS component.

Further information can be obtained from these experiments to elucidate interaction between the components of the polyblends and the molecular properties of the relaxing species. The most advanced theories of dielectric relaxation processes have related molecular

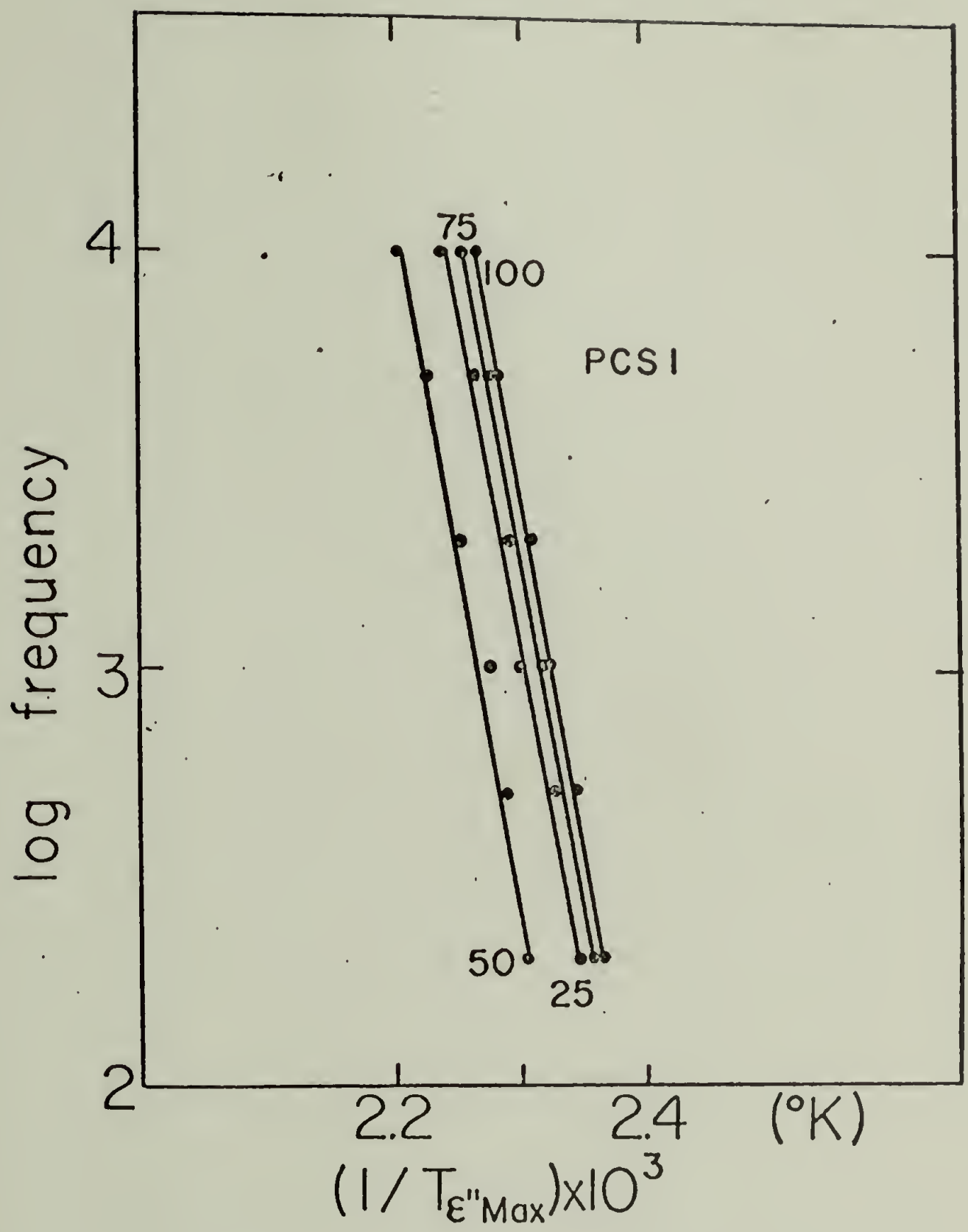

Figure 22. Dielectric Arrhenius plot for PPO/PCS-1 blends.

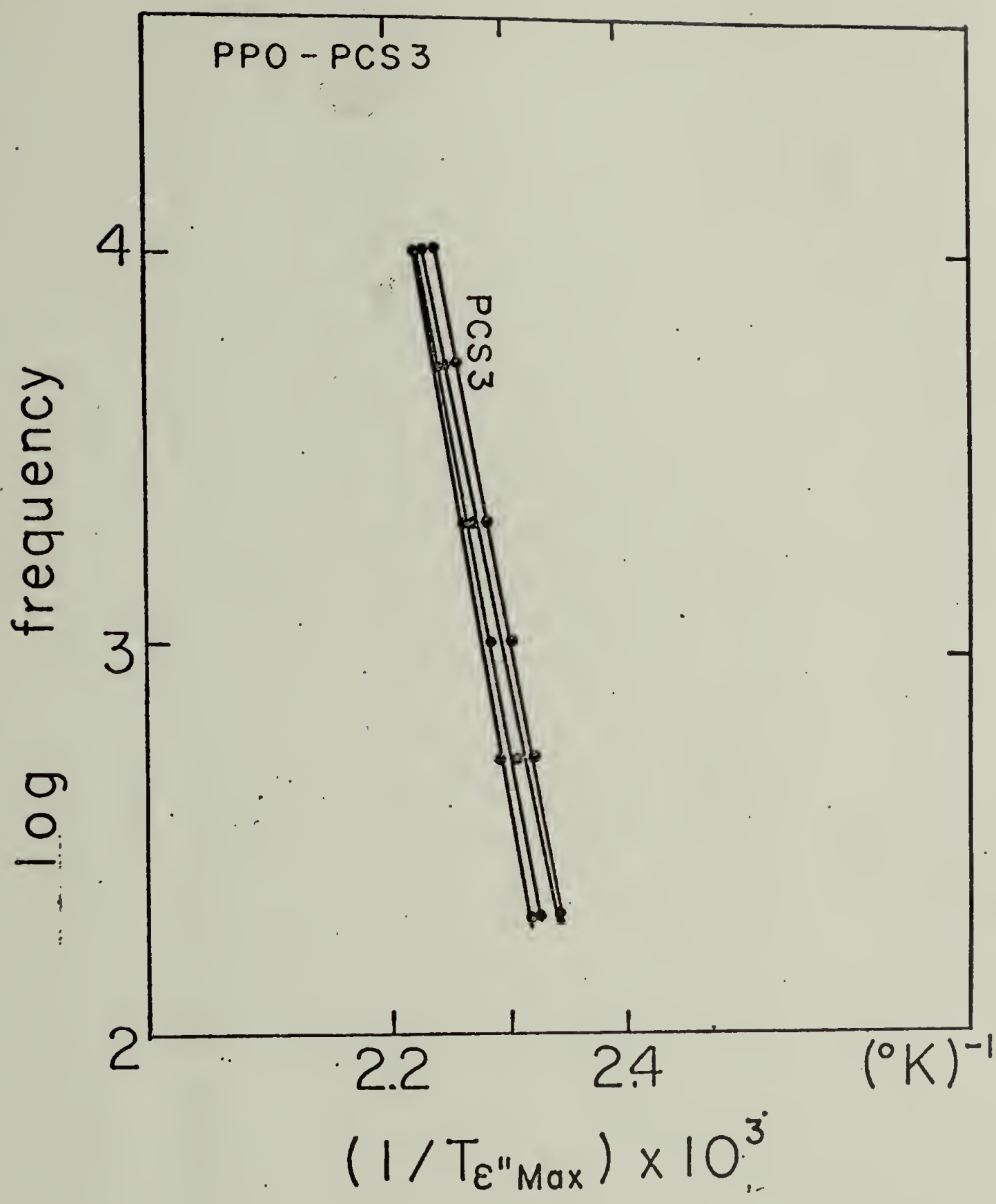

Figure 23. Dielectric Arrhenius plots for PPO/PCS-3 blends.

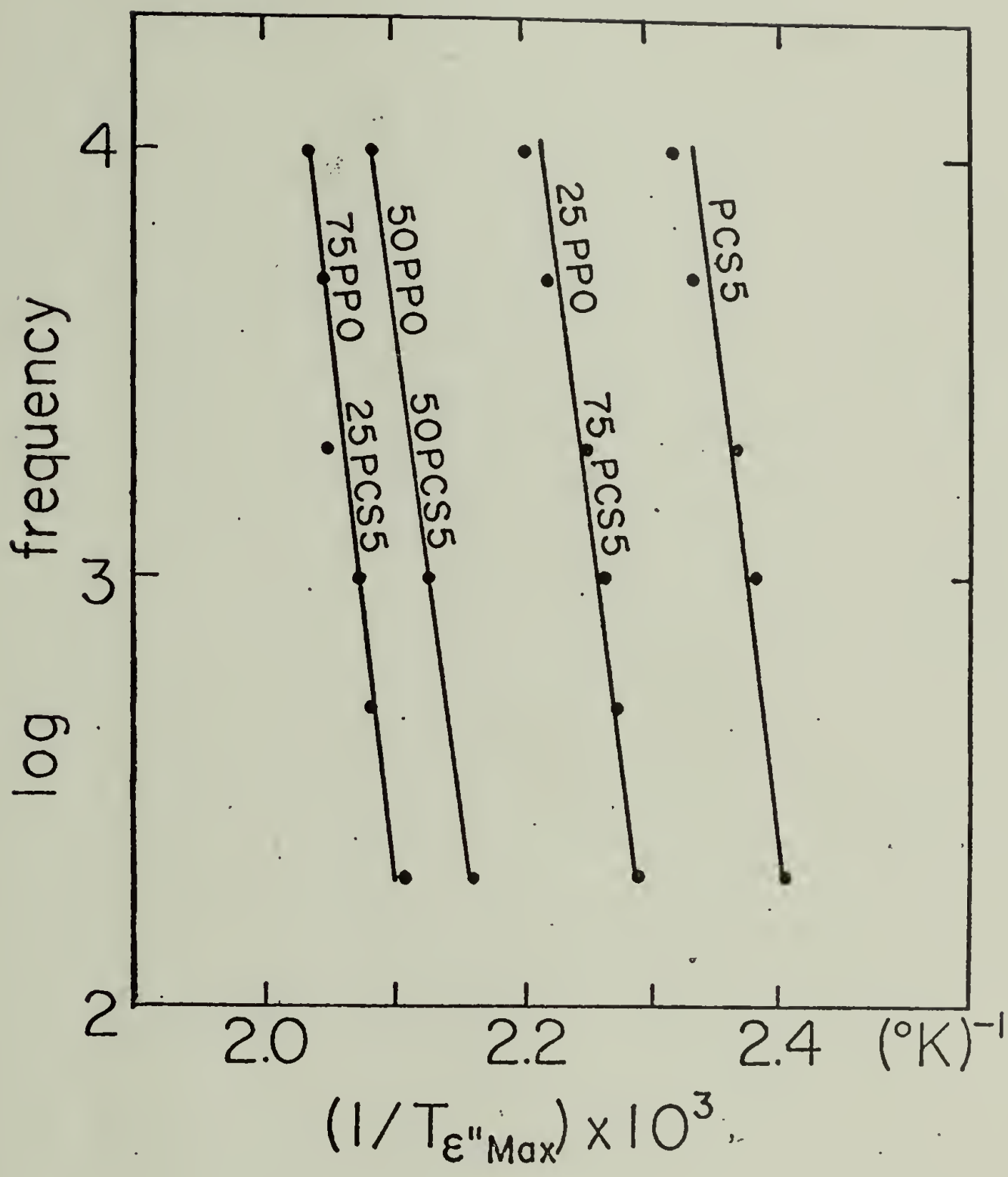

Figure 24. Dielectric Arrhenius plots for PPO/PCS-5 blends.

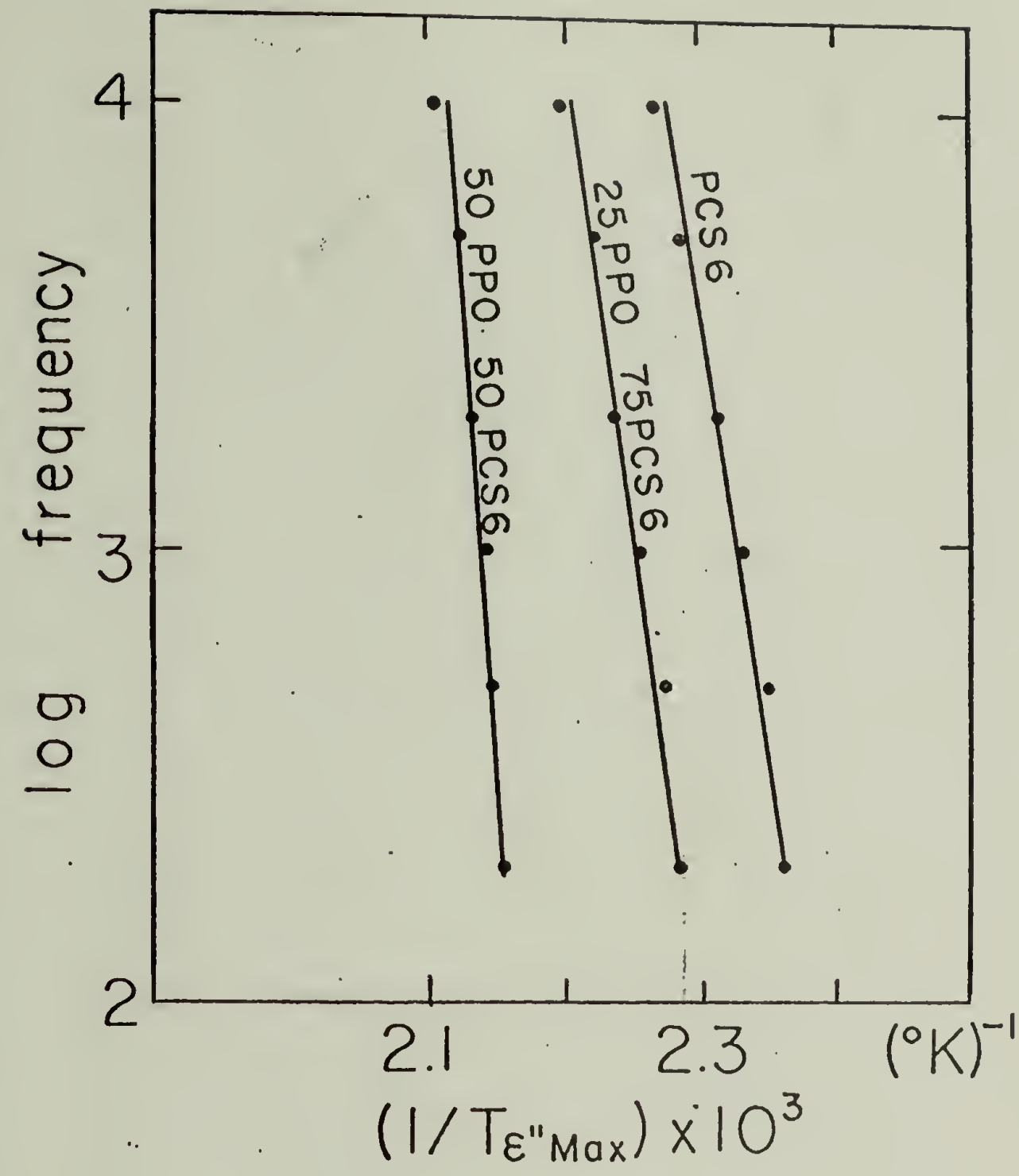

Figure 25. Dielectric Arrhenius plot for PPO/PCS-6 blends.

properties to the dielectic constant of the relaxed and unrelaxed states (ε_R and ε_U , respectively). The magnitude of the relaxation is then defined as the difference between ε_R and ε_U (i.e, the quantity ($\varepsilon_R - \varepsilon_U$)). (see Appendix II).

In the ideal experiment ε_R and ε_U are the limiting values of the dielectric constant at very low and very high frequencies, respectively, of a frequency range which traverses the entire relaxation spectrum. (These quantities are also referred to as ε_o and ε_∞ respectively.) Unfortunately, these experimental conditions did not, of course, exist for these studies. As the dielectric experimental frequency range was not broad enough to cover the entire relaxation range at any one temperature, the time-temperature superposition principle was utilized to generate dielectric relaxation master curves. Experimental plots of ε' versus log frequency produces an envelope of isothermal traces as shown in Figure 26 for a blend of 25/75:PPO/PCS-3. Standard horizontal shifting procedures[25] applied to these curves result in a continuous,sigmoidal shaped composite curve, the asymptotes of which represent ε_R and ε_U as shown in Figure 27.

This shifting procedure was analyzed to yield the constants C_1 and C_2 of the Williams, Landel and Ferry

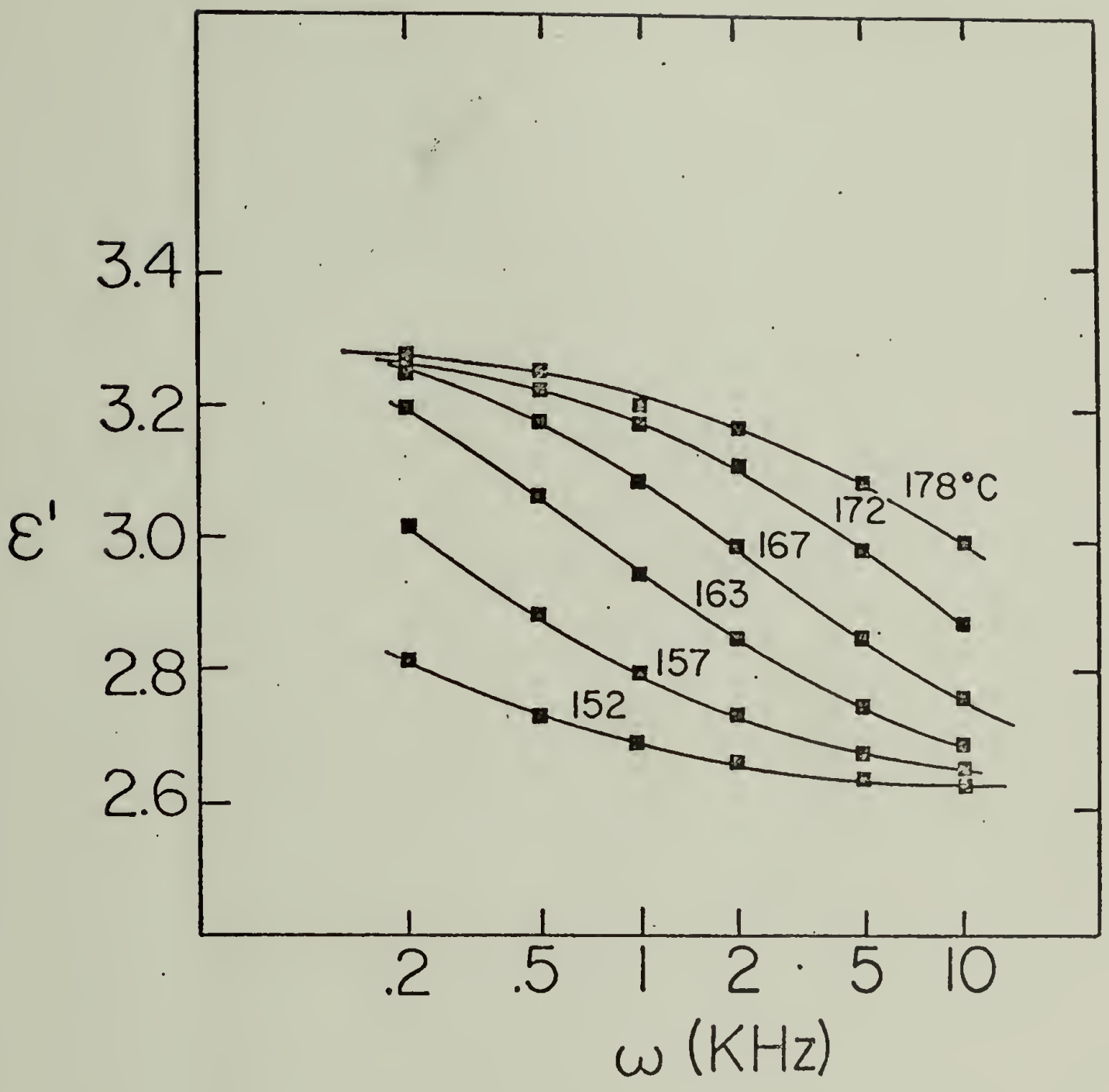

Figure 26. Typical isothermal traces of ε' versus ln frequency (25/75:PPO/PCS-3)

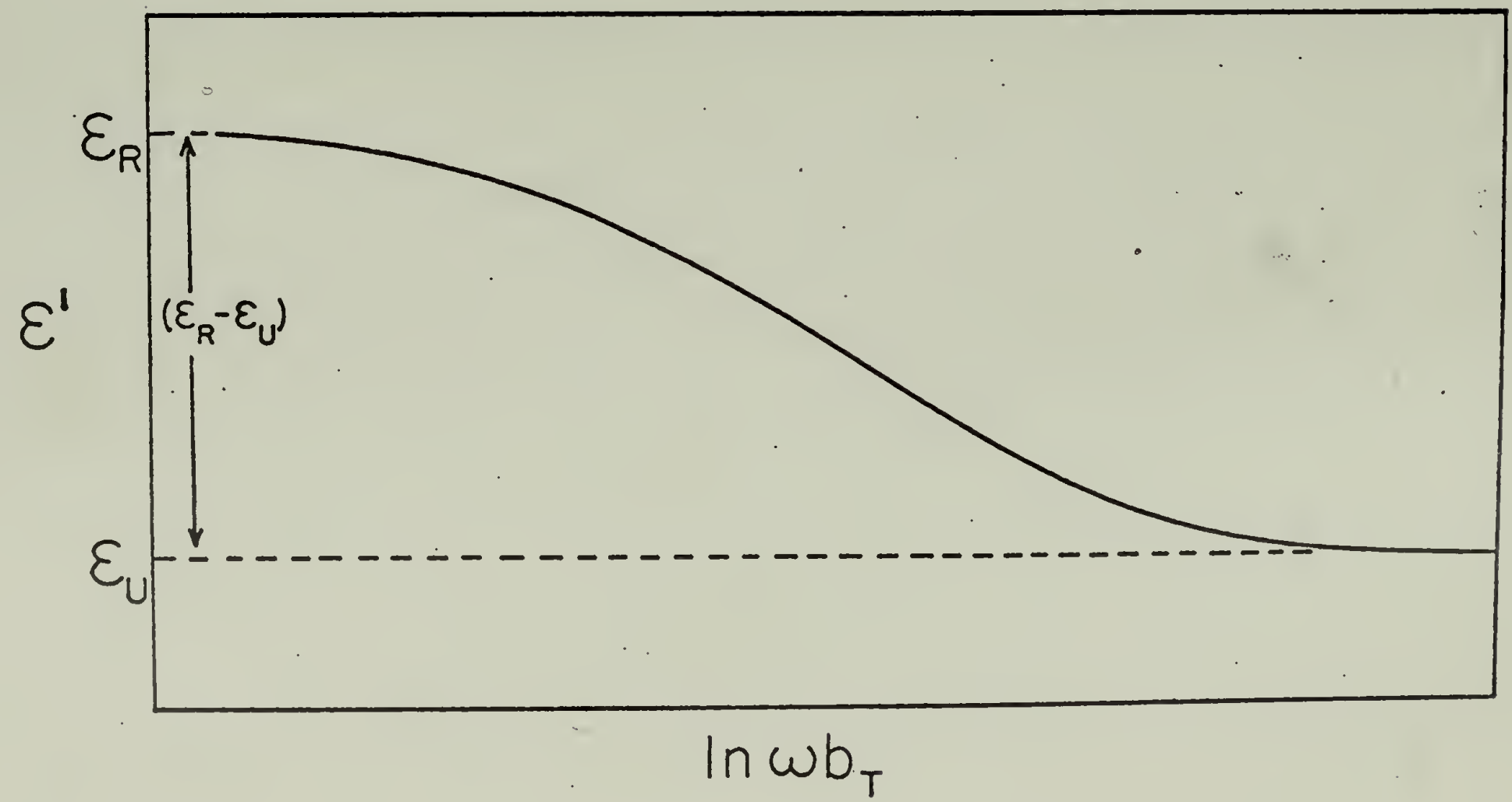

Figure 27. Typical composite ε' master curve (25/75:PPO/PCS-3).

(WLF) equation :[26]

$$\ln b_{\omega T} = \frac{- C_1 (T - Tg)}{C_2 + T + Tg} \qquad (18)$$

where the quantity $b_{\omega T}$ is the dielectric frequency shift factor, analogous to the mechanical shift factor a_T. The procedure of Ferry was followed to determine C_1 and C_2.[26] Equation 18 was rewritten in terms of T_∞ :

$$\ln b_{\omega T} = \frac{-C_1 (T - Tg)}{T - T_\infty} \qquad (19)$$

where

$$T_\infty = Tg - C_2 \qquad (20)$$

Values of $b_{\omega T}$ were plotted against the quantity, $[(T - Tg)/ (T - T_\infty)]$. T_∞ was adjusted until the plot was linear; $-C_1$ is the slope of this line; C_2 is the difference between Tg and T_∞. Table 2 lists WLF constants for the PPO/PCS blends. Within experimental accuracy, C_1 and C_2 were constant for the PCS copolymers and the PPO/PCS blends independent of blend compatibility characteristics. These values agree reasonably well with those obtained by dielectric relaxation studies for polystyrene of $C_1 = 13.7$ and $C_2 = 50.0$.[26]

Further application of the theory of dielectrics can relate macroscopic and molecular properties (see Appendix II for development) and elucidate the differ-

Table 2. WLF constants (dielectric) for PPO/PCS blends

Blend System	Tg (DSC)	C_1	C_2
PCS-1	123°C	12.5	53
25/75 : PPO/PCS-1	123	9.6	51
50/50 "	127	10.3	55
75/25 "	130	11.8	60
PCS-3	129	11.8	59
25/75 : PPO/PCS-3	130	10.5	60
50/50 "	130	10.0	60
75/25 "	130	10.6	58
PCS-5	120	10.3	52
25/75 : PPO/PCS-5	133	10.8	53
50/50 "	151	25.6	51
75/25 "	175	10.0	55
PCS-6	126	10.6	57
25/75 : PPO/PCS-6	137	9.1	53
50/50 "	158	8.0	55
75/25 "	181	9.6	55

ences between compatible and incompatible blends. Analysis of the dipole orientation correlation factor of the Frohlich equation yields information about the dipolar environment within the polymer blends:

$$g = \frac{9kT}{4\pi N\mu^2} \frac{(2\varepsilon_R + \varepsilon_U)(\varepsilon_R - \varepsilon_U)}{\varepsilon_R (\varepsilon_U + 2)^2} \qquad (21)$$

g = dipole orientation correlation factor
k = Boltzmann's constant
T = absolute temperature
N = number of dipoles per cm^3
μ_o = dipole moment of an isolated dipole unit
ε_R, ε_U = relaxed, unrelaxed dielectric constants

The value of μ used in this study is the dipole moment of an isolated p-chlorotoluene molecule (1.94 D) which is the generally accepted value for the p-chlorostyrene systems.[27,28] Considering short range interactions, the dipolar environment of a dipole i is related to g by :

$$g = 1 + z\overline{\cos\gamma} \qquad (22)$$

where $\overline{\cos\gamma}$ is the average cosine value of the angle γ between dipole i and its z nearest neighbors.

Within polymeric systems with dipoles at tetrahedral angles to the polymer chains (e.g., PCS copolymers) g values are less than unity due to chain configuration and hindered rotation (i.e., $\overline{\cos\gamma} < 0$).[12] Therefore as the effective dipole concentration decreases, the number

of nearest neighbors (z) decreases, and the correlation factor will increase. This concentration effect is demonstrated for the PCS copolymer series in Table 3. The "internal dilution" of the polar p-chlorostyrene by the nonpolar styrene moieties causes an increase in the correlation factor. This observation agrees with results for PCS-type random copolymers obtained by solution dielectric studies.[14]

Dipole orientation correlation factors were calculated for the PPO/PCS blend systems. (See Appendix III) Figure 28 plots g as a function of blend composition for the incompatible blends (PPO/PCS-1 and PPO/PCS-3), revealing that g is essentially constant across the blends' composition range. This constant g value is consistent with the fact that the relaxing PCS molecules aggregate in domains with no intimate mixing with PPO in these incompatible blends. The environment of a PCS dipole in such a blend is essentially the same as in the pure copolymer, resulting in constant g values for the copolymers and their respective blends.

However, the compatible blends (PPO/PCS-5 and PPO/PCS-6) display substantially different behavior as shown in Figure 29. As the PCS fraction of the blend decreases (i.e., as it is diluted with PPO), the correlation factor increases. This behavior is analogous to

Table 3. Effect of dipole concentration on orientation correlation factor (g) for PCS copolymers

PCS Copolymer	p-Cl styrene content (mole percent)	g factor
PCS-1	100	0.28 ± .02
PCS-3	68	0.35
PCS-6	60	0.37
PCS-5	47	0.41

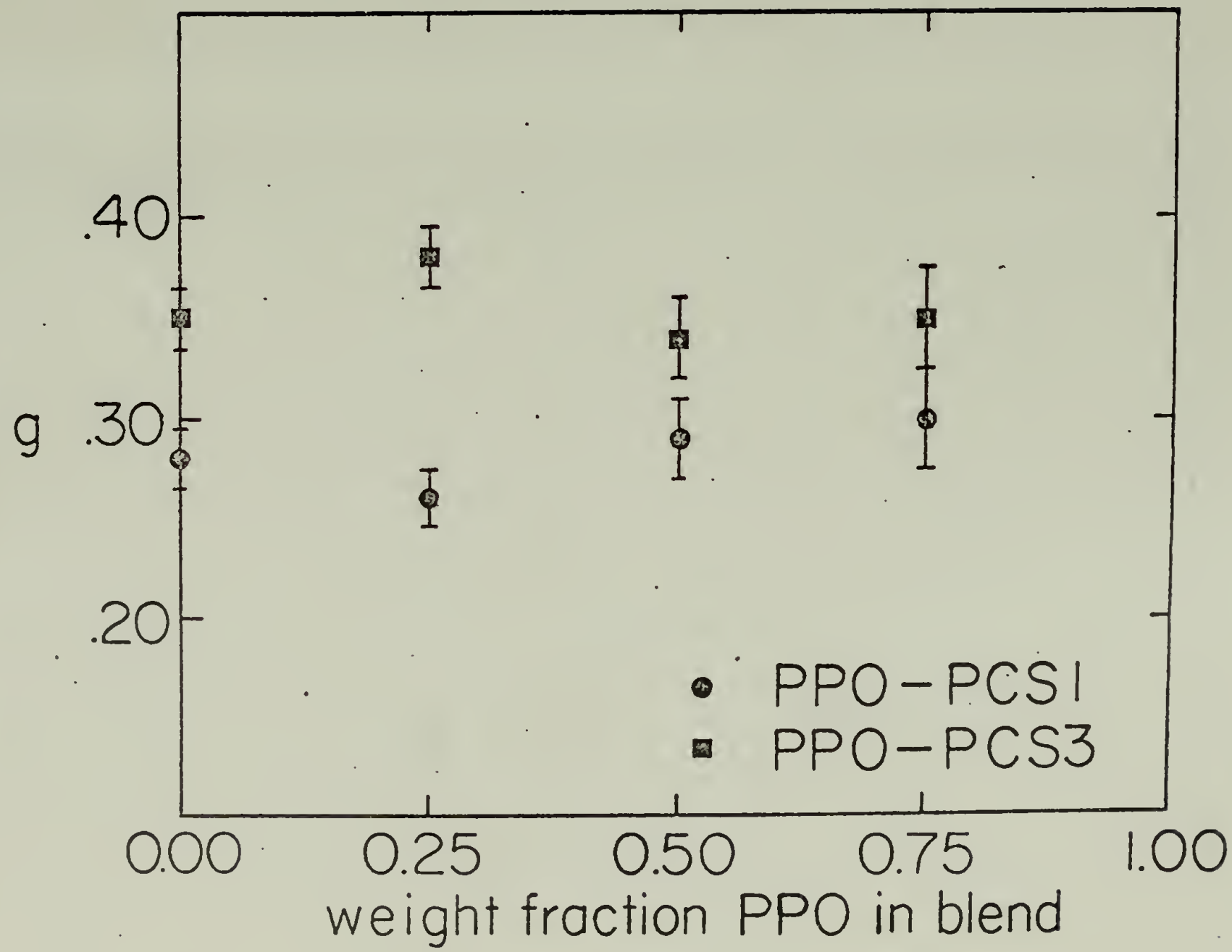

Figure 28. Compositional dependence of g factor for incompatible PPO/PCS blends.

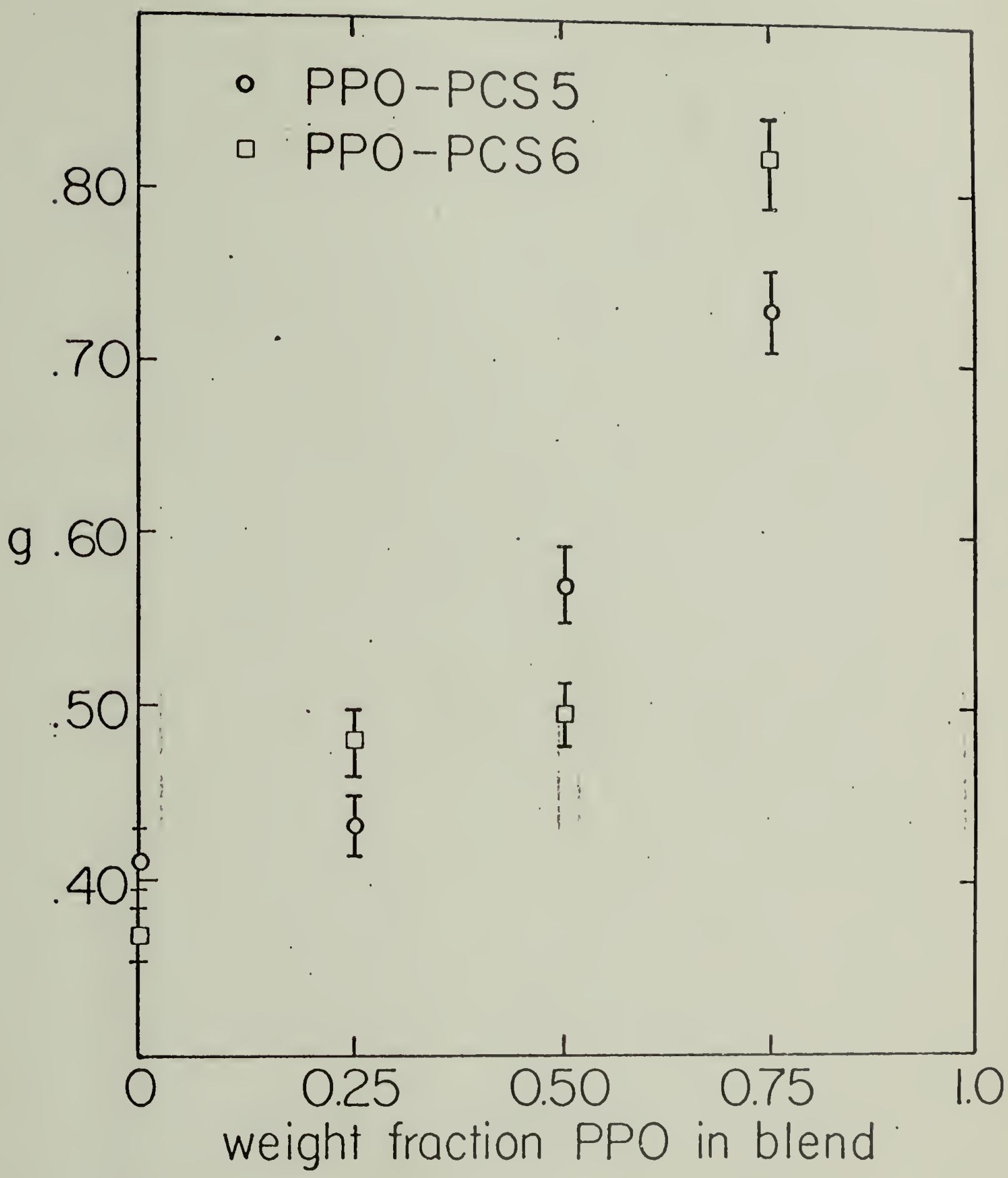

Figure 29. Compositional dependence of g factor for compatible PPO/Pcs blends.

dielectric properties of PCS copolymers in solution in which g increases as the solution concentrations become more dilute.[14] This increase may also partially result from chain expansion of the PCS molecules, parallel to the solution behavior of poly(p-Cl styrene) in low molecular weight solvents.[15]

From these dielectric relaxation studies, it is clear that the environment of the dipoles within the PCS chains changes as the compatible blend compositions vary. Presently, it is not possible to resolve the intermolecular (e.g., dilution) and the intramolecular (e.g., chain expansion) factors which affect the dipole orientation correlation factor. However, both of these factors are characteristic of systems of macromolecules in solution. Regardless of which factor is predominant in the influence of the g factor, this information indicates that there is intimate mixing between PPO and PCS-5 or -6 on the order which occurs in solutions of macromolecules in low molecular weight species. Otherwise, neither true dilution nor chain expansion could occur.

The compatibility characteristics of the PPO/PCS blends also affect other dielectric properties, especially the magnitude of the dielectric relaxation. These

differences in properties can be elucidated in terms of an extension of the Takayanagi two phase model [29] originally derived to analyze mechanical properties of semicrystalline polymers. Figure 30 represents the face of a unit cube of an idealized two phase system: phase 1 and phase 2 with the dielectric constants, ε_1 and ε_2, respectively. When subjected to an external electric field, E, in the prescribed direction, the composite material will display a dielectric constant, ε, the magnitude of which depends on the manner of interaction between the two phases. The two extreme modes of interaction are that the two phases can behave as though they are in a series arrangement ($\lambda = 1$) or in a parallel arrangement ($\phi = 1$). The resultant dielectric constant of the composite will be:

$$\varepsilon = \frac{\phi}{\frac{\lambda}{\varepsilon_1} + \frac{1-\lambda}{\varepsilon_2}} + (1-\phi)\,\varepsilon_2 \qquad (23)$$

This model of a heterogeneous material is a good approximation of the nature of the properties of the phase separated, incompatible blends. Figure 31 plots normalized relaxation magnitudes (i.e., magnitude of the blend relaxation divided by the magnitude of the pure PCS relaxation) as a function of blend composition. The solid line represents the series combination response;

the dashed line represents the parallel interaction. The experimental points for the incompatible systems (PPO/PCS-1 represented by ○, PPO/PCS-3 by ◆) fall within the theoretical envelope, indicating a combination of series and parallel modes of interaction. If the normalized relaxation magnitudes of the compatible blends were plotted as a function of blend composition, they would align more closely to the diagonal (i.e., solid, series model) line. This behavior indicates that for the compatible PPO/PCS blends, the relative normalized relaxation magnitudes are higher than for the corresponding incompatible systems.

A theoretical calculation of the dielectric constant of some incompatible blends can be performed from the theory of heterogeneous dielectrics. Given that the composition and domain shape of a composite are known, electrostatic theory predicts dielectric properties based on the dielectic properties of the components of the mixture. Generally, for a dispersion of a relaxing species (phase 1) in a non-relaxing matrix (phase 2), the following relationships have been developed:[30]

$$\frac{\varepsilon}{\varepsilon_1} = \frac{1 + A B \phi_1}{1 - B \psi \phi_1} \qquad (24)$$

Takayanagi
Two Phase Model

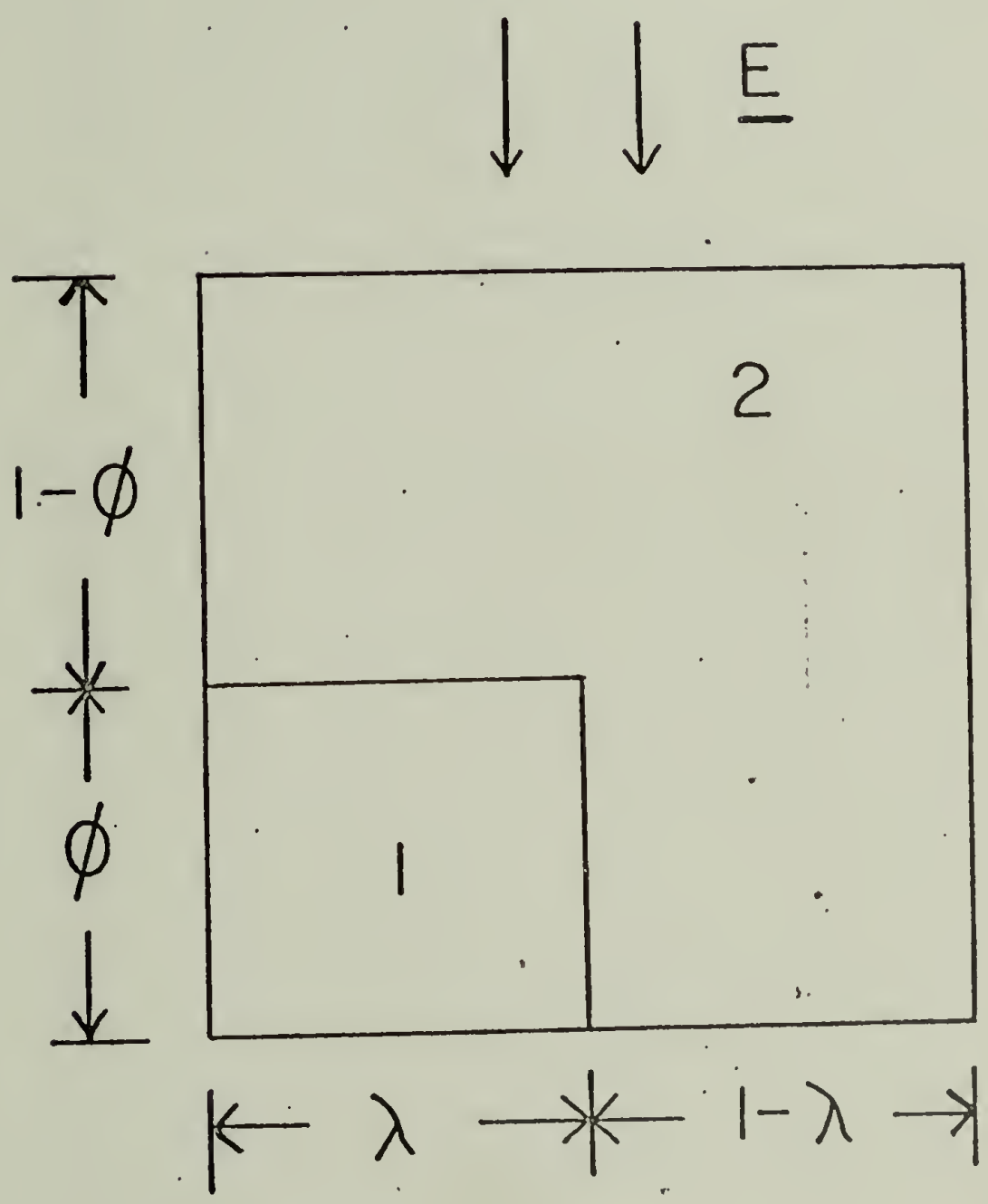

Figure 30. Description of Takayanagi model.

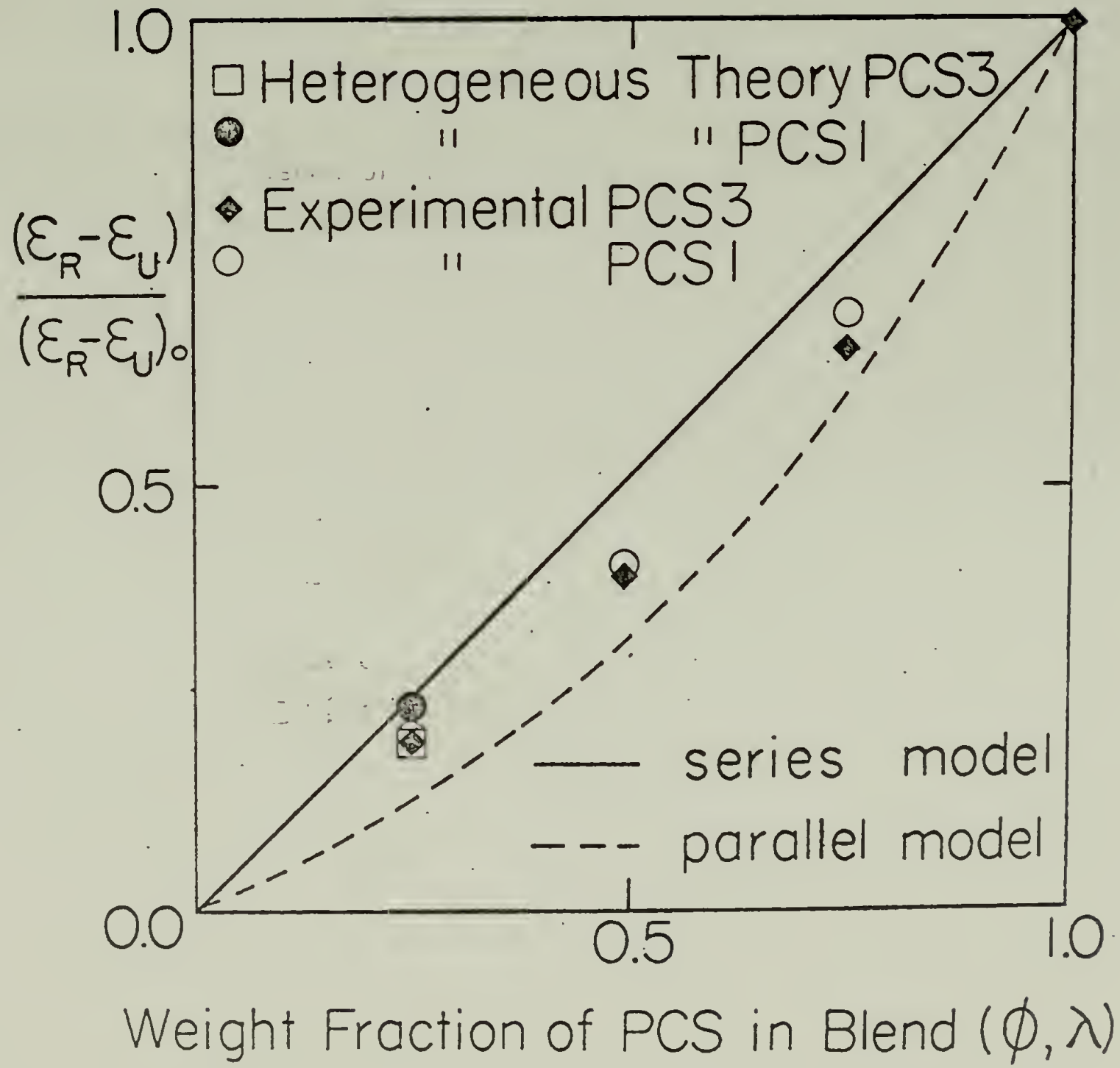

Figure 31. Compositional dependence of magnitude of relaxation for incompatible PPO/PCS blends.

$$A = \frac{1}{A_\varepsilon} - 1 \qquad (25)$$

$$B = \frac{(\varepsilon_1/\varepsilon_2) - 1}{(\varepsilon_1/\varepsilon_2) + A} \qquad (26)$$

$$\psi = 1 + \frac{1 - K}{K^2} \qquad (27)$$

In the above equations ε, ε_1,ε_2 are the dielectric constants of the mixture, phase 1 and phase 2, respectively; ϕ_1 and ϕ_2 are the phase volume fractions. A_ε is the depolarization factor and K is the maximum packing fraction, both of which are calculated from theory for a specific geometry of phase 1 (relaxing) domain shape. This theory is accurate for dispersions with $\phi_1 < 0.30$ with the domain sizes small compared to sample size. Therefore, this relationship is applicable to the incompatible blends of 75% PPO and 25% PCS-1 or -3. For randomly distributed spherical shaped domains (which describes the morphologies of these incompatible blends), the following parameters have been calculated: $A_\varepsilon = 3.0$ and $K = 0.64$.[30] Based on this theory, limiting values of ε were calculated for the above incompatible blends. The normalized theoretical values agree well with experimental values and are included in Figure 31.

D. Dynamic Mechanical Studies

Dynamic mechanical testing was utilized to determine the viscoelastic properties of the PPO/PCS blend systems. The blend samples were subjected to a sinosoidal shear stress as temperature and frequency were varied. Mechanical properties (e.g., storage and loss components of the shear modulus) were then calculated as previously described. The mechanical storage factor, G', and loss factor, G", is plotted as a function of temperature for a typical incompatible blend (PPO/PCS-3) at a frequency of 3.5 Hz in Figures 32 through 36. For the incompatible systems each blend exhibits two distinct damping peaks corresponding to the relaxations of the two immiscible components. However, when one of the incompatible components is present in small amounts ($\leq$ ca. 25%), the damping peak is of low intensity.

The mechanical properties of the compatible systems are more complex as illustrated in Figures 37 through 40 which plot G' and G" as a function of temperature for the PPO/PCS-6 system. For each blend, there is a primary loss peak maximum at a temperature intermediary to those exhibited by the two components. Figure 41 summarizes the compositional dependence of

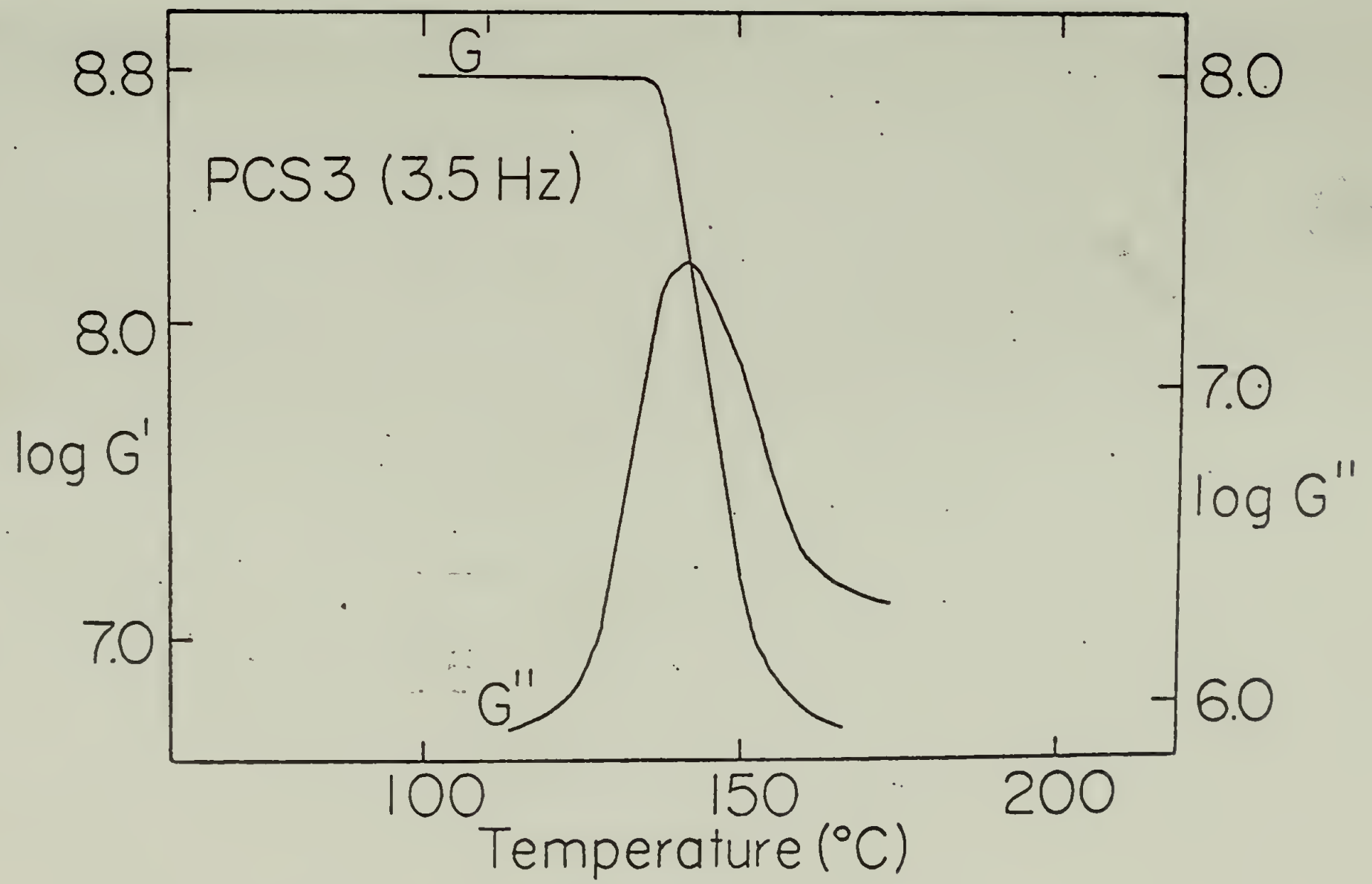

Figure 32. G',G'' as a function of temperature for PCS-3.

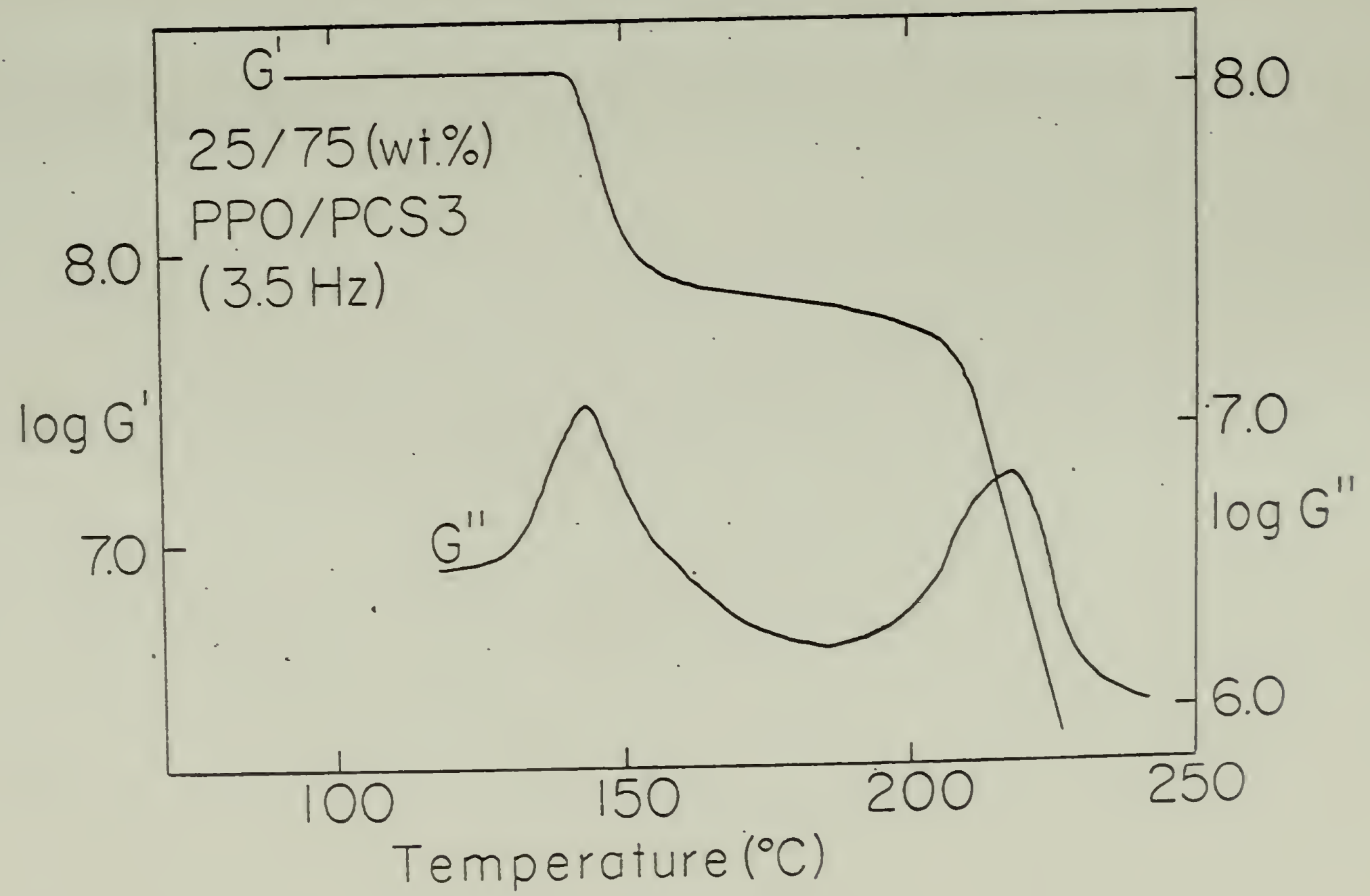

Figure 33. Temperature variation of G', G'' for 25/75:PPO/PCS-3.

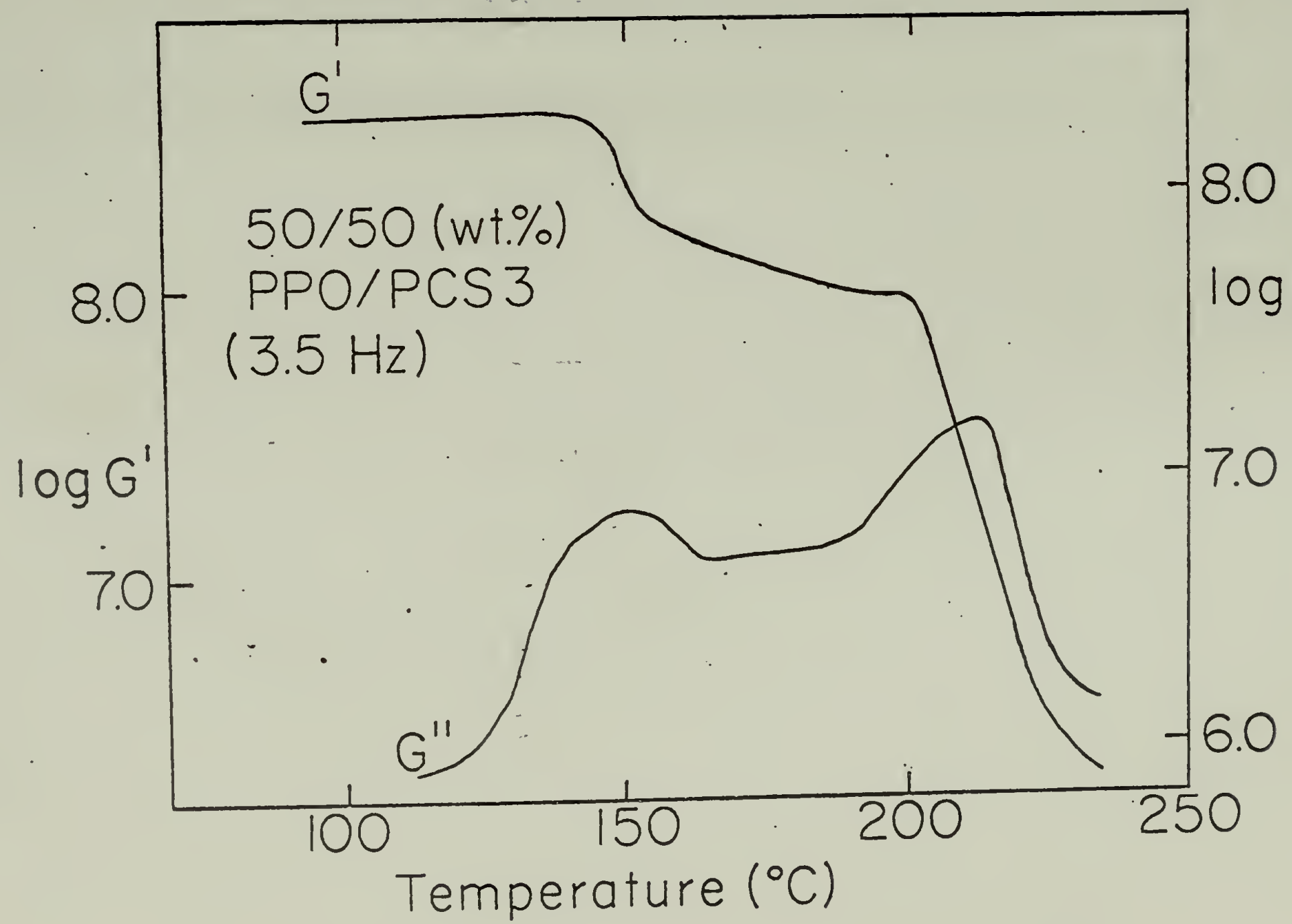

Figure 34. Temperature variation of G', G'' for 50/50:PPO/PCS-3.

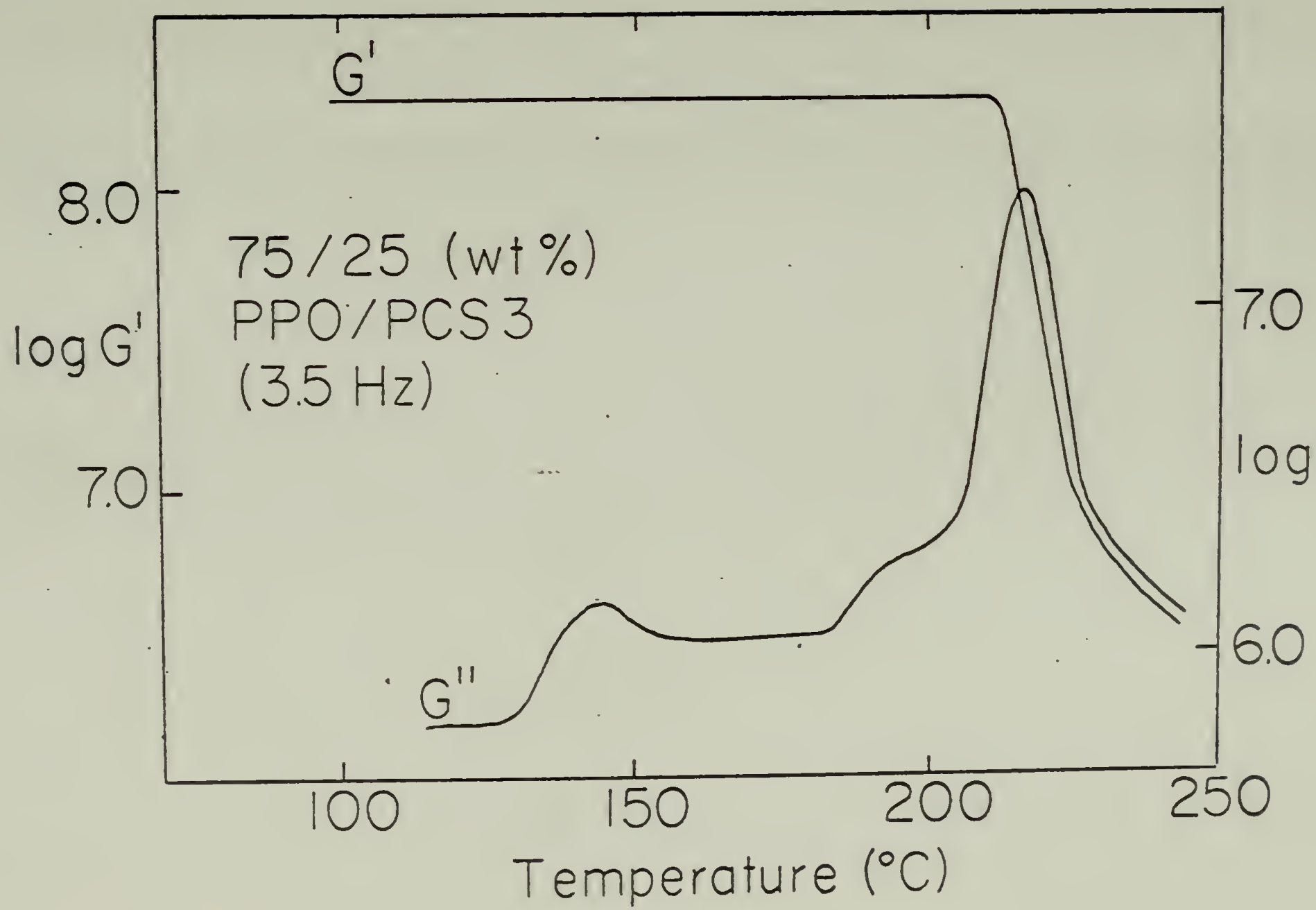

Figure 35. Temperature dependence of G', G'' for 75/25:PPO/PCS-3.

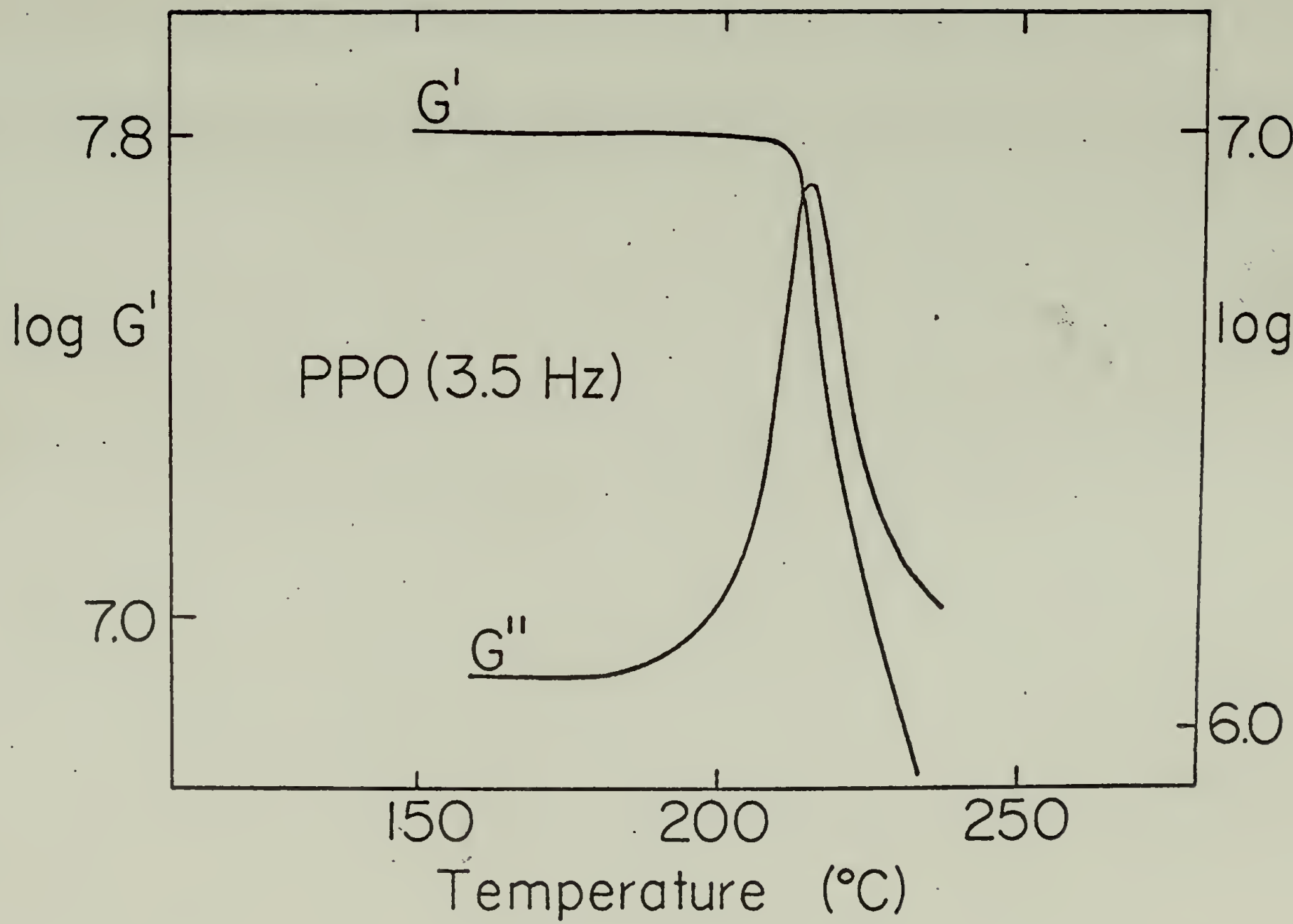

Figure 36. Temperature dependence of G', G'' for PPO.

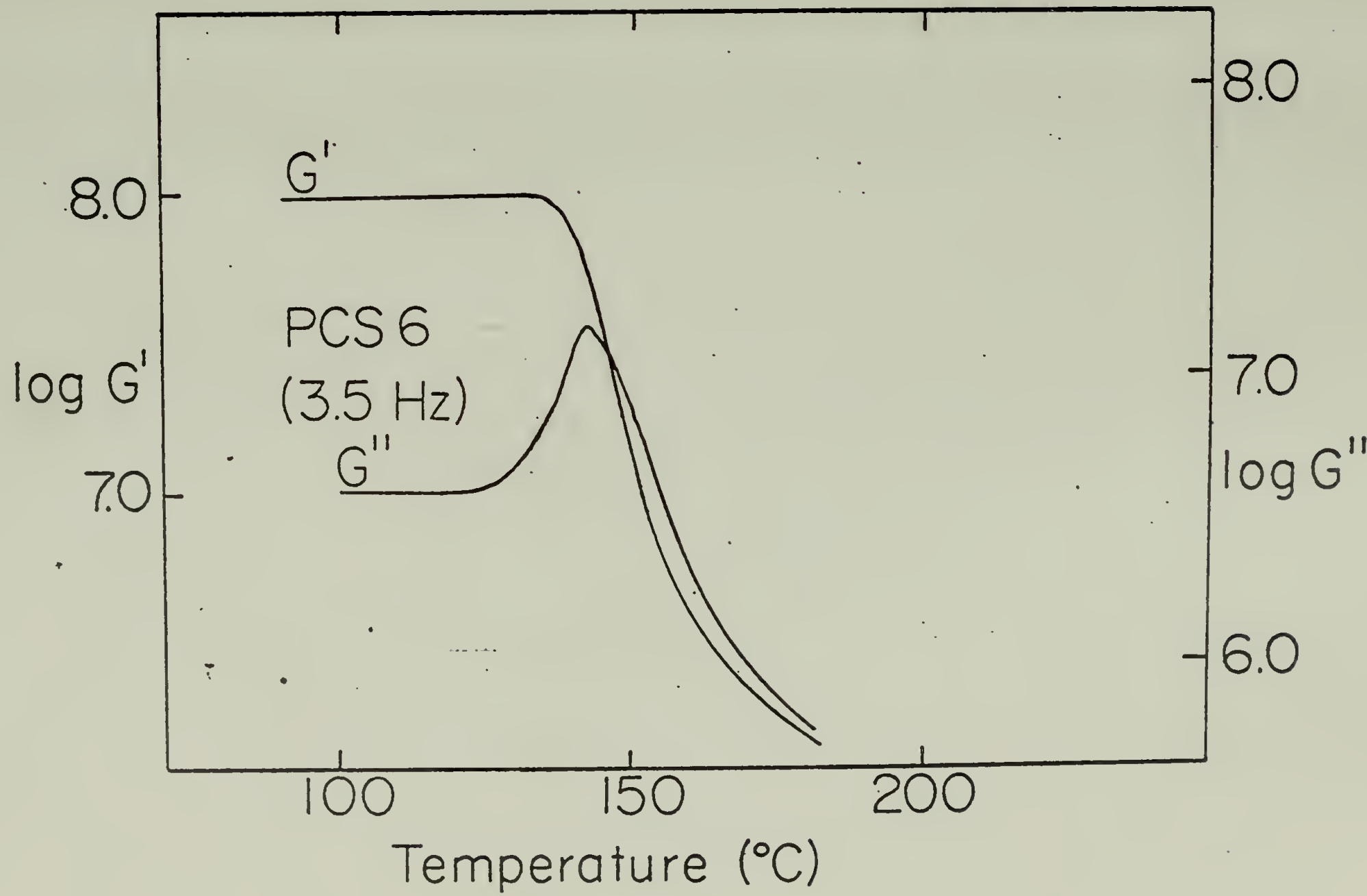

Figure 37. Temperature dependence of G', G'' for PCS-6.

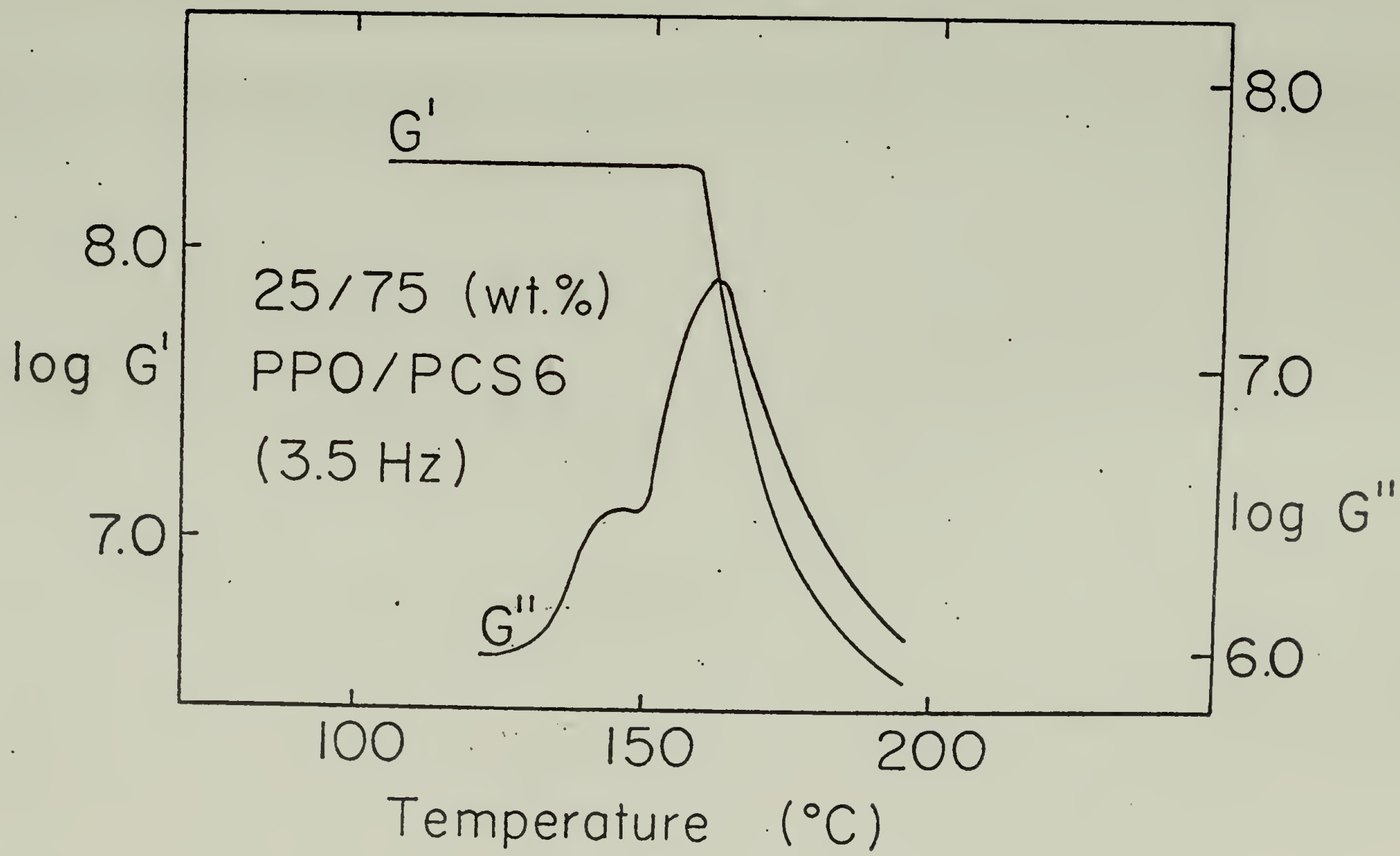

Figure 38. Temperature dependence of G', G'' for 25/75:PPO/PCS-6.

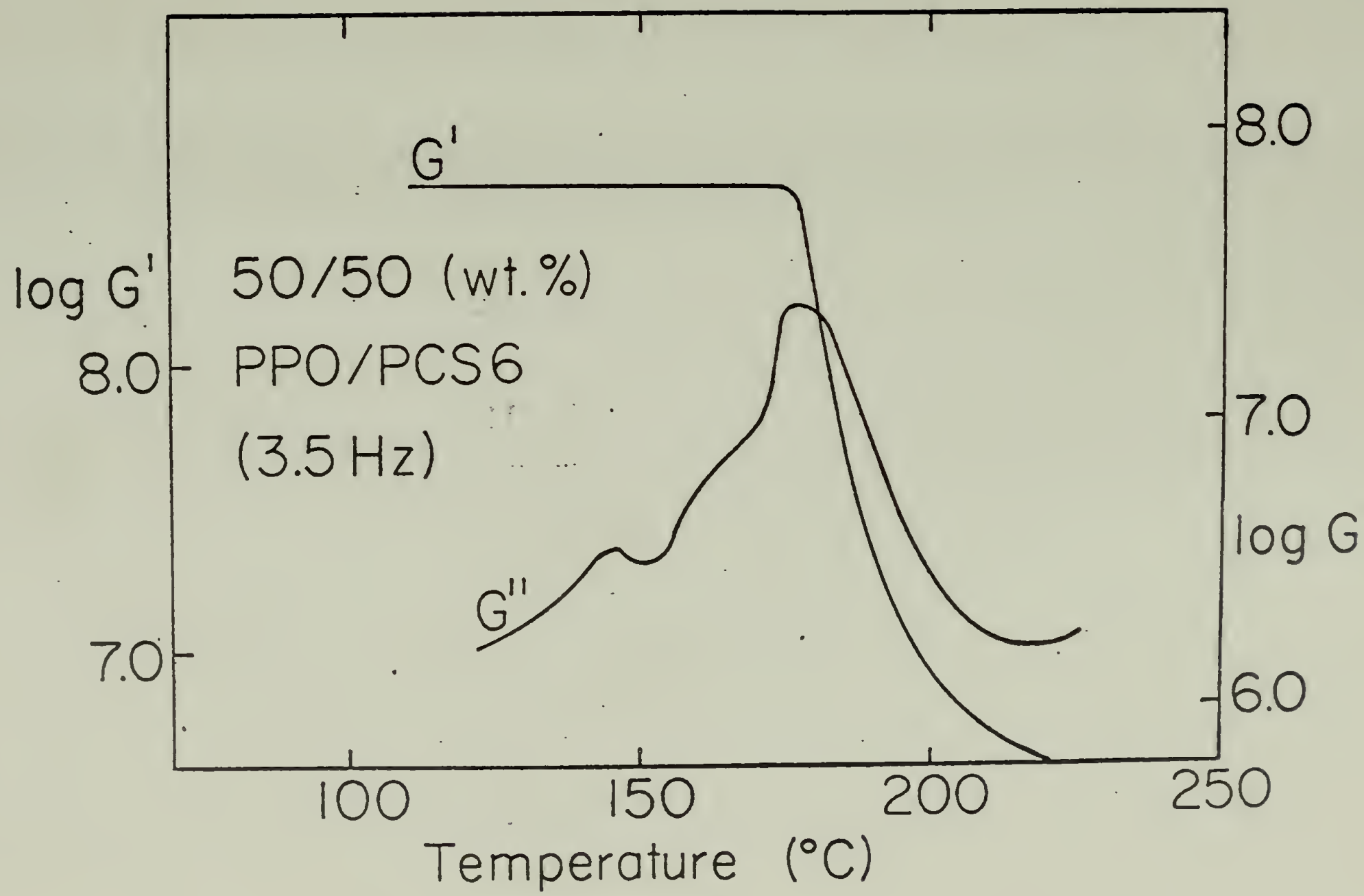

Figure 39. Temperature dependence of G',G'' for 50/50±PPO/PCS-6.

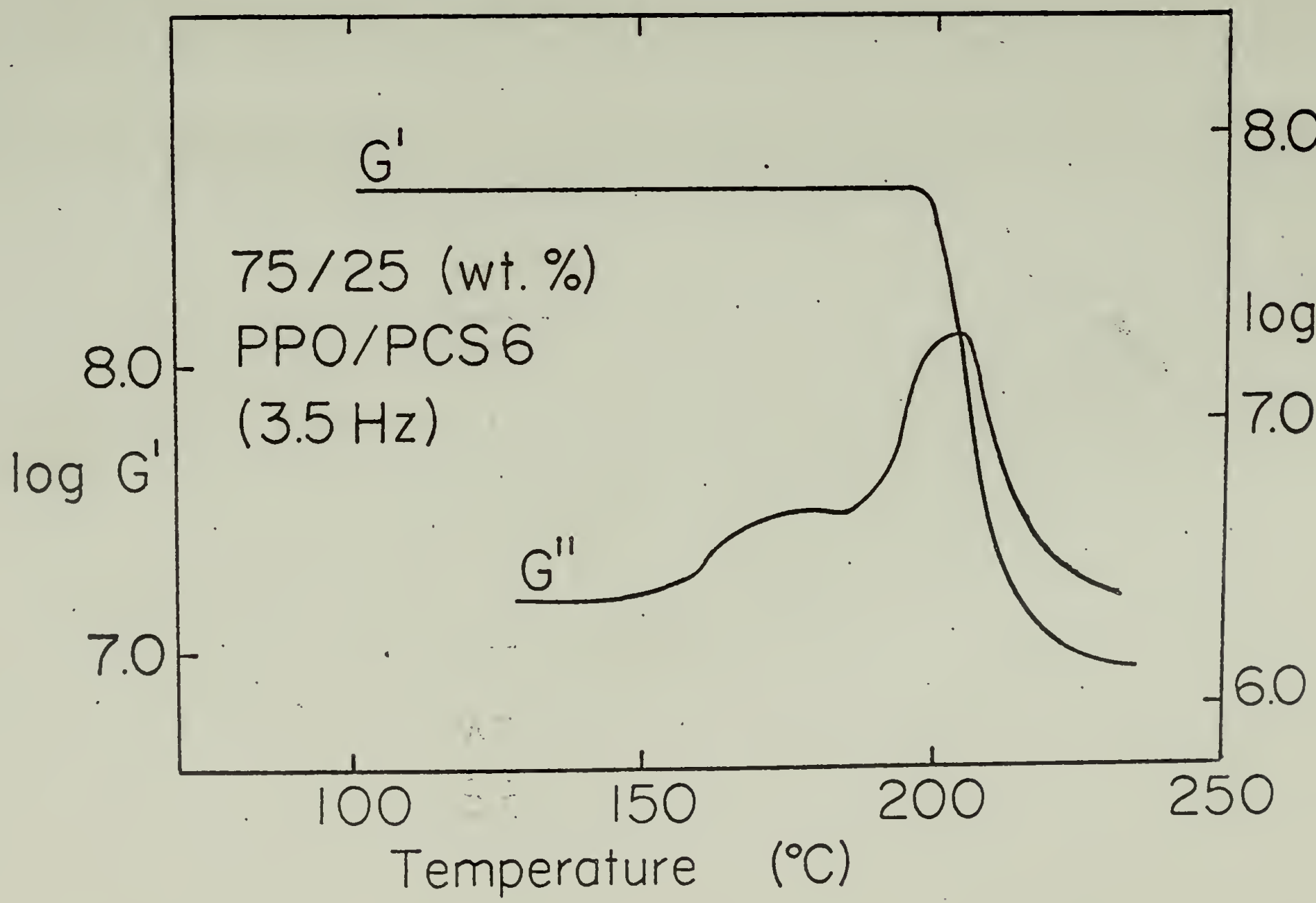

Figure 40. Temperature dependence of G', G'' for 75/25:PPO/PCS-6.

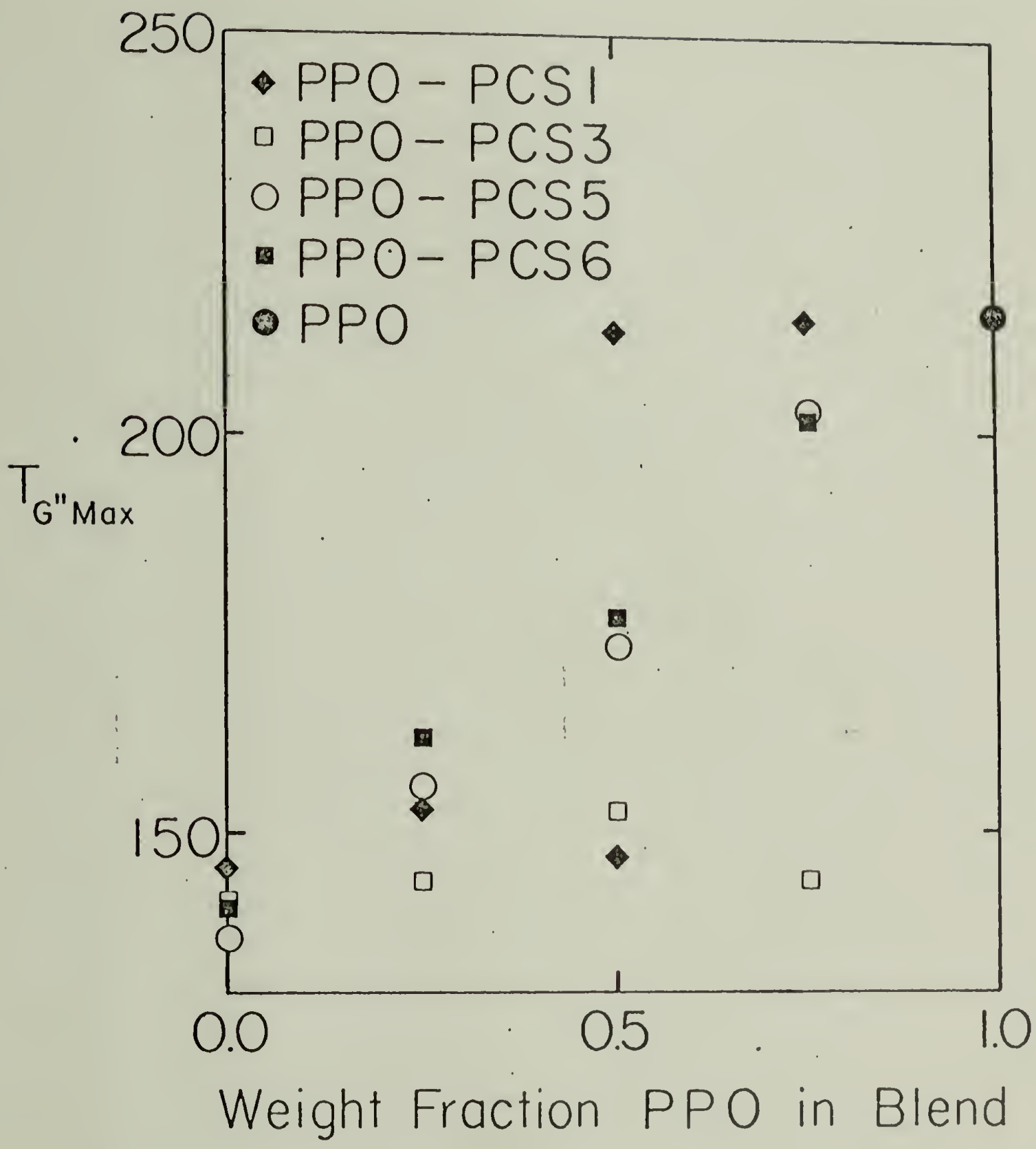

Figure 41. Compositional variation of $T_{G''max}$ for PPO/PCS blends.

$T_{G"max}$ (i.e., the temperature at which G" is a maximum) for the PPO/PCS blend systems at 110 Hz. A comparison of Figure 41 and Figure 20 (a plot of $T_{\varepsilon"max}$ versus blend compositions) indicates that compatibility characteristics cause similar effects in the resultant mechanical or dielectric relaxation properties.

In addition to the main relaxation peaks, the compatible blends exhibit secondary damping peaks at temperatures corresponding to the PCS relaxation; (these peaks were not included in Figure 41). No such secondary peaks were observed at higher temperatures which would be related to the PPO relaxation. Similar secondary peaks were observed in the PPO/polystyrene blend system, in which they were considered to result from the existence of PPO-rich and polystyrene-rich phases within the compatible system.[10] Analogously, the PCS-rich phase of the PPO/PCS compatible blends will exhibit a secondary relaxation at a temperature modified by the presence of PPO according to the general relationship:[10]

$$Tg = w_1 Tg_1 + w_2 Tg_2 \qquad (28)$$

where Tg refers to the secondary damping peak which results from a phase which contains weight fractions, w_1 and w_2, of components 1 and 2 which exhibit relaxations

at Tg_1 and Tg_2, respectively. Compositions of the PCS-rich phase (w_1) were calculated from the positions of the mechanical damping peaks, by rearranging Equation 28:

$$w_1 = \frac{Tg - Tg_1}{Tg_1 - Tg_2} \qquad (29)$$

Table 4 summarizes the results of this treatment for the compatible PPO/PCS blends. The estimates of w_1 are significantly higher than those reported by MacKnight et al. for the corresponding PPO/polystyrene blends.

Arrhenius plots for the dynamic mechanical data for the PPO/PCS-3 system are shown in Figure 42. The two G" peaks (one corresponding to each incompatible component) are represented by the symbols [x] (PPO) and [·] (PCS-3). The slopes of the plots are essentially constant for each relaxation over the composition range, indicating a constant transition activation energy for each component. Similar plots for the compatible systems are shown in Figures 43 and 44. As in the dielectric experiment, the activation energies are essentially constant across the compatible blend composition range.

Table 4. Weight fraction of PCS component (w_1) in PCS-rich phase

Sample	w_1
25/75 : PPO/PCS-5	0.95
50/50 "	0.92
75/25 "	0.58
25/75 : PPO/PCS-6	0.96
50/50 "	0.96
75/25 "	0.56
25/75 : PPO/polystyrene*	0.85
50/50 " *	0.64
75/25 " *	0.40

* Data of MacKnight *et al.*[10]

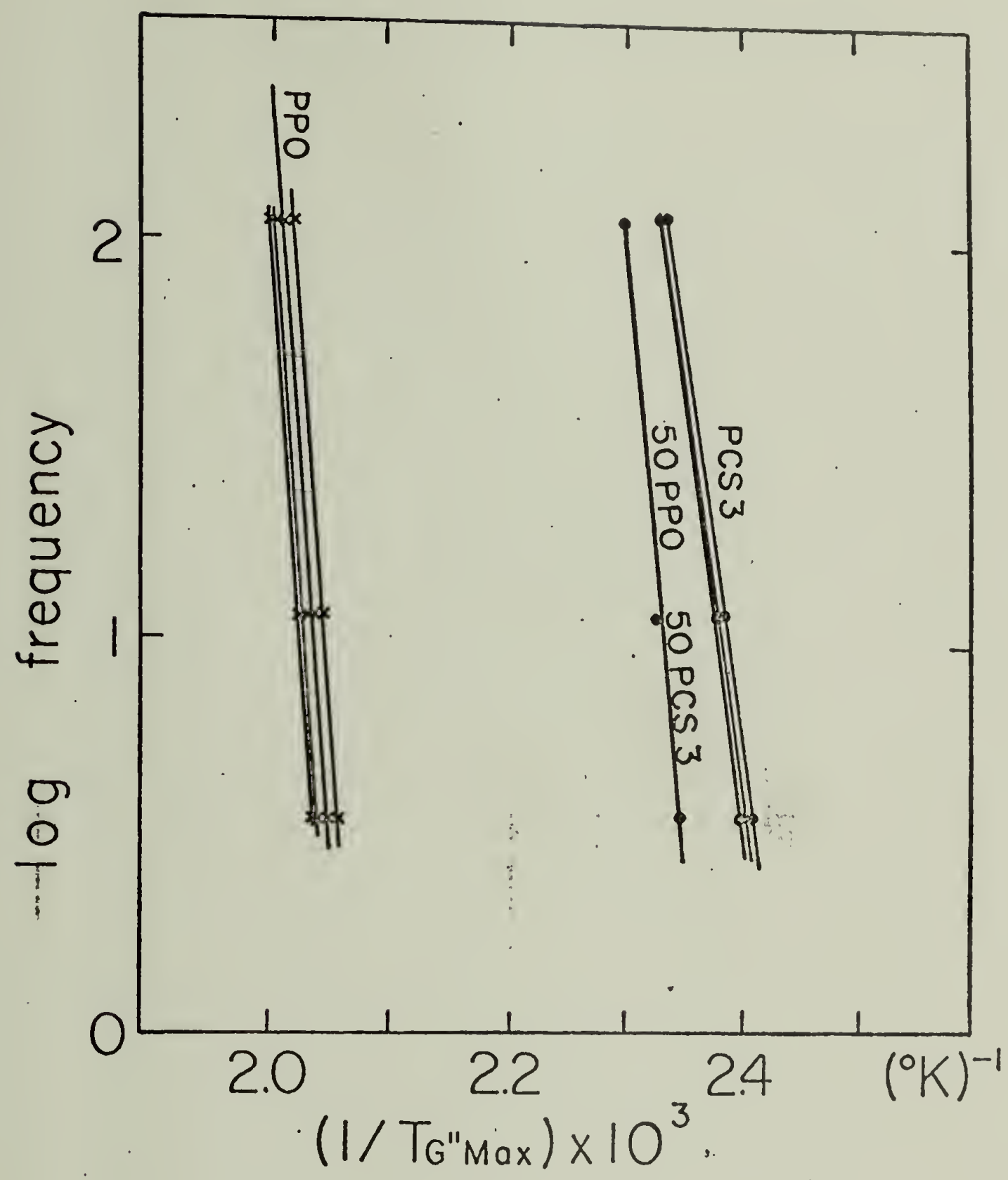

Figure 42. Dynamic mechanical Arrhenius plot for PPO/PCS-3 blends.

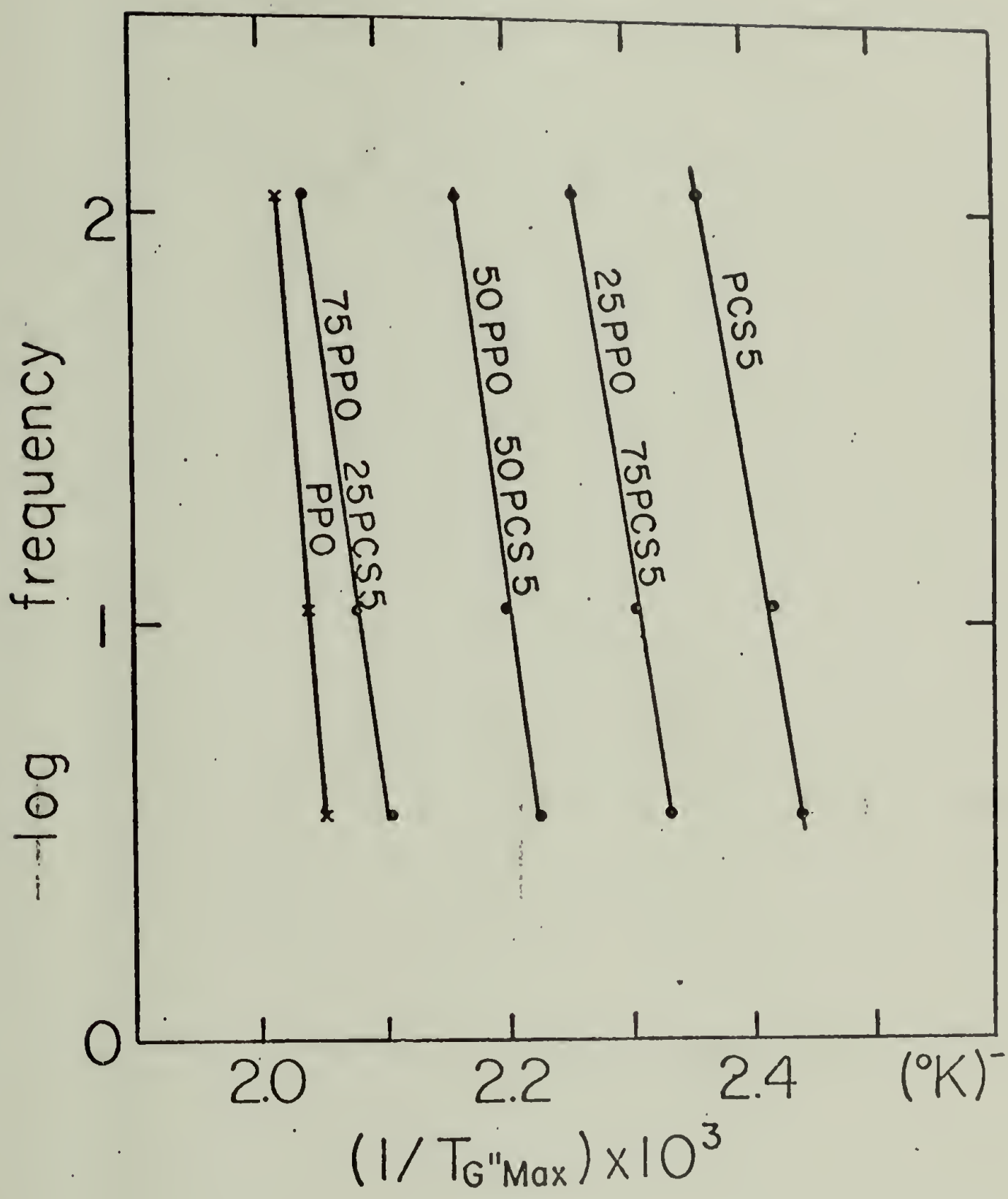

Figure 43. Dynamic mechanical Arrhenius plots for PPO/PCS-5 blends.

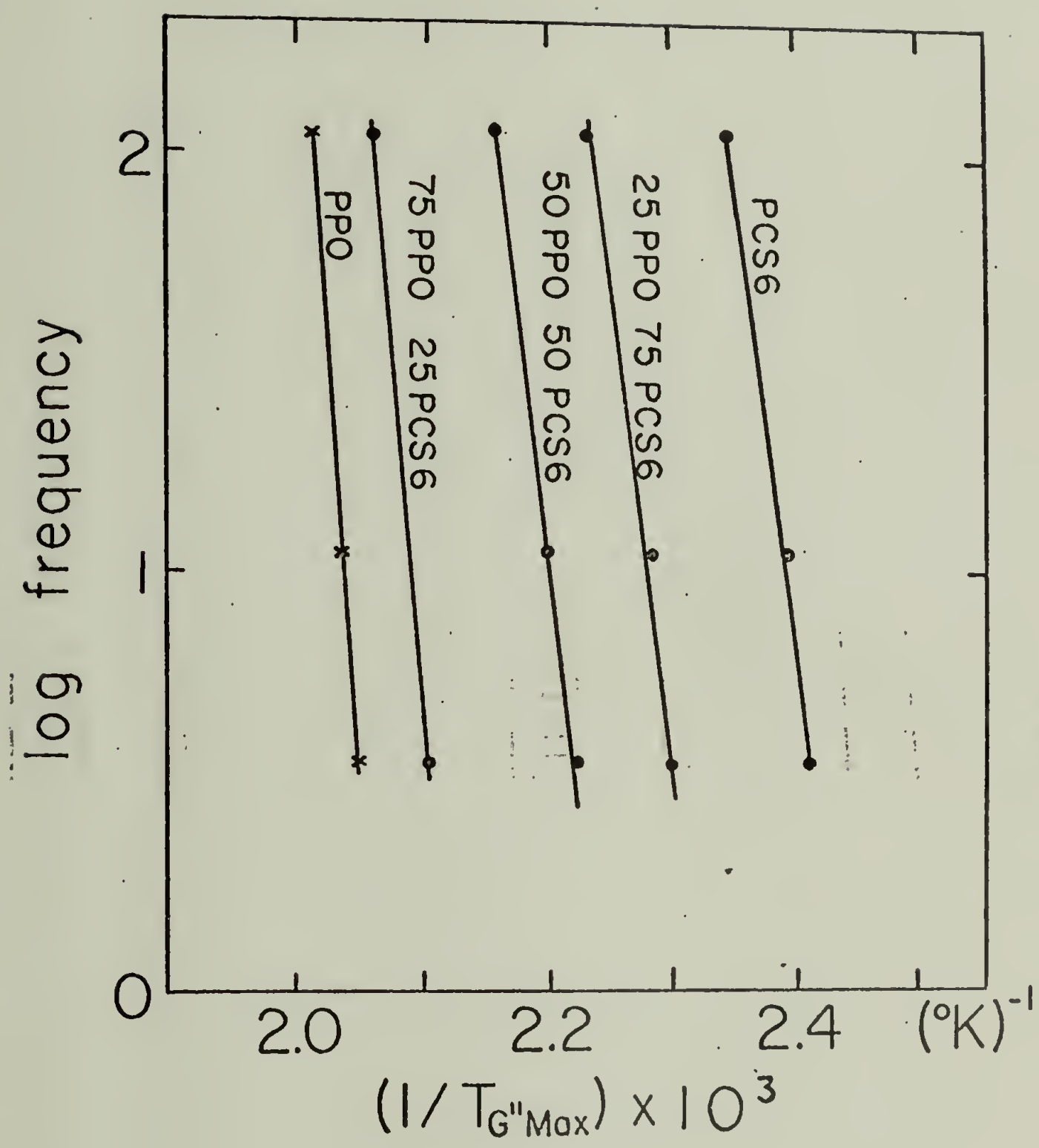

Figure 44. Dynamic mechanical Arrhenius plots for PPO/PCS-6 blends.

C H A P T E R I V

EVALUATION OF COMPATIBILITY THEORIES

The PPO/PCS polyblend system was analyzed in terms of the polymer blending/miscibility theory of Krause[5] in order to gain some insight into this system's chemically dependent compatibility characteristics. Krause's procedure[5] for the prediction of compatibility of polymer pairs was followed in order to correlate PCS copolymer composition and compatibility with PPO. The first step in this procedure is the calculation of the solubility parameters of each of the polymers on the basis of structural features. Using tabulated data,[36] the contributions of the various structural moieties to the solubility parameter were evaluated, as demonstrated in the examples for polystyrene and PPO. The solubility parameter, δ , is then :

$$\delta = \frac{\rho \ \Sigma F_i}{M} \qquad (30)$$

where ρ is the density of the polymer , ΣF_i is the sum of the structural feature contributions and M is the molecular weight of the polymer repeat unit.

Table 5 lists calculated values of the solubility parameters for the components of the PPO/PCS system.

It is in this initial step of the evaluation of the solubility parameters that major difficulties arise. For example, reported solubility parameters for polystyrene[34] range from 8.6 to 10.3 for both calculated and experimental values. Similarly, for PPO, an experimental value of 9.3 has been determined by viscometry[35]; this value differs significantly from the calculated value (9.45) when considering the critical limits of the compatibility theory. (For two polymeric components of molecular weights of 100,000, the critical difference in solubility parameters is 0.11.[5])

It is unsound (or, at least, difficult) procedure to apply a theory which basic feature requires more accuracy and/or precision than is possible. The inapplicability of the above theory is obvious upon analyzing Table 5. If the calculated solubility parameters are assumed to be accurate, PPO should be compatible with both PCS-3 and PCS-6 and possibly with PCS- 5, which is contrary to fact. Even if the experimental value of 9.3 is used for PPO, compatibility is not predicted with polystyrene. Similarly, other theories which utilize solubility parameters to assess compatibility contain this weakness; an example is the procedure which calculates critical ΔH_{mix} values.[37] It must be concluded that these approaches cannot be used to predict (or even

rationalize) compatibility of the PPO/PCS polyblend system.

Likewise, the structural dependence of the compatibility of this system cannot be generally rationalized in terms of specific polar interactions. One would expect the strongest interaction with PPO to occur in the most polar of the PCS family (i.e., that of the highest Cl content); however, PCS-1 and PCS- 3 are incompatible with PPO. Additionally, polymer pairs which demonstrate "pseudo-compatibility" due to specific interactions tend to be compatible only over a limited composition range. However, all PPO/PCS systems are consistent in their compatibility characteristics over their entire composition ranges.

Table 5. Evaluation of solubility parameters for PPO, PCS copolymers

Polymer	p-Cl styrene content (mole percent)	Compatibility with PPO	δ (calculated)
Polystyrene	0	yes	8.78 8.6 - 10.3 *
PCS-5	47	yes	9.33
PCS-6	60	yes	9.39
PCS-3	68	no	9.45
PCS-1	100	no	9.65
PPO	-	-	9.45 9.3 **

* Reported experimental and calculated values range.[34]

** Experimental value.[35]

Example 1. Calculation of solubility parameter (δ) for polystyrene.

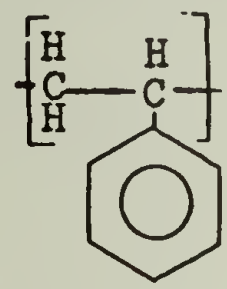

$\rho = 1.04$

$M = 104$

Group/Structural Feature	F_i
1 x $-\overset{H}{C}-$	131.5
1 x $-\overset{H}{\underset{\vert}{C}}-$	86.0
5 x $-\overset{H}{C}=$ (aromatic)	585.6
1 x $-\overset{\vert}{C}=$ (aromatic)	98.1
six member ring	- 22.4
	$\Sigma F_i = 877.8$

$$\delta = \frac{\rho \Sigma F_i}{M}$$

$$\delta = \frac{(1.04)(877.8)}{104} = 8.78$$

Example 2. Calculation of solubility parameter (δ) for PPO.

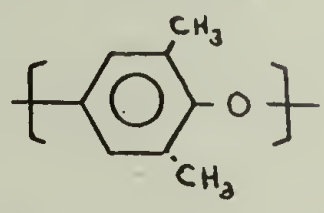

ρ = 1.06 M = 120

Group/Structural Feature	F_1
4 x -C= (aromatic)	392.5
2 x -C(H)= (aromatic)	234.2
2 x $-CH_3$	294.6
-O- (ether)	115.0
p-substitution	40.3
o,m- substitution	16.2
six member ring	- 22.4
	ΣF_1 = 1069.4

$$\delta = \frac{\rho \ \Sigma F_1}{M}$$

$$\delta = \frac{(1.06)(1069.4)}{120} = 9.45$$

A P P E N D I X I

RELATION OF DYNAMIC TESTING EXPERIMENTS AND POLYMER VISCOELASTIC RELAXATION PROCESSES

The dielectric and dynamic mechanical studies are electrical and mechanical analogues of the general dynamic experiment in which a viscoelastic material is subjected to a sinosoidally applied stress of a frequency, ω, at a temperature, T.[32] For the two dynamic experiments the stresses can be written as a function of time, t:

$$\sigma(t) = \sigma_o \sin \omega t \qquad \text{(A-1)}$$

$$E(t) = E_o \sin \omega t \qquad \text{(A-2)}$$

where $\sigma(t)$ is the time dependent mechanical stress and E(t) is the electric field strength (i.e., "electrical stress"). In response to the stresses, the resultant strains lag behind the stresses by a phase angle, δ :

$$\gamma(t) = \gamma_o \cos(\omega t - \delta_m) \qquad \text{(A-3)}$$

$$D(t) = D_o \cos(\omega t - \delta_e) \qquad \text{(A-4)}$$

where $\gamma(t)$ represents the mechanical strain and D(t) the electrical strain analogue, electric displacement;

δ_m and δ_e are the mechanical, electrical phase lag angles, respectively.

Following the standard definitions, the following terms are described in the complex notation:

$$G^* = \frac{\sigma^*}{\gamma^*} \qquad \text{(A-5)}$$

$$\varepsilon^* = \frac{D^*}{E^*} \qquad \text{(A-6)}$$

where G^* is the complex shear modulus and ε^* is the complex dielectric constant. These complex quantities can be represented as a combination of their respective storage and loss components:

$$G^* = G' + 1\,G'' \qquad \text{(A-7)}$$

$$\varepsilon^* = \varepsilon' - 1\,\varepsilon'' \qquad \text{(A-8)}$$

The "single prime" components (e.g., G', ε') refer to the storage functions or contributions due to displacements in phase with the applied stress. The "double prime" components (e.g., G'', ε'') are loss functions which represent energy dissipation due to strains out of phase with the applied stress. The commonly utilized parameter, tan δ, is a function of the above complex quantities:

$$\tan \delta_m = G''/G' \qquad \text{(A-9)}$$

$$\tan \delta_e = \varepsilon''/\varepsilon' \qquad \text{(A-10)}$$

These viscoelastic properties vary as a function of temperature and frequency across the relaxation region as shown in Figure A-1. At a constant temperature, as the frequency increases, the dielectric constant, ε', will decrease from a relaxed value, ε_R, to an unrelaxed value, ε_U. The shear modulus, G', will increase from a relaxed value, G_R, to an unrelaxed state having a modulus, G_U. The difference between the relaxed and unrelaxed quantities (e.g., $\varepsilon_R - \varepsilon_U$, $G_U - G_R$) is known as the magnitude of the relaxation. In this relaxation region the loss functions, ε'' and G", display peaks, reflecting an energy dissipation caused by a molecular relaxation process. The general behavior of these parameters can also be observed in the analogous experiment of traversing the relaxation region by variation of temperature at a fixed frequency.

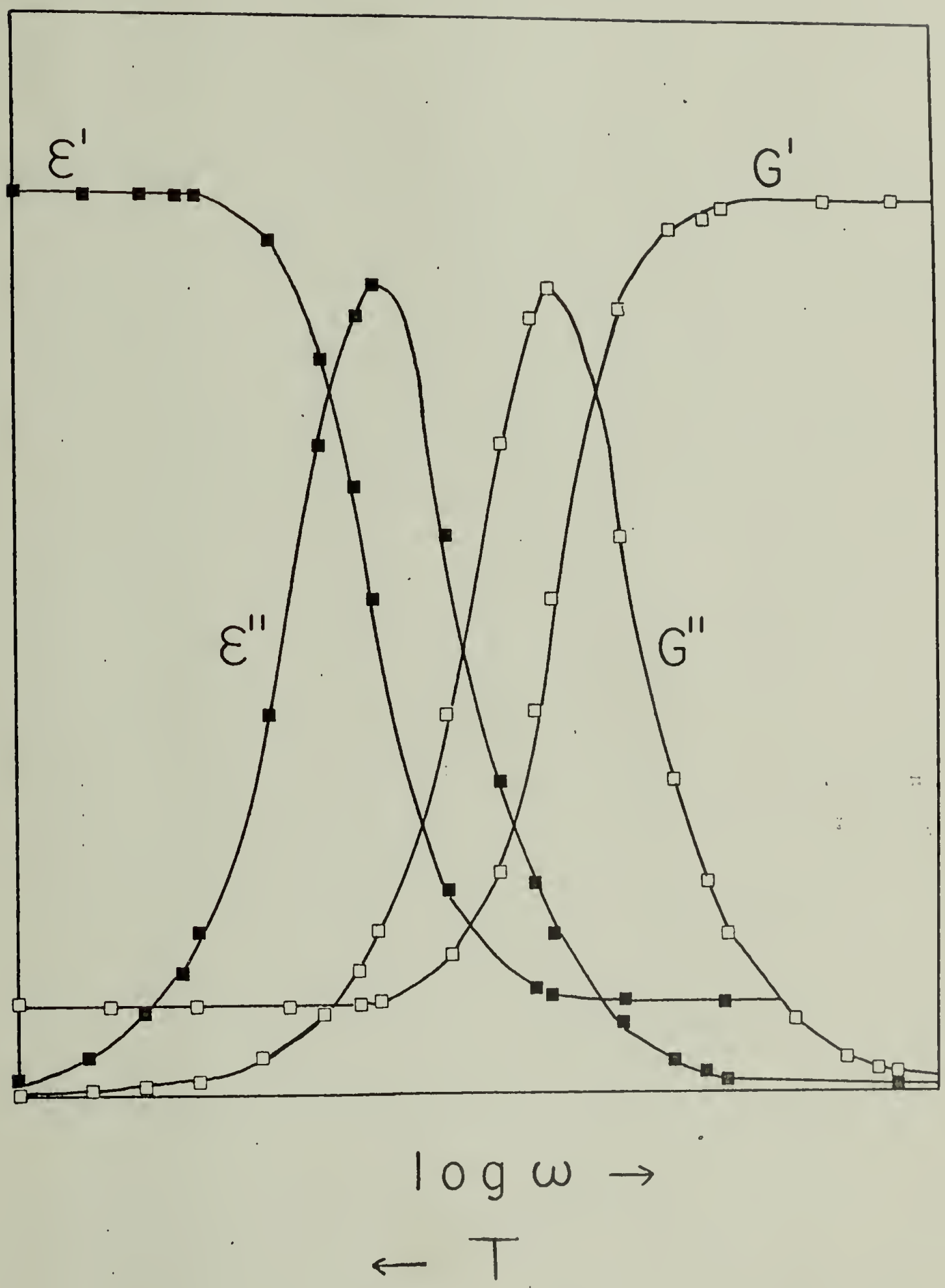

Figure A-1. Idealized variation of dynamic mechanical and dielectric properties as a function of frequency and temperature.

A P P E N D I X I I

DEVELOPMENT OF DIPOLE ORIENTATION CORRELATION ANALYSIS

The various developments of the theories relating macroscopic dielectric relaxation properties (e.g., ε_R, ε_U) and molecular properties (e.g., dipole moment, dipole orientations) follow the same general procedure, but successively deal more rigorously with molecular interactions.[33]

As a basis for these developments, consider the model of an infinite parallel plate capacitor assembly with a static electric field, $\underline{E}$. In a vacuum:

$$E = 4\pi\sigma \qquad \text{(A-11)}$$

where σ is the charge density of the electrode plates. Upon introduction of a dielectric material with a static dielectric constant, ε_R, the electic field is:

$$E = \frac{4\pi\sigma}{\varepsilon_R} \qquad \text{(A-12)}$$

The polarization, P, of the material is measured by the reduction of the field strength by the introduction of the dielectric into the field:

$$\begin{aligned} 4\pi P &= 4\pi\sigma - 4\pi\sigma/\varepsilon_R \qquad \text{(A-13)} \\ &= E(\varepsilon_R - 1) \end{aligned}$$

On a molecular scale the total electric moment ($\underline{m}$) of a molecule results from contributions from the permanent dipole ($\underline{\mu}$) and the induced dipole moment:

$$\underline{m} = \underline{\mu} + \alpha \underline{f} \qquad \text{(A-14)}$$

where α is the molecular polarizability and $\underline{f}$ is the effective field strength acting on the molecule. The total moment is related to the polarization by:

$$P = N \underline{m} \qquad \text{(A-15)}$$

where N is the number of dipoles.

A basic relationship between macro- and microscopic properties was developed by Debye to approximate the dielectric properties of noninteracting gaseous systems. In such a system the localized effective field strength is not perturbed by the presence of other individual molecules; i.e., $\underline{f} = \underline{E}$. When Equation A-14 is given in reference to $\underline{E}$, the quantity $\underline{\mu}$ is given as its projection on $\underline{E}$, (μ_E):

$$\mu_E = \mu_o \overline{\cos \theta} \qquad \text{(A-16)}$$

where μ_o is the dipole moment of an isolated molecule of the dielectric. The rotational potential energy of the dipole in the field is ($\mu_o E \overline{\cos \theta}$) ; the average

$\overline{\cos\theta}$ is determined by a statistical mechanical averaging process:

$$\overline{\cos\theta} = \frac{\int_0^{\pi} \cos\theta \exp(E\mu_o \cos\theta / kT) \sin\theta \, d\theta}{\int_0^{\pi} \exp(E\mu_o \cos\theta / kT) \sin\theta \, d\theta} \qquad \text{(A-17)}$$

$$= \frac{\mu_o E}{3\ kT} \qquad \text{(A-18)}$$

Combining Equations A-16 and -18 we obtain a value for the projection of $\underline{\mu}$ on $\underline{E}$:

$$\mu_E = \frac{\mu_o^2\ E}{3\ kT} \qquad \text{(A-19)}$$

The combination of Equations A-14 and -19 yields:

$$\underline{m} = \frac{\mu_o^2\ E}{3\ kT} + \alpha\ E \qquad \text{(A-20)}$$

Substituting for $\underline{m}$ using Equations A-13 and -15 and cancelling E, we obtain:

$$(\varepsilon_R - 1) = \frac{4\pi N\ \mu_o^2}{3\ kT} + 4\pi\alpha\ N \qquad \text{(A-21)}$$

At extremely high frequencies dipoles have no time to attain equilibrium causing the permanent dipole term to become negligible:

$$(\varepsilon_U - 1) = 4\pi N\ \alpha \qquad \text{(A-22)}$$

Combining Equations A-21 and -22, we arrive at a relationship between the magnitude of the dielectric relax-

ation and the molecular properties of systems of non-interacting molecules;

$$\varepsilon_R - \varepsilon_U = \frac{4\pi N \mu_o^2}{3 kT} \qquad (A\text{-}23)$$

The Onsager development made the theory applicable to dilute dipolar systems with long range dipole interactions. The model used for this treatment is a reference spherical cavity of a radius, a, within the dielectric medium which is subjected to an electric field, $\underline{E}$. A basic feature of this development includes the macroscopic interactions between the dipoles within and those outside the cavity. However, it excludes any short range interactions among the dipoles contained in the cavity. In this case the effective field, $\underline{f}$, on a dipole in the spherical region is a result of the cavity field ($\underline{G}$, resulting from the external field and the material surrounding the cavity) and the reaction field ($\underline{R}$, resulting from the dipoles within the sphere). Thus, Equation A-14 can be expressed appropriately:

$$\underline{m} = \underline{\mu} + \alpha (\underline{G} + \underline{R}) \quad . \qquad (A\text{-}24)$$

From electrostatic theory, $\underline{G}$ and $\underline{R}$ are related to the properties of the model:

$$\underline{G} = \frac{3\,\varepsilon_R}{2\,\varepsilon_R + 1}\,\underline{E} \qquad \text{(A-24)}$$

$$\underline{R} = \frac{1}{a^3}\,\frac{2(\varepsilon_R - 1)}{(2\,\varepsilon_R + 1)}\,\underline{m} \qquad \text{(A-25)}$$

The term μ is evaluated as a projection on $\underline{E}$ as in the Debye procedure. The rotational potential energy is:

$$U = -\frac{3\,\varepsilon_R}{2\,\varepsilon_R + 1}\,\mu E\,\overline{\cos\theta} \qquad \text{(A-26)}$$

The $\overline{\cos\theta}$ term is evaluated by an averaging process which reduces to the Langevin function:

$$\overline{\cos\theta} = \mathcal{L}\left[\frac{3\,\varepsilon_R}{2\,\varepsilon_R + 1}\,\frac{\mu E}{kT}\right] \qquad \text{(A-27)}$$

and when $E \ll kT$, i.e., at low field strengths, the following approximation is valid:

$$\overline{\cos\theta} \cong \frac{3\,\varepsilon_R}{2\,\varepsilon_R + 1}\,\frac{\mu E}{3kT} \qquad \text{(A-28)}$$

Similarly, $\underline{m}$ is expressed in terms of $\underline{E}$ and the polarizability is related to macroscopic parameters by the Clausius-Mosotti equation:

$$\alpha = \frac{\varepsilon_U - 1}{\varepsilon_U + 2} \, a^3 \qquad \text{(at high frequency)} \qquad \text{(A-29)}$$

The appropraite combination of the above equations yields the Onsager relationship:

$$\varepsilon_R - \varepsilon_U = \frac{4\pi N \mu_o^2}{9kT} \frac{\varepsilon_R (\varepsilon_U + 2)^2}{2\varepsilon_R + \varepsilon_U} \qquad \text{(A-30)}$$

Frohlich's treatment follows similar procedures but further includes the effects of interactions among the dipoles within the reference sphere. This dipolar interaction factor is introduced by including the generalized dipole vector product $\underline{\mu}\cdot\underline{\mu}$ in place of the term for the noninteracting systems:

$$\varepsilon_R - \varepsilon_U = \frac{4\pi N}{9kT} \frac{\varepsilon_R (\varepsilon_U + 2)^2}{2\varepsilon_R + \varepsilon_U} \, \underline{\mu}\cdot\underline{\mu} \qquad \text{(A-31)}$$

This treatment characterizes the influence of dipolar interactions in the dipole orientation correlation factor, g:

$$g = \frac{\underline{\mu} \cdot \underline{\mu}}{\mu_o^2} \qquad \text{(A-32)}$$

Generally, the quantity, $\underline{\mu}\cdot\underline{\mu}$ can be summed:

$$\underline{\mu} \cdot \underline{\mu} = \mu_o^2 + \mu_o^2 \sum_{j=1}^{N} \cos \gamma_j \qquad \text{(A-33)}$$

where a dipole i makes an angle γ_j with its N dipolar neighbors. In the Frohlich analysis of the simplified case of localized interactions:

$$\underline{\mu} \cdot \underline{\mu} = \mu_o^2 + z\mu_o^2 \overline{\cos \gamma} \qquad \text{(A-34)}$$

where z is the number of i's nearest neighbors which are associated with an average $\overline{\cos \gamma}$ value. Combining Equations A-32 and -33, g can be written as:

$$g = 1 + z \overline{\cos \gamma} \qquad \text{(A-35)}$$

Similarly, Equation A-31 can be written in the more familiar form:

$$g = \frac{9kT}{4\pi N \mu_o^2} \frac{(2\varepsilon_R + \varepsilon_U)(\varepsilon_R - \varepsilon_U)}{\varepsilon_R (\varepsilon_U + 2)^2} \qquad \text{(A-36)}$$

When this general treatment is applied to a system of isolated polymer chains, the correlation factor is summed over the length of the polymer chain:

$$g = 1 + \sum_{j=2}^{n} \cos \gamma_{1j} \qquad \text{(A-37)}$$

where the contributions of dipole j at an angle, γ_{1j}, with dipole 1 are summed over the n dipoles within the chain.

The evaluation of g for bulk polymers is more com-

plex as intermolecular as well as intramolecular dipole interactions must be considered:

$$g = 1 + \sum_{j=2}^{n} {}^{I}\cos\gamma_{1j} + \sum_{j} {}^{II}\cos\gamma_{1j} \quad \text{(A-38)}$$

where superscript I refers to intramolecular interactions (as in Equation A-37) and II refers to contributions from the interaction of dipole 1 (of chain I) with any dipole of any other chain.

A P P E N D I X I I I

ERROR ANALYSIS OF FROHLICH TREATMENT

The variance of a function calculated from experimentally determined quantities can be estimated by the standard procedure of error propagation analysis. Thus, if F is a function of variables, $F(x_1, x_2, \ldots, x_n)$, the fractional standard deviation ($\Delta F/F$) can be calculated from the standard deviation of the experimentally determined value, $(\Delta x_i/x_i)$,[38]

$$\left(\frac{\Delta F}{F}\right)^2 = \sum_i \left(\frac{\partial F}{\partial x_i}\ \frac{\Delta x_i}{x_i}\right)^2 \qquad \text{(A-39)}$$

By this method the standard deviation of the dipole orientation correlation factor (g) are calculated with respect to the variables ε_R and ε_U. The partial derivatives ($\partial g/\partial \varepsilon_R$, $\partial g/\partial \varepsilon_U$) were evaluated numerically via computer. The deviation of the experimental quantities ($\Delta \varepsilon_R$, $\Delta \varepsilon_U$) were determined by duplication of experiments and estimation of variability of extrapolations of $\varepsilon - \ln\omega$ plots.

REFERENCES

1. D.W. Fox and A.D. Wambach, German Patent, 2,331,826, (1974); blending of poly(ε -caprolactone) to improve the impact resistance of poly(butylene terephthalate).

2. J. Hrach and F. Breitenfellner, German Patent, 2,320,117, (1973); the modulus of poly(butylene terephthalate) is increased by blending with PET.

3. N. Asahara and H. Hasegawa, Japanese Patent, (74) 83,742, (1974); the melt viscosity of a Bisphenol-A polyester is reduced by blending with an alkyl iso-/tere phthalate.

4. A.J. Yu, in Multicomponent Polymer Systems, Advances in Chemistry Series, 99, (A.C.S., Washington, D.C., 1971), p.2.

5. S. Krause, J. Macromol. Sci.-Revs. Macromol. Chem., C7, 251, (1972).

6. The evaluation of thermodynamic principles and procedures parallels that of S. Krause, op. cit.

7. E.P. Cizek, U.S. Patent, 3,383,435, (1968).

8. This blend system is commercially identified by General Electric's trade name "Noryl"; physical properties reviewed by M. Kramer, J. Appl. Poly. Sci., Appl. Poly. Symposium, 15, 227, (1971).

9. W.J. MacKnight, F.E. Karasz and J. Stoelting, in Multicomponent Polymer Systems, Advances in Chemistry Series, 99, (A.C.S., Washington, D.C., 1971), p. 29.

10. W.J. MacKnight, F.E. Karasz and J.Stoelting, Poly. Eng. and Science, 10(3), 133, (1970).

11. A.R. Shultz and B.M. Gendron, paper presented at the Biennial Polymer Symposium, Ann Arbor, Michigan, June, 1972;
    b. A.R. Shultz, private communication;
    c. A.R. Shultz and B.M. Beach, Macromolecules, 7(6), 902, (1974).

12. P. Debye and F. Bueche, J. Chem. Phys., 19(5), 589, (1951).

13. M.V. Volkenstein, Configurational Statistics of Polymer Chains, (Interscience, New York, 1963), p.348.

14. G.P. Mikhailov, A.M. Lobanov and M.P. Platonov, Polymer Science USSR, 9, 2565, (1967).

15. L.L. Burshtein and T.P. Stepanova, Polymer Science USSR, 11, 2885, (1969).

16. H. Morawetz, Macromolecules in Solution, (Interscience, New York, 1965), p. 305.

17. T.M. Birshtein and O.B. Ptitsyn, Conformations of Macromolecules, (Interscience, New York, 1966), p.9.

18. R.F. Boyer and R.H. Boundy, Styrene: Its Polymers, Copolymers and Derrivatives, (Reinhold, New York, 1952), p. 936.

19. P.J. Flory, Principles of Polymer Chemistry, (Cornell University Press, 1953), p. 181.

20. A. Kotera et al., Nippon Kagakukai Bulletin, 39, 754, (1966).

21. L. McKenna, private communication.

22. General Radio Corp., 1620-A Assembly Operation Manual.

23. Toyo Corporation, DDV II-B Instruction Manual.

24. C.D. Han and T.C. Yu, J. Appl. Poly. Sci., 15, 1163, (1971).

25. J.D. Ferry, M.L. Williams and E.R. Fitzgerald, J. Phys. Chem., 59, 403, (1955).

26. J.D. Ferry, Viscoelastic Properties of Polymers, Second Ed., (Wiley Interscience, New York, 1970), p. 316.

27. A. Kotera et al., op. cit., 754.

28. M.V. Volkenstein, op. cit., p. 348.

29. M. Takayanagi, J. Poly. Sci., Part C, 15, 263, (1966).

30. L.E. Nielsen, J. Appl. Poly. Sci., 17, 3819, (1973).

31. L.D. Auger, private communication.

32. The development generally follows:

J. Aklonis, W.J. MacKnight and M. Shen, Introduction to Polymer Viscoelasticity, (Wiley, 1972)

N.G. McCrum, B.E. Read and G. Williams, Anelastic and Dielectric Effects in Polymeric Solids, (Wiley, New York, 1967).

33. The development generally follows:

H. Frohlich, Theory of Dielectrics, (Oxford Univ. Press, 1949)

N.G. McCrum, B.E. Read and G. Williams, op. cit.

34. J. Brandrup and E.H. Immergut, Polymer Handbook, (Interscience, New York, 1966), p. IV-341.

35. F.E. Karasz, private communication.

36. K.L. Hoy, J. Paint Technology, 42, 76, (1970).

37. B. Schneier, J. Appl. Poly. Sci., 17, 3185,(1973).

38. H.D. Young, Statistical Treatment of Experimental Data, (McGraw-Hill, 1962), p. 96.